Identification and characterization of Arabidopsis genes involved in tolerance to Fe deficiency-mediated chlorosis

Dissertation

zur Erlangung des
Doktorgrades der Naturwissenschaften (Dr. rer. nat.)

der

Naturwissenschaftlichen Fakultät I
– Biowissenschaften –

der Martin-Luther-Universität
Halle-Wittenberg

vorgelegt

von Frau Nicole Beate Schmid

geb. am 08.04.1983 in Heidenheim a.d. Brenz

Gutachter
1. Prof. Dr. Nicolaus von Wirén
2. Prof. Dr. Klaus Humbeck
3. Prof. Dr. Thomas Buckhout

Halle (Saale), den 28.05.2014

Parts of this thesis are published in:

Schmid NB, Giehl RFH, Döll S, Mock HP, Strehmel N, Scheel D, Kong X, Hider RC, von Wirén N, (2014): Feruloyl-CoA 6'-Hydroxylase1-Dependent Coumarins Mediate Iron Acquisition from Alkaline Substrates in Arabidopsis. Plant Physiology **164**: 160-172

Table of contents

1 Summary

Iron (Fe) is an essential nutrient for plants and although it is one of the most abundant elements in the earth's crust, the low solubility of this micronutrient in soils restricts its uptake by plants. Non-graminaceous plants acquire Fe through dissolution of Fe(III) precipitates, which is mainly mediated through rhizosphere acidification. Then reduction of ferric to ferrous Fe and subsequent uptake at the plasma membrane can occur. To date it still remains unclear how non-graminaceous plants access ferric Fe in the rhizosphere and overcome the problem of low Fe solubility and impeded Fe reducibility in high pH soils. Thus, this study aimed at identifying molecular components that mediate Fe acquisition under alkaline soil conditions.

The present thesis started with the establishment of a screening approach that allowed the screening of a collection of approximately 3,500 T-DNA insertion lines of *Arabidopsis thaliana* in conditions that simulated the low Fe availability in alkaline substrates. This approach enabled the identification of two T-DNA insertion lines, *myb72-1* and *f6'h1-1*, that exhibited decreased tolerance to Fe deficiency-mediated chlorosis on calcareous substrate. Both lines showed strong chlorosis that could be restored by the addition of Fe-EDDHA. Furthermore, qRT-PCR analysis revealed that the corresponding genes are strongly up-regulated in response to Fe deficiency in roots of wild-type plants.

In *f6'h1*, the expression of a gene that encodes the 2-oxoglutarate-dependent dioxygenase Feruloyl-CoA 6'-Hydroxylase1 (F6'H1) is disrupted. Localization studies with *proF6'H1:GUS* and *proF6'H1:F6'H1:green fluorescence protein* (GFP) lines revealed that F6'H1 localization is restricted to roots. In addition, F6'H1 expression is induced mainly in the basal zone of the primary root and extends to cortical and rhizodermal root cells under Fe deficiency. Thus, F6'H1 expression coincides with that of other Fe acquisition genes, namely *FIT*, *IRT1* and *FRO2*. Further analysis showed that under Fe deficiency, F6'H1 is required for the biosynthesis of fluorescent coumarins that are released into the rhizosphere in a FIT-dependent manner. Interestingly, in the other T-DNA insertion line *myb72,* where the expression of the gene that encodes the R2R3-MYB-like transcription factor MYB72 is disrupted, the biosynthesis of fluorescent metabolites is also impaired in conditions of Fe deficiency.

Scopoletin was the most prominent coumarin found in Fe-deficient wild-type root exudates but failed to mobilize Fe(III), while esculetin, i.e. 6,7-dihydroxycoumarin, occurred in lower amounts but was effective in Fe(III) mobilization. Nevertheless, not only esculetin but also scopoletin as well as esculin, the glucoside of esculetin, were able to prevent *f6'h1* mutant plants from Fe deficiency-induced chlorosis. In vitro assays showed that esculetin acts as a catechol-type siderophore and forms stable complexes with Fe(III) ($\log K_f$ = 17.1) only at alkaline pH. At low pH, esculetin exhibits also reducing abilities, since esculetin-bound Fe(III) alleviated *fro2* mutant plants from Fe deficiency and mediated Fe(III) reduction, even in the absence of a plasma membrane-bound reductase. The fact that scopoletin and esculin were able to avoid chlorosis in *f6'h1* plants might be attributed to their possible de-glycosylation and de-methylation in the rhizosphere, which is supposed to yield compounds with Fe(III)-mobilizing capacity like esculetin. This was indicated for esculin by a colorimetric assay that detects Fe(III)-esculetin complex formation.

The results presented in this thesis indicate that Strategy I plants, usually employing a reduction-based strategy to acquire Fe from soils, release secondary metabolites with Fe(III)-chelating and -reducing properties to assist Fe acquisition in high pH soils.

2 Introduction

2.1 The importance of iron for plants

Iron (Fe) is an indispensable element for virtually all forms of life as its deficiency detrimentally affects growth and development of plants and humans likewise (Beinert et al., 1997; Masse and Arguin, 2005). In resource-poor areas where people mainly rely on staple crops like rice, maize or wheat for their micronutrient and specifically Fe intake, the crop Fe status is of crucial importance (White and Broadley, 2005; Welch, 2002). However, Fe deficiency is not only a problem in developing countries, but also prevails in industrialized countries, therefore making Fe deficiency-induced anemia a widespread life-threatening disease that affects more than 2 billion people all over the world (WHO; http://www.who.int/nutrition/topics/ida/en/; Kobayashi et al., 2013; Mayer et al., 2008; Frossard et al., 2000). Fe deficiency is also a worldwide agricultural problem, especially in calcareous soils, that cover about 30% of the arable land worldwide (see section 2.1.2 for more details about soil Fe availability) (Kobayashi et al., 2013; Lucena, 2007). Even though plants require relatively low amounts of Fe for optimal plant growth, the concentration of Fe in the soil solution should be around 10^{-9} to 10^{-4} M, whereby plants typically accumulate 50 to 150 µg g^{-1} dry weight (Guerinot and Yi, 1994; Hansch and Mendel, 2009), the lack of adequate amounts of this micronutrient present in their system severely affects their growth, yield and quality (Kobayashi et al., 2013). The first symptom that becomes visible in a plant suffering from Fe deficiency is the yellowing of interveinal regions of young leaves. Proportional to the degree of the deficiency, this yellowing eventually expands to the whole leaves and turns them light yellow or even white (Chen and Barak, 1982). This condition is called chlorosis and refers to an impaired chlorophyll biosynthesis due to the absence of sufficient Fe. Carotenoids are then the sole remaining leaf pigments (von Wirén, 1994; Marschner, 2012; Abadia and Abadia, 1993).

Many plant species, as for example soybean, peanut, sorghum, rice, corn or wheat suffer from Fe deficiency under various conditions all over the world and as a result exhibit impaired growth and limited yield (Hansen et al., 2007). Even in fruit trees, such as kiwifruit, peach, pear, various citrus species and grapevine, which

have a relatively low Fe requirement, Fe deficiency still represents one of the most severe challenges for obtaining high yields and fruit quality. This represents a serious problem especially when these plants are grown on calcareous soils as they prevail in many Mediterranean habitats found in France, Italy, Greece or Spain (Abadía et al., 2004; Álvarez-Fernández et al., 2007; Rombola and Tagliavini, 2007). There are several fertilization or cultural management strategies commonly used to counteract the development of Fe deficiency on the field. These practices include acidifying the soil with ammonium salts or sulfur (S) supplies, applying foliar or soil Fe fertilizer, irrigation and drainage management or intercropping with Fe-efficient graminaceous species (Hansen et al., 2007; Chen and Barak, 1982; Cesco et al., 2006). However, these methods still exhibit shortcomings or could be developed even further.

The improvement of existing strategies or the development of new ones, which include breeding approaches and genetic engineering, require profound and comprehensive knowledge of Fe homeostasis on both molecular and physiological levels. The aim of the next sections is to give an overview of the functions, the occurrence and the factors that determine the availability of this important metallic micronutrient that is required by plants for many different biochemical functions (Marschner, 2012).

2.1.1 Fe within plants and its physiological functions

Fe is essential for all plants since the proper function of many enzymes and thus life-sustaining processes depend on the presence of this metal. For example, energy-generating processes like photosynthesis and mitochondrial respiration require sufficient amounts of Fe. Almost 90% of Fe found in leaf cells is located in chloroplasts (Kim and Guerinot, 2007) where it is indispensable for the proper structure and functionality of the thylakoid membranes (Marschner, 2012). Furthermore, the biosynthesis of chlorophyll and heme structure precursors like δ–aminolevulinic acid (ALA) or protoporphyrinogen depend on Fe (Marschner, 2012). Fe also plays a role in nutrient assimilation as it determines cofactors that are required for the function of nitrate, nitrite and sulfite reductase enzymes. In addition, the biosynthesis of hormones such as ethylene, gibberellic acid and

jasmonic acid and the production and scavenging of reactive oxygen species (ROS), osmoprotection, nitrogen fixation and pathogen defense also rely on Fe or rather Fe-containing enzymes (Hansch and Mendel, 2009; Ishimaru et al., 2006).

The reason for the versatile functions of Fe in part lies in its ability to change reversibly its oxidation state (ferric (Fe^{3+}) ↔ ferrous (Fe^{2+})). This 'talent' enables this highly reactive transition metal to accomplish electron transfer through reversible redox reactions, but on the same time also forces the plant to keep Fe uptake and cellular Fe homeostasis tightly controlled. Whenever Fe occurs in its free ionic form, it can produce ROS such as superoxide ($O2^{\cdot-}$) or hydroxyl radicals ($OH^{\cdot}$) as illustrated in the following reactions (Marschner, 2012):

i) $O_2 + Fe^{2+} \rightarrow O_2^{\cdot-} + Fe^{3+}$

ii) $H_2O_2 + Fe^{2+} \rightarrow Fe^{3+} + OH^- + OH^{\cdot}$ (Fenton reaction)

iii) $O_2^{\cdot-} + H_2O_2 \xrightarrow{Fe} O_2 + OH^{\cdot} + OH^-$ (Haber-Weiss reaction)

Hydroxyl radicals can be very toxic as they can damage many cellular components. In particular DNA, proteins, lipids or sugars are endangered by these radicals. Hence a cell usually prevents Fe to exist in a free form and therefore Fe is rather tightly bound or incorporated in proteins. The Fe chelator nicotianamine (NA) for example functions in protecting plants from oxidative damage, since once complexed by NA, Fe becomes Fenton-inactive (von Wirén et al., 1999). In fact, NA is a versatile metabolite that can form complexes with both Fe(II) and Fe(III) at alkaline pH and is ubiquitous to all higher plants (Scholz et al., 1992). Excess amounts of Fe can also be 'secured' in a nonreactive form bound to ferritin, an 24-subunit plastidic Fe storage protein that has pivotal significance in protecting plants from oxidative stress (Ravet et al., 2009; Briat et al., 2010). Alternatively, Fe can be stored in the vacuole where it is linked to organic acids (Curie et al., 2009).

Proteins that contain Fe are distinguished depending on the form in which Fe is incorporated in the protein. There are proteins that bind Fe directly, as it is the case with ferritins (Hansch and Mendel, 2009). In other proteins Fe is integrated in their cofactors like heme or the Fe-S clusters (Hansch and Mendel, 2009). In heme structures, reduced Fe is bound by four nitrogen atoms of a porphyrin ring. The two remaining coordination bonds of Fe are available for interactions with

other molecules such as oxygen (O_2), nitric oxide (NO) or carbon monoxide (CO), which ultimately determine the functionality of hemeproteins. In principle, heme Fe can then serve as a source or sink of electrons. Proteins where hemes represent the prosthetic group are of crucial importance to plants (Paoli et al., 2002). Amongst them are leg-hemoglobins (oxygen binding and transport) or the cytochromes that are needed in redox systems in chloroplasts and mitochondria (photosynthetic and respiratory cytochromes for electron transfer). Heme-proteins also play a role in the production or scavenging of free radicals (antioxidative enzymes such as catalase, peroxidase and NADPH oxidase) or in the catalyzation of mono-oxygenation reactions (cytochrome P450 enzymes) (Hansch and Mendel, 2009). On the other hand, in Fe-S clusters, Fe is either incorporated to inorganic S or to the thiol group of cystein or a combination of both (Marschner, 2012). Most frequently occurring are Fe_2S_2, Fe_3S_4 or Fe_4S_4 clusters that are able e.g. to mediate electron transfer, represent substrate binding sites or shape the structure of proteins (Beinert et al., 1997; Hansch and Mendel, 2009). Due to their structural variety, proteins with Fe-S clusters can accomplish many functions for example as electron carriers (e.g. ferredoxin) or regulator proteins (e.g. aconitase) (Hansch and Mendel, 2009).

Irrespective of its function, Fe is more or less needed in all plant parts and thus must be rigorously distributed to reach various tissues and organelles. This path of Fe throughout the plant includes several chelation, oxidation/reduction and transport processes. Symplastic Fe is complexed by chelators like citrate or nicotianamine to maintain Fe in solution, thus facilitating its short- and long-distance transport (Kim and Guerinot, 2007) (see Table 1 for structures). Transporters mediating the transport of Fe, Fe-chelates or Fe-chelators are distributed all over the plant. Examples of such transporters are the *Arabidopsis* transporter FERRIC REDUCTASE DEFECTIVE 3 (FRD3) of the multidrug and toxin efflux (MATE) family which mediates citrate efflux into the xylem (Rogers and Guerinot, 2002; Durrett et al., 2007) or several members of the YELLOW STRIPE-LIKE (YSL) transporter family that are involved in Fe-NA transport throughout the plant (Curie et al., 2009). Ferric iron is transported by vacuolar membrane-based Arabidopsis transporters that are members of the NRAMP (NATURAL RESISTANCE ASSOCIATED MACROPHAGE PROTEIN) family of metal transporters (Lanquar et al., 2005), the VACUOLAR IRON TRANSPORTER 1

(VIT1) that is required for vacuolar Fe uptake (Kim et al., 2006) or the plasma membrane-located A*rabidopsis* IRON REGULATED 1/Ferroportin1 (IREG1/FPN1) protein, which possibly mediates vascular Fe loading (Morrissey et al., 2009).

2.1.2 Fe in the soil – occurrence and availability

Besides representing the major constituent of the Earth's inner core (Alfè et al., 2002), Fe is also highly abundant in its crust, being the most abundant metal after aluminum (Marschner, 2012). In soils, the total Fe content varies between 0.2 and 5% (Scheffer and Schachtschabel, 2002) and ferric oxids like hematite (α-Fe_2O_3) and goethite (α-FeOOH) are the prevailing forms of Fe(III)-bearing minerals (Chen and Barak, 1982). It is generally acknowledged that mineral soils contain total Fe concentrations ranging from 20 to 40 g kg^{-1}, whereof crops remove approximately 1 to 2 kg Fe ha^{-1} annually (Marschner, 2012). The Fe pools present in the soil are divided mainly into: (1) the ionic and complexed form in solution, (2) the part that is specifically adsorbed onto mineral or organic surfaces, (3) the part of live or dead soil biomass and (4) the fraction of insoluble inorganic precipitates. Ultimately, these different forms of Fe are crucial for the availability of this element to plants (Varanini and Pinton, 2007; Frossard et al., 2000). In general, organically bound Fe is supposed to be more accessible to plants than the inorganic insoluble ones (Varanini and Pinton, 2007; Frossard et al., 2000).

The problem that plants generally face when acquiring Fe from the soil is clearly not related to its quantity but rather to the availability of Fe in conditions that allow plant growth (Guerinot and Yi, 1994). Usually, free ionic Fe in the aqueous soil solution is the preferential form for Fe uptake by plants, but its appearance depends on the release of Fe from the solid phase of the soil. This process in turn depends on soil pH, redox conditions, cation exchange capacity, the activity of microorganisms, organic matter content and soil structure and water content (Frossard et al., 2000). Fe solubility and dissolution rates are low in high pH, calcareous soils (Lucena, 2007). In fact, in agricultural soils the pH values can vary strongly (Frossard et al., 2000) and the significance of the pH for the Fe nutrition of plants is enormous. A pH drop of one unit can boost Fe solubility up to 1000 fold (Hansen et al., 2007). If the pH of the soil solution decreases

dramatically, ferric Fe concentrations can increase up to 10^{-9} M (see reaction i; Buchanan et al., 2000).

i) $Fe(OH)_3 + 3H^+ \leftrightarrow Fe^{3+} + 3\ H_2O$

In well-aerated soils, Fe precipitates with phosphates or hydroxide ions already at slightly acidic to alkaline pH levels (Lemanceau et al., 2009; Marschner, 2012). In general, the oxidation of Fe^{2+} to Fe^{3+} makes Fe relatively insoluble, thus Fe solubility strongly depends on the soil redox potential. Under aerobic conditions, Fe^{2+} is oxidized thus rendering mostly Fe^{3+}. However, ionic Fe concentration in the soil solution is about 10^{-15} M and thus quite low (Kim and Guerinot, 2007) and those of inorganic Fe species like $Fe(OH)_2^+$, $Fe(OH)_3$ and $Fe(OH)_4^-$ is 10^{-10} M or even lower (Marschner, 2012), thus not meeting a plant's requirement. Yet in the soil solution, Fe is often chelated by soluble organic ligands such as bacterial or fungal siderophores (see section 2.1.3) or humic substances, thus keeping Fe in solution and available to plants (Buchanan et al., 2000; Varanini and Pinton, 2007). Fe-humate complexes, for example, are able to move Fe towards plant roots presenting an available Fe source for all plant species (Varanini and Pinton, 2007).

The presence of calcium carbonate ($CaCO_3$) and/or bicarbonate (HCO_3^-) are additional factors that influence Fe solubility in the soil, as they influence soil pH by pH buffering according to the reactions (Zuo et al., 2007):

ii) $CaCO_3 + H_2O + CO_2 \leftrightarrow Ca^{2+} + 2HCO_3^-$

iii) $HCO_3^- + H^+ \leftrightarrow H_2O + CO_2$

Increasing amounts of hydrogen ions (low soil pH) are generally favored in conditions of decomposed organic matter and intensive rainfall as plenty of carbon dioxide (CO_2) is produced and soil water concentrations are increased (reaction iii) (Zuo et al., 2007). The influence of this bicarbonate buffer system on the expression of Fe deficiency symptoms in plants strongly depends on the plant species and the utilized Fe acquisition strategy.

2.1.3 Fe chelation and Fe chelators

In conditions of low Fe availability, various microbes and some plants species (see section 2.2.1 for plant siderophores) have the ability to produce and release siderophores in order to increase Fe solubility in the rhizosphere (Terano et al., 2002; Stintzi et al., 2000; Leong and Neilands, 1976). The rhizosphere is defined as the root surrounding soil that is influenced by root activity (Hinsinger, 1998). Such siderophores, Greek for Fe carriers, are low-molecular-weight compounds (< 2000 daltons) with a very high affinity for Fe and are able to form water soluble complexes with Fe^{3+} (Hider and Kong, 2010). Once complexed by a siderophore, the Fe ion becomes more stable and is 'protected' from precipitation. If all six valencies of Fe are connected, Fe is 'secured' and is prevented from interacting any further. In siderophores, Fe(II) and Fe(III) can be coordinated by six ligands forming an octahedral geometry. Frequent donor atoms (ligands) for Fe coordination are negatively charged oxygen atoms which possess very high affinity for Fe(III). Nitrogen or sulfur atoms are also present in various siderophores (Hider and Kong, 2010). Siderophore ligands are very diverse, but bidentate ligands like hydroxamates, catechols or α–hydroxycarboxylates predominate (Leong and Neilands, 1976) (see Table 1 for structure). In general, the redox potential of Fe-siderophore complexes is highly negative, with values below -300 mV (Hider and Kong, 2010). This feature leaves Fe(III)-complexes rather 'redox-immobile' and largely prevents the formation of hydroxyl radicals in aerobic conditions (Hider and Kong, 2010) (see section 2.1.1). Moreover, Fe(III) complexes are thought to be more stable than Fe(II) complexes. Therefore, in order to release Fe from such a complex, the complexed Fe(III) is often reduced to yield a less stable Fe(II) complex (Hider and Kong, 2010).

Examples of microbial siderophores are ferrichromes, which are produced by fungi or bacterial enterobactin, that forms extraordinary stable complexes with Fe(III). Further examples are pyoverdine and ferrioxamines, both also being synthesized by bacteria (Marschner et al., 2011) (see Table 1 for structure). The benefit of bacterial siderophores in supporting plant Fe nutrition has been described. Radzki et al. (2013) showed that chlorophyll and Fe content of Fe-starved tomato plants increased after treatments with siderophores from the bacterial strain *Chryseobacterium* spp. C138. There are also many examples of synthetic Fe

chelators, which are frequently used for Fe fertilization in agricultural plant production. EDTA (ethylenediaminetetraacetic acid), HEDTA (N-(2-hydroxyethyl)-ethylenediaminetriacetic acid) and EDDHA (ethylenediamine-N,N'-bis(2-hydroxyphenylacetic acid)) (see Table 1 for structure) are amongst the most widespread examples. EDDHA is a particularly outstanding Fe chelator since it forms stable chelates with Fe(III) over a pH range from 4 to 10. In contrast, complexes where Fe is chelated by EDTA or HEDTA become unstable at pH > 6, thus these chelators are more suitable for acid soils or for foliar application. In plant nutrition, chelators, either of microbial or commercial origin, basically function as 'Fe shuttles' as they help plants to access spatially and chemically unavailable soil Fe by 'transporting' it to the root surface. Once Fe is dissociated from the complex, some chelators remain in the soil and can be used repeatedly.

Table 1. Structure of Fe ligands with their major functional groups.

Type	Structure	Name	Reference
Siderophore ligands	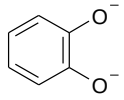	Catecholate	(Hider and Kong, 2010)
	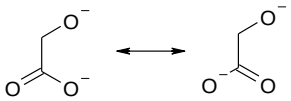	α–hydroxycarboxylates	(Hider and Kong, 2010)
	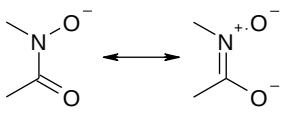	Hydroxamates	(Hider and Kong, 2010)
Synthetic chelators	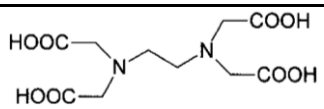	Ethylenediaminetetra acetic acid (EDTA)	(von Wirén et al., 2000)
	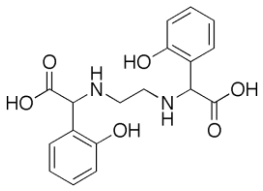	Ethylenediamine-N,N'-bis(2-hydroxyphenylacetic acid) (EDDHA)	(García-Marco et al., 2006)
	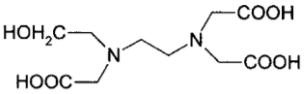	N-(2-hydroxyethyl)-ethylenediaminetriac etic acid (HEDTA)	(von Wirén et al., 2000)

Continuation of Table 1: Structure of Fe ligands with their major functional groups.

Organic acid	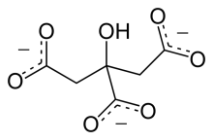	Citrate	(Silva et al., 2009)
Plant chelators	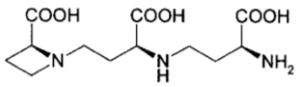	Nicotianamine	(von Wirén et al., 2000)
Phytosiderophores	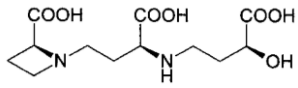	Deoxymugineic acid	(von Wirén et al., 2000)
	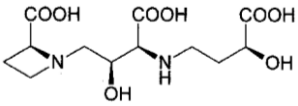	Mugineic acid	(von Wirén et al., 2000)
Microbial siderophores	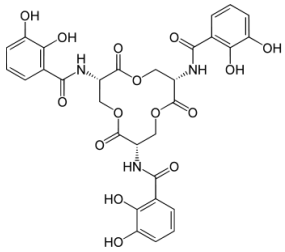	Enterobactin	(Neilands, 1981)
	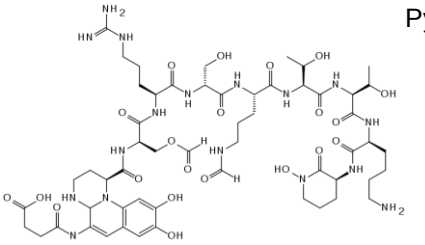	Pyoverdine	(Wendenbaum et al., 1983)
	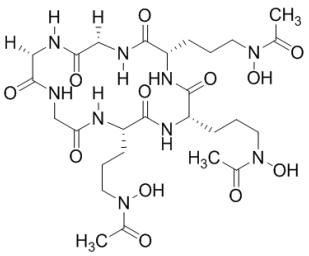	Ferrichrome	(Neilands, 1981)

2.2 Acquisition of Fe by plants – physiological and molecular mechanisms

Plants as sessile organisms cannot migrate to a given source of nutrients when the abundance or availability of nutrients in the rhizosphere becomes scarce.

Thus, plants rely on their ability to mobilize the nutrients they need. Nutrient acquisition by plants is commonly defined as the combined action of nutrient mobilization in the rhizosphere and their subsequent uptake or transfer into the root (Hinsinger, 1998). This is of particular importance for Fe, as this element is not sufficiently available in the aqueous soil solution and thus requires special mechanisms to increase its availability for plants (see section 2.1.2) (Marschner, 2012). Hence, to overcome the problem of low Fe bioavailability a mere increase in Fe uptake-related processes is not sufficient. To overcome this problem, plants have developed strategies that combine the mobilization of Fe from sometimes hardly available soil reserves and their subsequent uptake (Hider and Kong, 2010; Kobayashi and Nishizawa, 2012). Depending on the plant species, two different strategies (Strategy I and II; Römheld and Marschner, 1986) have evolved. Both are described in more detail in the following sections.

2.2.1 Chelation-based Fe acquisition (Strategy II)

Almost 40 years ago, it was demonstrated in rice and oat plants that roots release Fe-chelating compounds, especially in response to Fe deficiency (Takagi, 1976). Nowadays it is well established that graminaceous plants such as barley, maize and wheat employ a Fe acquisition strategy that relies on the release of mugineic acid-type (MA), hexadentate chelators, so-called phytosiderophores (PS) (Takagi et al., 1984; Nozoye et al., 2011). The release of phytosiderophores is mediated by the major facilitator superfamily (MFS) TRANSPORTER OF MUGINEIC ACID 1 (TOM1) in rice and by HvTOM1 in barley, whose expression in roots is increased upon Fe deficiency (Nozoye et al., 2011). Once in the rhizosphere, these organic compounds form complexes that bind ferric Fe with their amino and carboxyl groups. They then diffuse back to the roots and are taken up as an intact Fe(III)-phytosiderophore complex via the plasma membrane-bound transporter YSL (YELLOW STRIPE1-LIKE) without the requirement of a reduction step (Curie et al., 2001; Schaaf et al., 2004). *Zm*YS1 and *Hv*YS1 are high-affinity Fe(III)-MA transporter identified in maize and barley, respectively (Curie et al., 2001; Murata et al., 2006) (Figure 1).

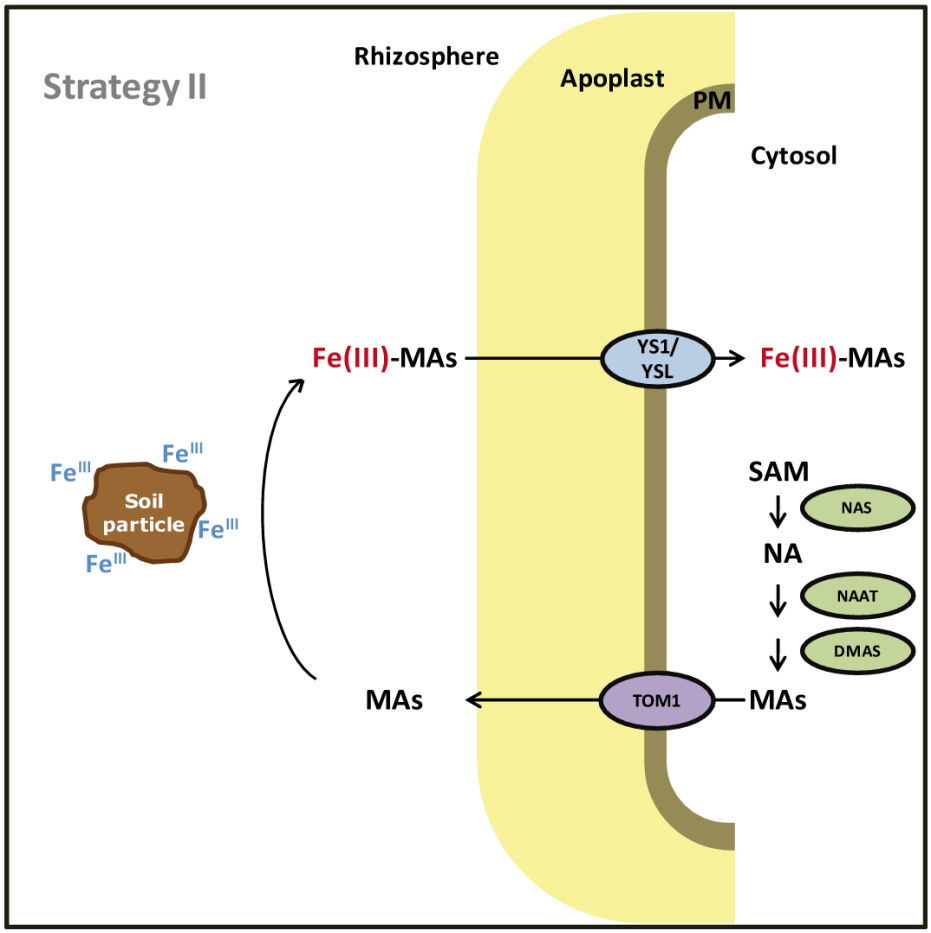

Figure 1. Chelation-based Fe acquisition (Strategy II) in graminaceous plants. Abbreviations: YS1/YSL, YELLOW STRIPE 1/YELLOW STRIPE 1-LIKE; TOM1, transporter of mugineic acid; SAM, S-adenosyl-L-methionine; NA, nicotianamine; MA, phytosiderophores of the mugineic acid family; NAS, nicotianamine synthase; NAAT, nicotianamine aminotransferase; DMAS, deoxymugineic acid synthase; PM, plasma membrane. Illustration according to Kobayashi and Nishizawa (2012).

The growth and yield of most graminaceous plants is not strongly impaired when these plants are cultivated in calcareous or alkaline soils, since the biosynthesis, the release and the chelating ability of mugineic acids is largely insensitive to high soil pH (Römheld and Marschner, 1986). Mugineic acids are non-proteinogenic amino acids and commonly contain six functional groups that coordinate ferric Fe (Ma and Nomoto, 1996). They are synthesized from S-adenosyl-L-methionine (SAM) via nicotianamine (NA) and 2'-deoxymugineic acid (DMA). The consecutive enzymatic reactions for this synthesis are mediated by the enzymes nicotianamine synthase (NAS), nicotianamine aminotransferase (NAAT) and deoxymugineic acid synthase (DMAS) (Bashir et al., 2006) (Figure 1). While nicotianamine is common to all plant species, the conversion of nicotianamine to mugineic acid-type

phytosiderophores is restricted to graminaceous species (Kobayashi and Nishizawa, 2012). DMA represents the first active phytosiderophore and represents the precursor for the synthesis of other MAs, such as 3-hydroxymugineic acid (HMA), 3-epihydroxymugineic acid (epi-HMA) or avenic acid A (Ma et al., 1999; Kobayashi et al., 2001). When plants experience Fe deficiency, the synthesis of MAs is increased (Ma et al., 1995) and the extent of MA synthesis and secretion largely defines the tolerance of a species towards conditions of low Fe availability. Barley and wheat, for example, release much more phytosiderophores when exposed to Fe deficiency than maize or sorghum and consequently their tolerance to high pH-induced chlorosis is much higher (Hinsinger, 1998).

In rice, phytosiderophore-mediated Fe acquisition is regulated by the bHLH transcription factor *OsIRO2* (Ogo et al., 2006; Hindt and Guerinot, 2012). Under Fe deficiency *OsIRO2* is up-regulated and in experiments where this transcription factor was overexpressed, increased expression of genes involved in phytosiderophore synthesis and transport was observed (Ogo et al., 2006; Hindt and Guerinot, 2012). Other positive regulators of the Fe-deficiency response are OsIDEF1 and 2 (iron deficiency-responsive element 1 and 2 (IDE1 and 2) - binding factor 1 and 2), that belong to the plant-specific transcription factor family ABI3/VP1 (ABSCISIC ACID INSENSITIVE 3/VIVIPAROUS 1) and NAC (NO APICAL MERISTEM, *Arabidopsis* transcription factor, and CUP-SHAPED COTYLEDON) (Hindt and Guerinot, 2012; Kobayashi and Nishizawa, 2012). Both *OsIDEF1* and 2 regulate Fe deficiency-inducible genes, but they regulate predominantly distinctive functions (Kobayashi and Nishizawa, 2012). OsIDEF1 acts upstream of *OsIRO2* and its transcript levels are independent of the plant's Fe status (Kobayashi et al., 2007). Interestingly, a constitutive *OsIDEF1* expression in rice plants increases the tolerance of these plants towards Fe deficiency (Kobayashi et al., 2007).

2.2.2 Reduction-based Fe acquisition (Strategy I)

All dicots, including *Arabidopsis thaliana*, and non-graminaceous monocots employ a so-called reduction-based strategy (Strategy I) to acquire Fe from the

soil (Kim and Guerinot, 2007; Kobayashi and Nishizawa, 2012). This three-step mechanism requires the interplay of several proteins localized in the root epidermis. Fe acquisition in Strategy I plants includes an enhanced release of protons into the rhizosphere, a process that is mainly related to Fe deficiency-induced H^+-ATPases (proton-translocating adenosine triphosphatases), like *AHA2* in Arabidopsis (Santi and Schmidt, 2009). The released protons decrease the pH of the rhizosphere and thereby facilitate the dissolution of Fe(III) precipitates. Furthermore the release of phenolics and flavins also has been associated with facilitating Fe mobilization (Lucena et al., 2007). Fe(III) then mainly occurs in a chelated form and must reach the proximity of the root plasma membrane, where ferric Fe is then reduced to ferrous Fe by the plasma membrane-bound FERRIC CHELATE REDUCTASE2 (FRO2) (Robinson et al., 1999; Connolly et al., 2003). This reduction step is a prerequisite for the subsequent transport of Fe^{2+} across the plasma membrane via the IRON-REGULATED TRANSPORTER1 (IRT1) (Eide et al., 1996; Varotto et al., 2002; Vert et al., 2002) (Figure 2).

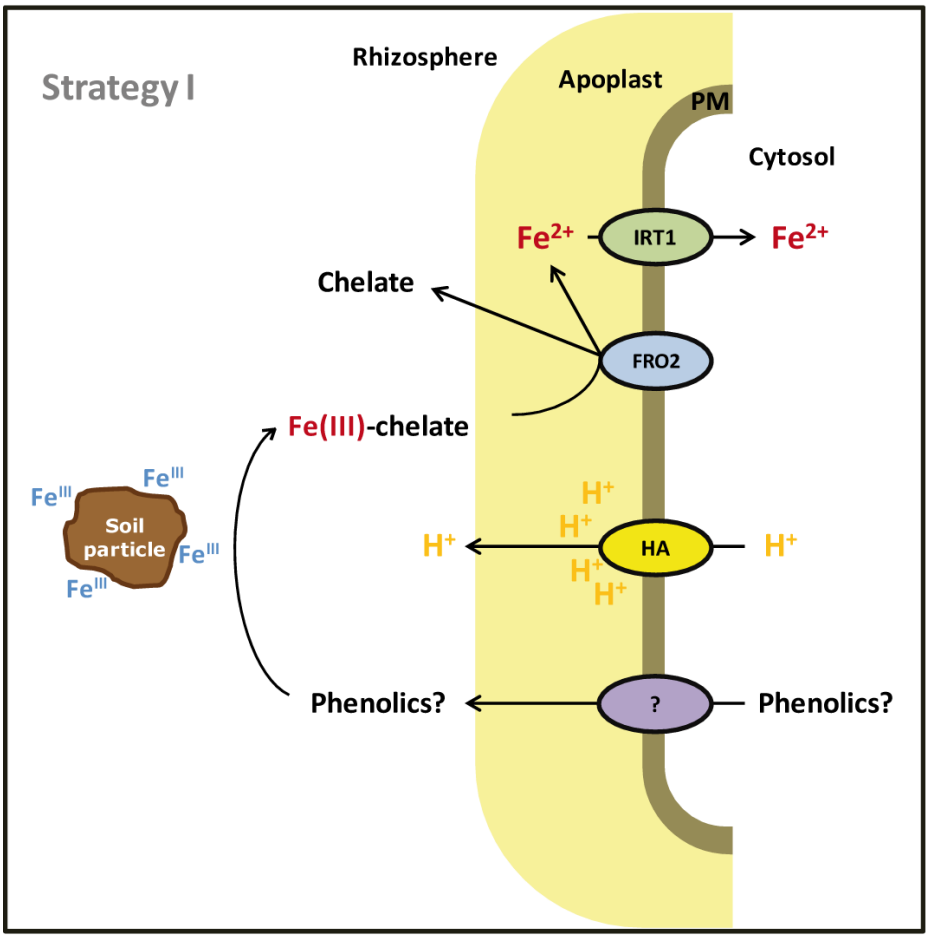

Figure 2. Reduction-based Fe acquisition (Strategy I) in non-graminaceous plants. Abbreviations: IRT1, iron-regulated transporter; FRO2, ferric-chelate reductase oxidase; HA, H^+-ATPase; PM, plasma membrane. Illustration according to Kobayashi and Nishizawa (2012).

At the transcriptional level the individual components of the Strategy I are regulated by the cooperative action of the basic helix-loop-helix (bHLH) transcription factors FIT (FER-LIKE IRON DEFICIENCY-INDUCED TRANSCRIPTION FACTOR) and bHLH38 and bHLH39 (Colangelo and Guerinot, 2004; Jakoby et al., 2004; Yuan et al., 2008). The highly coordinated transcriptional regulation of the Fe acquisition machinery allows plants enhancing Fe intake when Fe is limited or when the plant's demand for Fe has increased (Giehl et al., 2009). Similar to *FRO2* and *IRT1*, *FIT* expression is enhanced in outer root cells in conditions of Fe deficiency (Colangelo and Guerinot, 2004). In a microarray analysis, FIT was identified as the closest homolog to the *FER* gene from tomato which is also induced by Fe deficiency (Colangelo and Guerinot, 2004). Proteins of this superfamily can form homo- or heterodimers and contain a conserved bHLH domain comprising of ~18 hydrophilic and basic amino acids that

enables DNA binding (Colangelo and Guerinot, 2004). FIT seems to be regulated by Fe deficiency in two ways. On the one hand, *FIT* transcript and protein levels both accumulate in conditions of Fe deficiency (Meiser et al., 2011). On the other hand, to finally initiate FIT activity, an Fe deficiency signal is required. Sivitz et al. (2011) has proposed that the FIT protein level is post-transcriptionally regulated through proteasome-mediated degradation that is regulated by nitric oxide and ethylene (Meiser et al., 2011). This mechanism continuously ensures a rapid turnover of 'freshly synthesized' FIT protein, thus enabling quick responses to changes in the cellular Fe status (Meiser et al., 2011). Furthermore, Fe deficiency responses are linked with the ethylene pathway (Lingam et al., 2011). A yeast two-hybrid screening revealed that FIT can interact with two transcription factors of the ethylene pathway, namely ETHYLENE INSENSITIVE 3 (EIN3) and ETHYLENE INSENSITIVE 3-LIKE1 (EIL1), thereby most likely preventing FIT from degradation. This in turn leads to increased FIT abundance and thus enhanced expression of Fe acquisition genes (Lingam et al., 2011). Besides bHLH38 and bHLH39, two other members, of the Ib subgroup of the bHLH gene family in Arabidopsis, AtbHLH100 and AtbHLH101, have also been shown to interact with FIT and to induce *FRO2* and *IRT1* promotor-driven expression in yeast cells (Wang et al., 2013). Since triple knock-out mutants of *AtbHLH38* or *AtbHLH39* with *AtbHLH100* and *AtbHLH101* led to Fe deficiency-induced chlorosis, *AtbHLH100* and *AtbHLH101* also appear to play a role in the regulation of Fe-deficiency responses (Wang et al., 2013).

Arabidopsis is an eligible model plant for the study of Fe acquisition mechanisms in non-graminaceous plants. Genes encoding FRO2 and IRT1 for example, were initially characterized in Arabidopsis before they were identified in other dicot species (Eckhardt et al., 2001; Cohen et al., 2004; Li et al., 2004). Besides *FRO2*, there are seven other members of the ferric chelate reductase (FRO) gene family in Arabidopsis. They are expressed in different tissues and membranes throughout the plant and respond differently to conditions of Fe deficiency (Mukherjee et al., 2006). Proteins of the FRO gene family belong to the flavocytochrome superfamily, which possess binding sites for FAD and NADPH and hence are capable of transporting electrons across membranes to reduce ferric chelates (Robinson et al., 1999; Mukherjee et al., 2006). FRO2 is predominantly expressed upon Fe deficiency in the outer root cell layers (Connolly et al., 2003; Mukherjee et

al., 2006). In an attempt to achieve increased Fe accumulation in plants, Connolly et al. (2003) generated transgenic plants overexpressing *FRO2*, as Fe^{3+} reduction is often suggested to be a rate-limiting step in Fe uptake. However, even though increased *FRO2* expression led to an enhanced tolerance to low Fe conditions, it turned out that *FRO2* overexpression could only increase ferric-chelate reductase activity under Fe deficiency, implying a post-transcriptional regulation of FRO2 by Fe itself or by the plant's Fe nutritional status.

Because of the strong chlorotic phenotype that develops in plants defective in *IRT1* expression (Henriques et al., 2002; Varotto et al., 2002; Vert et al., 2002), it is very likely that this high-affinity Fe transporter represents the main entry route of Fe into roots. IRT1 was first identified through functional expression in yeast, as it successfully restored growth of the Fe deficiency-sensitive *Saccharomyces cerevisiae* yeast strain *fet3fet4* (Eide et al., 1996). This transporter is a member of the zinc-regulated transporter ZRT/IRT-like protein (ZIP) family and besides Fe(II) also mediates uptake of other divalent metals like zinc (Zn(II)), manganese (Mn(II)), cadmium (Cd(II)), and cobalt (Co(II)) (Eide et al., 1996; Korshunova et al., 1999). ZIP proteins have been described to have eight putative transmembrane domains, with their N- and C-terminal ends located outside of the plasma membrane. By performing heterologous expression studies in yeast, Rogers et al. (2000) demonstrated that substrate specificity of IRT1 can be altered through mutations in amino acid residues that are involved in metal recognition and transport. Such modifications might be potentially valuable in preventing the accumulation of 'unwanted' metals especially in Fe-deficient plants (Rogers et al., 2000), where the FIT-dependent transcriptional expression of *IRT1* is strongly induced in the outer cell layers of roots (Vert et al., 2003; Colangelo and Guerinot, 2004). IRT1 levels in plants are rigorously regulated to ensure optimal metal uptake. Barberon et al. (2011) could show that the abundance of IRT1 is post-translationally controlled via monoubiquitin-dependent endocytosis that is not regulated by the plant Fe status. In fact, IRT1 continuously cycles between the plasma membrane and the trans-Golgi network/early endosomes or is degraded in the vacuole when IRT1 protein abundance needs to be adjusted. This trafficking of IRT1 is controlled through monoubiquitination on several cytosol-exposed lysine residues. Overexpression of IRT1 led to increased protein abundance but did not result in an increased level of plasma membrane-located IRT1 (Barberon et al.,

2011). By screening E3 ubiquitin ligase mutants for altered IRT1 degradation, Shin et al. (2013) identified IRT1 DEGRADATION FACTOR1 (IDF1). Loss of this gene not only led to altered degradation of IRT1 and the loss of IRT1-ubiquitin complexes but also increased tolerance to Fe deficiency. IDF1 directly interacts with IRT1 and in absence of the IDF1 RING-type E3 ligase activity, IRT1 levels increase, implying that IDF1 is directly needed for IRT1 degradation.

In high pH environments, rhizosphere acidification becomes crucial for Strategy I-type Fe acquisition. AHA2 is one of twelve H^+-ATPases in Arabidopsis (Palmgren, 2001) and is largely involved in this process. H^+-ATPases are plasma membrane-located proton pumps that depend on the hydrolysis of ATP. They decrease apoplastic pH since they extrude protons that accumulate extracytoplasmically (Palmgren, 2001). This acidification of the rhizosphere then contributes to weaken Fe-O bonds through protonation (Schwertmann, 1991) and thus increases Fe solubility. Furthermore, it ensures proper function of Fe(III) chelate reductase by providing an environment that hinders the rejection of negatively charged Fe chelates from the cell wall (Schmidt, 2006; Santi and Schmidt, 2009). Similar to *IRT1* and *FRO2*, *AHA2* up-regulation in response to Fe deficiency depends on FIT but seems not to be co-regulated with *IRT1* and *FRO2* (Ivanov et al., 2012). Furthermore, the chronology of the three main steps of Strategy I Fe acquisition is not yet clearly understood. Whilst FRO2 and IRT1 activity are basic requirements for Fe uptake, it is often speculated that proton extrusion rather fulfills a supportive task (Santi and Schmidt, 2009). Compared to the increased activity of the Fe(II) chelate reductase upon Fe deficiency, the process of rhizosphere acidification is not ubiquitous to all Strategy I species (Schmidt, 2006) and is rather low in Arabidopsis roots (Santi and Schmidt, 2009). *AHA2* is expressed in shoots and roots mainly in the vascular tissue, but also in cortical and epidermal cells (Fuglsang et al., 2007). Under Fe deficiency its expression is increased (Colangelo and Guerinot, 2004), but interestingly, this increase is prevented in conditions of a pH > 7.5 (Santi and Schmidt, 2009). In the same study it was found that *FIT*, *FRO2* and *IRT1* transcript abundance was also less increased by Fe deficiency at high pH. In the case of *FRO2* and *IRT1*, high pH led to an increased expression also in conditions of Fe sufficiency. These observations clearly emphasize the pH-dependency of Strategy I-type Fe acquisition.

2.2.3 Fe mobilization of Strategy I plants

To date, it still remains unknown how non-graminaceous plants access ferric Fe in the rhizosphere and overcome the problem of low Fe solubility and impeded Fe reducibility in high pH soils. One assumption is that Strategy I plants induce additional mechanisms to assist and/or complement the reduction-based Fe acquisition machinery. In this regard, it has been shown that Fe deficiency also stimulates the exudation of organic compounds, such as phenolics, organic acids, sugars and flavins (Römheld and Marschner, 1983; Welkie, 2000; Jin et al., 2007; Rodriguez-Celma et al., 2011). These compounds usually represent the majority of released metabolites of Fe-deficient plants (Tato et al., 2013; Jin et al., 2008) and some of them could help plants to mobilize sparingly available Fe from the rhizosphere soil or from the root apoplast. In fact, intermediates of the tricarboxylic acid cycle such as citrate or malate have been reported to occur in root exudates (Jones, 1998; Ma et al., 2001; Zhang et al., 1997). Besides representing a rhizospheric carbon source that also acts as chemoattractant for microbes, organic acids are thought to acidify the soil and chelate sparingly available nutrients like Fe (Dakora and Phillips, 2002). Nevertheless their effectiveness or significance in Fe chelation is contested since organic acids are relatively easy adsorbed by the soil surface or degraded by microorganisms (Uren, 2007). Furthermore, Fe complex formation and stability with these organic acids sharply decreases with increasing pH (Jones, 1998; Neumann and Römheld, 2007). Thus, in alkaline soils the release of organic acids might have a rather supportive character in assisting the overall amount of solubilized Fe and to favor Fe chelation by more efficient chelators (Reichard et al., 2007). In the case of phenolics, studies by Jin et al. (2007) indicated that this class of compounds may take over a direct role in the solubilization and utilization of apoplastic Fe. For instance, when phenolic compounds released by roots of red clover were removed from the nutrient solution by a synthetic adsorbent, plants developed symptoms of Fe deficiency and an increased accumulation of Fe in the root apoplast of Fe-deficient plants was observed (Jin et al., 2007). Likewise, the re-utilization of Fe that is precipitated in the stele of rice roots involves the efflux of the phenols protocatechuic acid and caffeic acid via the MATE (MULTIDRUG AND TOXIN EXTRUSION) transporter PEZ1 (PHENOLICS EFFLUX ZERO1) (Ishimaru et al., 2011a).

Phenolics are aromatic compounds possessing one or more hydroxyl groups and are mainly synthesized by the phenylpropanoid pathway using aromatic amino acids (phenylalanine, tyrosine, tryptophan) as precursors (Frossard et al., 2000). The cytosol-based synthesis of phenylpropanoids can be adjusted quickly in response to unfavorable conditions such as wounding, pathogen infection, oxidative stress, UV-irradiation or nutrient deficiencies (Tato et al., 2013; Cesco et al., 2010). Interestingly, many enzymes of this pathway are Fe regulated, as revealed by iTRAQ (Isobaric Tag for Relative and Absolute Quantification) differential liquid chromatography-tandem mass spectrometry (Lan et al., 2011). *In vitro* studies have shown that phenolic compounds can chelate and reduce Fe(III) (Andjelkovic et al., 2006; Mladenka et al., 2010). However, it is noteworthy that the overall reducing capacity of the phenolics released by Fe-deficient roots is many orders of magnitude below that of the ferric chelate reductase (Römheld and Marschner, 1983). Thus, the chemical action and precise nutritional function of the phenolic compounds released by Fe-deficient plants still remains unknown.

Over the last decades, the search for molecular players involved in Fe homeostasis has been based on various screening approaches with Arabidopsis, a relatively 'Fe-efficient' plant. For example, FRO2 (*frd1-1* mutation), the main ferric chelate reductase, was discovered by screening a population of ethyl methanesulfonate (EMS)-mutagenized and transfer-DNA (T-DNA)-tagged lines for alterations in Fe deficiency-induced Fe(III) chelate reduction (Yi and Guerinot, 1996; Robinson et al., 1999). Furthermore, Roschzttardtz et al. (2011) performed a genetic screen for regulatory elements of Fe uptake by screening EMS-mutagenized *proIRT1*:LUC lines. Such very successful screening approaches had in common that they were based on the identification of phenotypes that required either the complete absence or presence of fully available Fe. Therefore, these approaches are potentially neglecting components and plant genes that might be involved in facilitating Fe-acquisition or -utilization efficiency in conditions where Fe is only sparingly available. In terms of Fe acquisition, detection of impaired Fe uptake or suppressed root morphological, physiological or biochemical responses might require the presence of Fe in order to be detectable by an inferior performance of any given mutant in comparison to wild-type plants. Thus, future attempts in identifying novel molecular players involved in these processes may

profit from screening approaches based on low Fe availability, rather than complete absence of Fe.

2.3 Aim of the study

The ability of non-graminaceous plants to acquire Fe is strongly reduced in calcareous alkaline soils. Under these conditions, protons released to increase Fe solubility are buffered and the activity of the plasma membrane-bound ferric chelate reductase is suppressed. Nevertheless, Strategy I plants growing under these conditions are able to access ferric Fe in the rhizosphere and must thus, at least in part, be capable of overcoming low soil Fe availability. Therefore, it was hypothesized that so far unidentified components are involved in Fe acquisition by Strategy I plants. Consequently, the aim of the present study was to identify molecular components that mediate Fe acquisition under alkaline soil conditions. To accomplish this goal, a screening approach was designed that allows the identification of genes involved in plant tolerance to Fe deficiency-mediated chlorosis. In this forward genetic approach, a collection of homozygous T-DNA insertion mutants of Arabidopsis was chosen to serve as gene pool. This approach had the advantage that the identity of the deleted genes in these lines was easy to access and thus would allow an immediate start with the characterization of a gene, once a promising phenotype is discovered.

The main part of the thesis is devoted to the characterization of two T-DNA insertion lines and their affected gene functions. Initially, this required the verification of the dependence of the observed phenotype on Fe deficiency and included studies on Fe deficiency-regulated gene expression.

The successful phenotype verification was then followed by a more detailed investigation of the second identified T-DNA insertion line. Firstly, the tissue-specific gene localization was studied in conditions of Fe deficiency. Since previously a role in secondary metabolism had been assigned to this gene, biochemical analyses were carried out to study the synthesis and secretion of several secondary metabolites in mutant and wild-type plants in response to Fe deficiency. Further studies were performed to elucidate the chemical action of the

secreted metabolites and their involvement in individual steps of Strategy I-type Fe acquisition.

Finally, the thesis closes with a discussion on the significance and the role of the two identified genes in the process of Fe acquisition and integrates the findings of this study into a comprehensive model. Furthermore, suggestions are made regarding the elucidation of remaining gaps in Fe acquisition under conditions of low Fe availability.

3 Materials and Methods

3.1 Plant materials

In the present study, the *Arabidopsis thaliana* accession line Columbia-0 (Col-0) was used as wild type. The following T-DNA insertion and mutant lines in the Col-0 genetic background were used: *f6'h1-1* (At3g13610; SALK_132418C), *f6'h1-2* (At3g13610; SALK_050137C), *fit* (*fit-3* allele (Jakoby et al., 2004)), *frd3-3* (Delhaize, 1996), *myb72-1* (At1g56160; SAIL_713_G10 Syngenta), *myb72-2* (At1g56160 MYB72; SALK_052993), *35S:MYB72* (Van der Ent et al., 2008) - the latter two lines kindly provided by Prof. Dr. Corné M.J. Pieterse, *irt1* (Varotto et al., 2002) and *35S:FIT* (Jakoby et al., 2004). In addition, the *frd1-1* (*fro2*) mutant (Yi and Guerinot, 1996) and its respective wild-type (colgl1-1) kindly provided by Prof. Dr. Ute Krämer were also used in this study.

3.2 Growth conditions on substrate and mutant screening

In order to screen for mutants with reduced ability to acquire Fe from soils with high pH, 3500 homozygous T-DNA insertion lines (SALK Institute, Alonso et al., 2003) were grown on peat-based substrate ('Klasmann Substrat 1'). The pH of the substrate was either maintained at pH 5.6 or increased to pH 7.2 by the supplementation of 20 g kg^{-1} calcium carbonate ($CaCO_3$) and 12 g kg^{-1} sodium bicarbonate ($NaHCO_3$). Plants were cultivated in 54 pot trays and in each pot 3 to 5 plants were allowed to grow. In three pots of the tray wild-type (Col-0) and *frd3-3* mutant plants, which show chlorosis even under ample Fe availability (Durrett et al., 2007), respectively were included. Each insertion mutant was grown on one pot on non-limed substrate at pH 5.6 and on two positions on limed substrate as described above at pH 7.2. The trays were placed inside a conditioned growth chamber with a 22°C/18°C and 9/15-h light/dark regime at a light intensity of 120-150 µmol photons m^{-2} s^{-1}. The screen consisted of visually assessing the appearance and intensity of Fe deficiency symptoms (e.g. chlorosis in young leaves) in insertion lines grown at pH 7.2 as compared to both the same insertion line grown on pH 5.6 or wild-type and *frd3-3* mutant plants grown on pH 7.2.

Experiments in growth substrate were carried out as described above for 13 days. Depending on the experiment, 2.0 mL of a 0.5 g L^{-1} Fe-sequestrene (6% Fe(III)-

EDDHA, Syngenta), or 29 mM esculin (Roth) or 34 mM esculetin (Roth) solution were supplied three times usually during 4 days to assess whether these compounds could alleviate Fe deficiency symptoms of plants.

3.3 Growth conditions on agar plates

In experiments with agar plates, seeds were surface sterilized with a solution containing 70% (v/v) ethanol and 0.05% (v/v) Triton X-100. Seeds were then sown on sterile plates containing half-strength (½) MS medium (Murashige and Skoog, 1962) (Duchefa Biochemie B.V.) with 40 or 75 µM Fe-EDTA (Fluka Analytical), supplemented with 0.5% sucrose, 2.5 mM MES (pH 5.6 or pH 7.2, adjusted with KOH) and 1% (w/v) Difco agar (Becton Dickinson). The plates were incubated at 4°C for 2 days to synchronize seed germination. Afterwards, the agar plates were kept in a vertical position inside growth cabinets under a 22°C/18°C and 10/14-h light/dark regime and light intensity adjusted to 120 µmol photons m^{-2} s^{-1}.

After 10 days, seedlings were transferred to various treatments, depending on the experiment. The agar plates contained ½ MS medium supplemented or not with Fe (see Figure legends). In the latter case, 50 µM ferrozine (Serva®) was added to the medium. When investigating the effect of different coumarins on preventing Fe deficiency in plants the following conditions were used: The pH of ½ MS agar medium was adjusted to 5.6 or 7.2 by KOH (Roth) and buffered by 2.5 mM MES. Iron was supplemented as 50 µM $FeCl_3$ (Merck). These plates received either no additional treatment (no treatment) or were supplemented with 160 µM Na-EDTA, 500 µM esculetin (Roth), 500 µM esculin (Roth) or 50 or 500 µM scopoletin (Sigma Aldrich). Plants were assessed after 6 days.

3.4 Imaging, scanning and fluorescence imaging of plants

Photographs of plants grown on substrate were taken with a Canon Digital IXUS 70, maintaining the same settings in manual modus. Plants grown on agar plates were scanned by an Epson Expression 10000XL scanner at a resolution of 300 dpi. Root fluorescence was imaged by a fluorescence imaging system Quantum ST4[24]. Excitation was adjusted by epi-UV at 365 nm and the emitting light was filtered by a 440 nm-filter (F-440M58). The images were taken with the help of the “Quantum-capt version 15.17” software (Döll, 2013).

3.5 Chlorophyll and shoot Fe determination

Whole shoot samples were incubated at 4°C for 24 hours in *N,N'*-dimethyl formamide (Merck) for determination of chlorophyll concentrations. The absorbance at 647 nm and 664 nm was then determined in the extracts following the protocol described by Porra et al. (1989). For Fe measurements, seeds or whole shoot samples were dried for 48 hours at 65°C and digested with HNO_3 (Merck) in polytetrafluoroethylene vials in a pressurized microwave digestion system (UltraCLAVE IV; MLS GmbH, Leutkirch, Germany). Iron concentrations were analyzed by inductively-coupled plasma optical emission spectrometry (ICP-OES; iCAP 6500 dual OES spectrometer; Thermo Fischer Scientific, Waltham, U.S.A.) equipped with a glass spray chamber Mira Mist nebulizer. Element standard (Fe) was prepared from certified reference single standards from CPI-International (USA). The ICP multi-element standard solution VIII (Merck) and the certified reference material 1515 apple leaves (NIST) were used for quality control.

3.6 Ferric-chelate- and coumarin-dependent Fe(III)- reduction assays

In order to determine the ferric-chelate reductase activity, ten-day-old plants were transferred for 6 days to ½ MS media containing Fe (+Fe; 75 µM Fe(III)-EDTA) or without Fe and 50 µM ferrozine (Serva®) (-Fe). The ferric-chelate reductase activity was then measured according to the protocol described in Waters et al. (2006). Briefly, plants were placed in a reaction solution containing 0.2 mM $CaSO_4$, 5 mM MES (pH 5.5), 0.2 mM ferrozine (Serva®), and 0.1 mM Fe(III)-EDTA (or 0.1 mM Fe(III)-esculetin, depending on the experiment). After 30 min, ferric-chelate reductase activity was determined by measuring the absorbance of the solution at 562 nm and was expressed in µmol Fe(II) g^{-1} FW h^{-1}.

Coumarin-dependent Fe(III) reduction was assessed by measuring the formation of Fe(II) at 562 nm every 30 min during 4 hours. When comparing the pH dependency of Fe(III) reduction, the Fe source during the reaction was 0.05 mM Fe(III)-EDTA or Fe(III)-esculetin (Roth) and the pH of was adjusted to pH 5.6 or pH 7.2. In addition, in order to investigate the Fe(III) reduction capability of different coumarins, 0.1 mM esculetin (Roth), 0.1 mM esculin (Roth) or 0.1 mM scopoletin

(Sigma Aldrich) were added to the reaction solution (buffered with 1 mM MES to pH 5.6) as described above.

3.7 Assay to test for coumarin modifications

To determine the de-glycosylation or de-methylation of esculin or scopoletin, a method based on Edberg et al. (1977) and Trepeta and Edberg (1987), originally developed for the discrimination between esculin hydrolysing and non-hydrolysing bacteria, was used. The presence of esculetin was detected by the formation of a dark-brown Fe-esculetin complex. Wild-type (Col-0) and *f6'h1-1* plants were grown for 12 days on ½ MS (75 µM Fe-EDTA) before transfer for 6 days either on ½ MS without Fe and 50 µM ferrozine (-Fe) or with 75 µM Fe-EDTA (+Fe). Plants were incubated for 6 hours on ½ MS solution supplemented (+) or not (-) with 2.7 mM esculin or scopoletin at pH 5.6 or 7.2. In this solution, Fe was supplied in the form of 1.9 mM ammonium ferric citrate (Roth). The formation of the Fe(III)-esculetin complex was measured at 460 nm (Ormö et al., 1992; Salama et al., 1978; McBryde, 1964). As blank, the absorption at 460 nm of the respective solutions without esculin (-esculin) or scopoletin (-scopoletin) was used.

3.8 Cloning and plant transformation

A 3.230 bp fragment containing 2.064 bp of the promoter region and open reading frame (ORF) of *F6'H1* was amplified from the genomic DNA of *Arabidopsis thaliana* (accession Col-0) plants. Genomic DNA was extracted according to the manufacturer's instructions of the DNeasy Plant Mini Kit from Qiagen. The Phusion High-Fidelity DNA Polymerase (Finnzymes, Thermo Fisher Scientific) was used for amplification. The following primers were used: At3g13610_Prom_5' (5'-caccCAGATTCACATTCATAAGTTC-3') and At3g13610_ORF_3'o.S. (5'-GATCTTGGCGTAATCGACGGTTTTC-3'). The resulting amplicon was cloned into the pENTR/TOPO entry vector according to the manufacturer's instruction (Invitrogen). This fragment was then subcloned into the Gateway plant expression vector pGWB4 (no promoter, C-sGFP) by the recombination of attL and attR sites (LR reaction) following the instruction manual provided by Invitrogen. To study the tissue localization of *F6'H1* expression via GUS, the 2.064 bp promoter region of *F6'H1* was amplified from genomic DNA using the primers At3g13610_Prom_ 5' (5'-caccCAGATTCACATTCATAAGTTC-3') and At3g13610_Prom_3'o.S. (5'-

TGGAATAAAAAAGATAGGAGC-3'). The fragment was cloned into the pENTR/TOPO entry vector and then transferred by LR reactions as described above to the pGWB3 vector (no promoter, C-GUS).

For the overexpression of *F6'H1* under the control of the 35S promoter, the ORF was amplified either from the genomic DNA (obtained as described above, for line 3b and 5h) with the primers At3g13610 ORF 5`35S (5`caccACAACACAATCAAAATCCC -3`) and At3g13610 ORF 3`35S m.S. (5`-TCAGATCTTGGCGTAATCGACGG- 3`) or from cDNA (obtained as described in section 3.10; for lines 18a, 18l, 20j and 21l) with primers At3g13610 ORF 5`35S ATG (5`-caccATGGCTCCAACACTCTTGACAAC- 3`) and At3g13610 ORF 3`35S m.S. (5`-TCAGATCTTGGCGTAATCGACGG- 3`). The resulting fragments were treated as described above and ultimately transferred to the pGWB2 vector. The plant expression vectors pGWB2, pGWB3 and pGWB4 were kindly provided by Tsuyoshi Nakagawa (Research Institute of Molecular Genetics, Shimane University, Matsue, Japan). The *Agrobacterium tumefaciens* strain C58C1 (pGV2260) was used to transform wild-type (Col-0) plants with these binary vectors according to the floral dip protocol (Clough and Bent, 1998). Plant transformants were selected on agar medium containing 35 µg mL^{-1} kanamycin. For each transgenic construct generated for localization studies, at least 8 independent T1 lines were analyzed and pictures of representative expression patterns are shown. T1 of plant transformants produced for overexpression of *F6'H1* were selected on agar medium containing 35 µg mL^{-1} kanamycin and 80 µg mL^{-1} ticarcillin. For selection of the T2 lines only kanamycin-based selection was conducted and homozygous resistant lines used for experiments.

3.9 Histochemical and microscopy analyses

The tissue localization of *F6'H1* was determined by histochemical staining of the GUS activity in Arabidopsis seedlings transformed with the construct *ProF6'H1-1:GUS*. *ProF6'H1-1*-dependent GUS activity was assessed by incubating roots or whole seedlings in a solution containing 0.4 mg mL^{-1} of 5-bromo-4-chloro-3-indolyl-b-D-glucuronide, 50 mM sodium phosphate, pH 7.2, and 0.5 mM ferrocyanide and 0.5 mM ferricyanide. After 12 hours of incubation at 37°C, plant samples were cleared and mounted according to the procedure described by Malamy and

Benfey (1997). At least 10 seedlings per independent transgenic line and treatment were analyzed with a conventional light microscope (Axioskope, Zeiss, Germany) connected to a CCD camera (Axiocam HRc, Zeiss, Germany). The software AxioVision Rel. 4.8 (Zeiss, Germany) was used for imaging.

GFP-dependent fluorescence in roots of *ProF6'H1-1-F6'H1-1-GFP* lines were detected with a confocal microscope LSM 510 Meta (Carl Zeiss MicroImaging GmbH, Jena, Germany). Roots were stained with propidium iodide (10 µg mL^{-1}) for 10 min. GFP-dependent fluorescence was detected by excitation at 488 nm with an argon laser and filtering the emitting light at 505 to 530 nm. The 488 nm excitation and 458-514 nm emission lines were used to image the propidium iodide-derived fluorescence.

Naturally occurring root fluorescence was detected with the same confocal microscope by excitation at 364 nm and the emitting light filtered at 385 to 450 nm (Döll, 2013). Presented are overlays of fluorescence and bright-field images. The software LSM 510 release 3.2 (Zeiss) was used for adjustments and image recording.

3.10 Gene expression analysis

Plants were grown axenically on agar plates as described in 3.3 and total RNA was extracted from roots of either Fe-sufficient or deficient Col-0 or *fit* mutant plants using a modified version of the single-step method (Chomczynski and Sacchi, 1987). For reverse transcription of RNA into cDNA, the RevertAid First Strand cDNA Synthesis Kit of Fermentas (St. Leon-Rot, Germany) and oligo-dT-primers were used and RNA samples treated previously with RQ1 RNase-Free DNase (Promega). The cDNA samples were then used to investigate gene expression by quantitative real-time PCR (q RT-PCR) with the Mastercycler ep *realplex* (Eppendorf, Hamburg, Germany) and the iQ SYBR Green Supermix (Bio-Rad Laboratories, Hercules, CA, USA). The expression of *F6'H1* was assessed by using specific primers, as suggested by Schippers et al. (2008) (P109F6'H1for: 5'-TGATATCTGCAGGAATGAAACG-3'; P110F6'H1rev: 5'-GGGTAGTAGTTAAGGTTGACTC-3'). For *MYB72* expression, primers P86MYB72for: 5'- TCATGATCTGCTTTTGTGCTTTG–3' and P87MYB72rev: 5'–ACGAGATCAAAAACGTGTGGAAC–3' according to Van der Ent et al. (2008)

were chosen. To assess *IRT1* expression the following primers were used: P99IRT1For 5'-CGGTTGGACTTCTAAATGC-3' and P100IRT1Rev 5'-CGATAATCGACATTCCACCG-3' (Seguela et al., 2008). In addition, the expression of the house-keeping gene *UBIQUITIN2 (UBQ2)* was also determined by using the primers P32UBQ2-For: 5'-CCAAGATCCAGGACAAAGAAGGA-3'; P33UBQ2-Rev: 5'-TGGAGACGAGCATAACACTTGC-3' (Giehl, 2011). Relative expression was calculated according to Pfaffl (2001).

3.11 Collection of root exudates and root extractions

Root exudates were collected from 14-day-old plants grown axenically for 4 days on Fe-sufficient (75 µM Fe-EDTA) or deficient (no added Fe and 50 µM ferrozine added) solid medium. The plants were carefully transferred from the agar plates to a 12-well plate (12 plants per well) containing 5 mL of ultrapure water per well (Millipore). The plates were placed inside bowls covered with PVC film to prevent dehydration. The trays were kept under 22°C with constant illumination (120 µmol photons m^{-2} s^{-1}). After 6 hours, the solution containing the root exudates was collected. The exudates of 144 plants were combined into one replicate. These solutions were concentrated in a rotary evaporator (Rotavapor R-210/215, Büchi). Evaporated samples were then resuspended in 10 mL 100% methanol and sonicated for 5 min, and finally concentrated to 0.5 mL using a Christ ALPHA RVC centrifugal evaporator. In the case of fluorescence-free root exudates, the complete exudates were loaded on a SepPack C18 cartridge (Water, Wildford, MA, USA). The column was washed three times with 10% (v/v) methanol (Maslak, 2002) and the combined fluorescence-free flow-through and wash solution was used for the Fe(III) mobilization assay.

In order to extract phenolic compounds from roots, 100% methanol was added to frozen root samples (400 µL methanol per 100 mg roots) and the samples were homogenised using a tissue homogenizer (Precellys 24, Bertin technologies, Montigny-le-Bretonneux, France) and zirconium silicate (58%) grinding beads (diameter 1.0-1.2 mm; RIMAX ZS-R, Mühlmeier GmbH, Bärnau, Germany) for 2 x 45 sec at 5500 rpm. After centrifugation (16400 rpm/28500 x *g*, at 4°C for 10 min) the supernatant was transferred into a new tube and the pellet was resuspended again with the same amount of methanol and the second supernatant was

combined with the first. An aliquot of this sample was then diluted to 80% (v/v) with the acidic solvent from the aqueous phase of the HPLC before injection (Korn et al., 2008).

3.12 Fe mobilization assays and Fe-coumarin complex determination

Iron mobilization capacity was determined by incubating different compounds or root exudates with freshly prepared 0.1 mM Fe hydroxide at pH 7.2. Samples were incubated at constant shaking for 2 hours. Afterwards the solutions were filtered by Chromafil® CA-45/25 (0.45 µm pore) filters. The Fe concentrations in the filtrates were detected by sector-field high-resolution inductively coupled plasma mass spectrometry (HR)-ICP-MS (ELEMENT 2, Thermo Fisher Scientific, Germany). Element standards were prepared from certified single standards from CPI-International (USA). ^{56}Fe was used as external standard and ^{103}Rh as internal standard for matrix correction. The ICP multi-element standard solution VI (Merck) was used for quality control. Alternatively, the accumulation of Fe-coumarin complexes in these filtrates were measured photometrically at 460 nm (Ormö et al., 1992; Salama et al., 1978; McBryde, 1964).

3.13 Determination of coumarins in root extracts and exudates by UPLC-FLD

Root extracts and exudates were subjected to separation by a Waters Acquity ultra performance liquid chromatography (UPLC) system fitted with an Acquity UPLC® photodiode array (PDA) detector and an ACQUITY UPLC® fluorescence detector (FLD). This separation method followed the protocol described by Yonekura-Sakakibara et al. (2008). Briefly, the Waters Acquity UPLC system was equipped with a BEH phenyl column (Waters Acquity UPLC BEH Phenyl Column, 130Å 2.1 x 100 mm, 1.7 µm) and an Acquity UPLC BEH Phenyl VanGuard pre-column (130Å, 1.7 µm, 2.1 mm x 5 mm). The column temperature was set to 35°C. The gradient was linear from 0 min, 100% solvent A (0.1% (v/v) formic acid in 18 MΩ ultrapure water) to 10 min, 40% solvent B (0.1% (v/v) formic acid in acetonitrile). Solvent B was brought up to 100% after each run to clean the column

and the initial conditions were restored in a delay of 3.5 min. Samples were evaluated with UV detection at 280 nm and fluorescence detection at 300/400 nm, 336/438 nm and 360/450 nm.

3.14 Determination of coumarin concentrations in root extracts and exudates via UPLC-ESI-ToF-MS

UPLC-electrospray ionization-time-of-flight (ESI-ToF) was carried out with a Dionex Ultimate 3000 UPLC system (Thermo Fisher Scientific Inc. Waltham, MA, USA) coupled to an ultra high resolution time-of-flight mass spectrometer (UHR-TOF-MS, maXis impact, Bruker Daltonics, Bremen, Germany). The HPLC conditions were those as described above. ESI was carried out in positive mode. MS settings were optimized for small to medium molecules established on the coumarin standards esculin, esculetin, scopolin and scopoletin (Döll, 2013) (mass range 50 m/z – 1,000 m/z, capillary voltage 4000 V, nebulizer 3 bar, dry gas 11 L min^{-1}, dry temperature 260°C, hexapole radio frequency voltage (RF), 40 volt, peak-to-peak (Vpp), funnel 1 RF 300 Vpp, funnel 2 RF 300 Vpp, prepulse storage time 5 µs, transfer time 50 µs, low mass 40 m/z, collision cell RF 500 Vpp, collision energy 8.0 eV). Calibration was performed externally before each run with 10 mM sodium formate, using a calibration mode quadratic + HPC (for High Precision Calibration). Data analysis was carried out with Compass DataAnalysis V.4.1 and Compass QuantAnalysis V2.1 (Bruker Daltonik GmbH, Bremen, Germany).

4 Results

4.1 Establishment of a screening system to identify genes with reduced tolerance to Fe deficiency-mediated chlorosis

In order to identify novel genes or components that are involved in Fe acquisition in *Arabidopsis thaliana,* a mutant collection was intended to be screened on a growth substrate that simulates an intact, high pH rhizosphere. Under neutral or alkaline pH, the availability of Fe is strongly decreased (Connolly et al., 2003). As a consequence, wild-type (Col-0) plants grown on alkaline substrate exhibit mild symptoms of Fe deficiency, expressing in retarded growth and leaf chlorosis. Therefore, various mixtures of calcium carbonate ($CaCO_3$) and bicarbonate ($NaHCO_3$) or $CaCO_3$ and calcium oxide (CaO) added to a peat-based substrate were tested for their potential to increase and buffer the substrate pH (Mengel et al., 1984; Boxma, 1972; Lucena, 2000; Marschner, 2012).

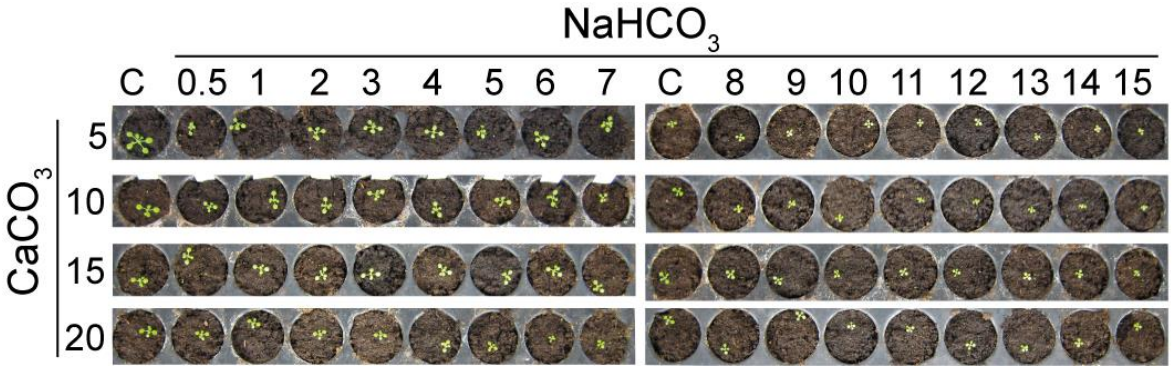

Figure 3. Growth of wild-type (Col-0) plants on several combinations of $CaCO_3$ and $NaHCO_3$ to test for calcareous conditions that induce mild chlorosis. C = control (non-limed substrate), $NaHCO_3$ concentrations from 0.5 to 15g kg^{-1} at constant $CaCO_3$ concentrations ranging from 5 to 20g kg^{-1}. Plants were grown for 17 days in short day conditions.

Several combinations of $CaCO_3$ and CaO were added to the substrate and evaluated but not considered any further, as the development of Fe deficiency-induced chlorosis strongly varied among individual plants (data not shown). Amongst the tested combinations of $CaCO_3$ and $NaHCO_3$ (Figure 3), the addition of 20 g kg^{-1} of $CaCO_3$ and 12 g kg^{-1} of $NaHCO_3$ increased the pH to 7.2 and led to the development of slight chlorosis in leaves of wild-type plants when grown for

two to three weeks on this substrate (Figure 3). Therefore, this combination of calcareous buffers was considered as most suitable for the design of the substrate (referred to as limed substrate throughout this thesis) for the screening.

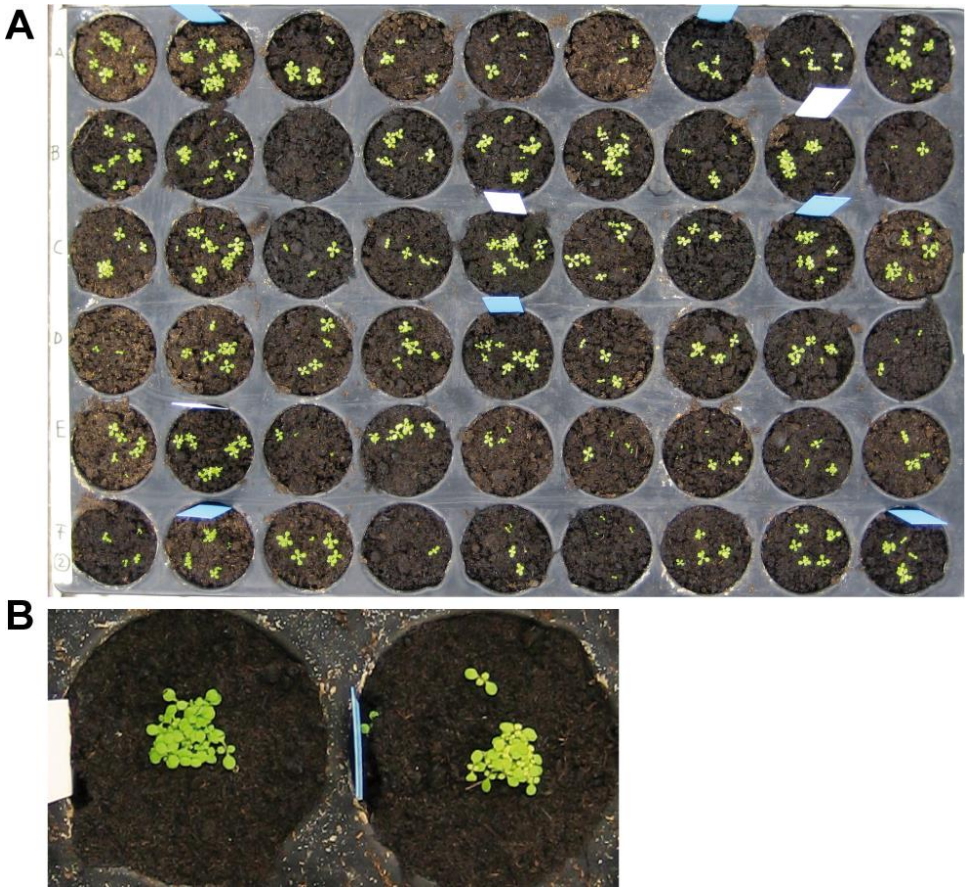

Figure 4. Representative example of a tray as it occurred during the screening. (A) Wild-type (Col-0) (white label) and *frd3-3* (blue label) plants were grown repeatedly as controls in the same tray. (B) The two control lines in magnified view. Plants were grown on limed substrate.

The screening collection consisted of about 7,000 homozygous, non-redundant T-DNA insertion lines from *Arabidopsis thaliana* (Alonso et al., 2003). Plants were cultivated in trays containing 54 pots and on each pot within such a tray, 3 to 5 individual plants carrying the same T-DNA insertion were allowed to grow (Figure 4A). On non-limed substrate at pH 5.6, each insertion mutant was grown in one pot and on limed substrate at pH 7.2, two pots per insertion line were assigned. As controls, wild-type (Col-0) and *frd3-3* mutant plants, the latter showing chlorosis even under ample Fe availability (Durrett et al., 2007), were included in three pots within each tray (Figure 4B). The screen consisted of visually assessing plant size

as well as the appearance and intensity of Fe deficiency symptoms (mainly chlorosis in young leaves) in insertion lines grown at pH 7.2 as compared to both the same insertion line grown on pH 5.6 or to wild-type and *frd3-3* mutant plants grown on the same tray at pH 7.2. Once a noticeable phenotype was spotted, the line was selected and the phenotyping repeated. A correction of leaf chlorosis attained by the addition of Fe-EDDHA was defined as condition for assuming the chlorosis of a particular line to be Fe deficiency-related.

Figure 5. Phenotype of several mutants identified during the screening process. (A) Wild type (Col-0) and (B to D) T-DNA insertion lines grown on non-limed substrate (pH 5.6). These insertion lines showed chlorosis that could not be reverted by supplying highly soluble Fe-EDDHA. The genes predicted to be disrupted by T-DNA insertions are: (B) At3g48720, transferase family protein; (C) At5g52440, thylakoid membrane delta pH translocation pathway component protein; and (D) At1g50770, aminotransferase-like, plant mobile domain family protein.

During the screening, the phenotype of over 3,500 T-DNA insertion lines was recorded and several of them displayed interesting phenotypes such as bright leaves, meristematic or veinal chlorosis (Figure 5) that could not be related to Fe homeostasis (data not shown). Two insertion lines fulfilled the prerequisites to be selected for more detailed analysis. They both developed strong chlorosis when grown on limed substrate and the addition of Fe-EDDHA led to a regreening of these insertion lines. These lines carry defects in the genes At1g56160 and At3g13610 and are further described in sections 4.2 and 4.3.

4.2 Isolation of a T-DNA insertion line expressing strong chlorosis under calcareous conditions: *myb72*

4.2.1 Phenotype of *myb72-1* with defective expression in At1g56160 in different growth systems

The growth of the T-DNA insertion line SAIL_713_G10 (*myb72-1*) was compared on non-limed (pH 5.6) and limed substrate (pH 7.2) (Figure 6A). This line harbors a T-DNA insertion in a gene that encodes the R2R3-MYB-like transcription factor MYB72 (Kranz et al., 1998; Van der Ent et al., 2008). When grown at pH 5.6, the phenotype of *myb72-1* plants did not differ from wild-type plants. However, at pH 7.2 a strong chlorosis developed in *myb72-1* whilst the wild type remained slightly chlorotic (Figure 6A). In contrast, on agar plates the performance of *myb72-1* either supplied with readily available Fe or in complete absence of Fe did not differ significantly from wild-type plants in terms of shoot Fe and chlorophyll concentrations (Figure 7).

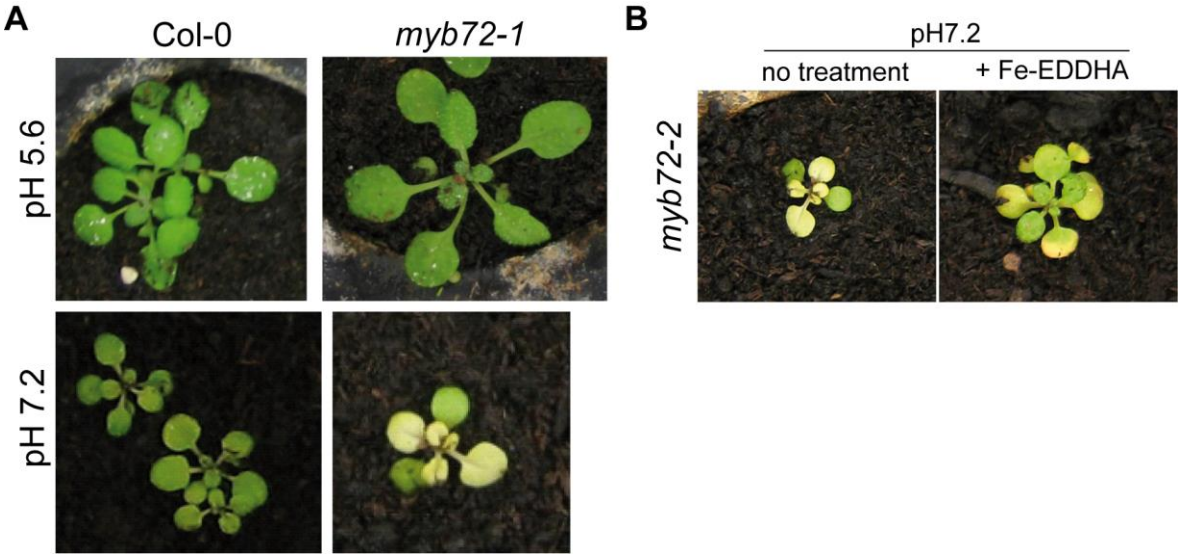

Figure 6. The phenotype of the *myb72-1* and *myb72-2* T-DNA insertion lines grown on substrate. Twenty six day-old plants either grown on non-limed substrate at pH 5.6 (A) or on limed substrate at pH 7.2 (A, B). In (B) plants on the right are supplied with 2.0 mL of a 0.5 g L^{-1} Fe-sequestrene (6% Fe(III)-EDDHA) solution (+Fe-EDDHA) for 7 days before the end of the experiment.

Since the strong chlorosis of the *myb72-1* insertion line that appeared on limed substrate could be reverted by adding generous amounts of Fe-EDDHA (Figure

6B), the defective gene was presumed to play a role in Fe homeostasis. Hence, the expression of *MYB72* in response to Fe deficiency was studied by quantitative real-time PCR (qRT-PCR). This analysis revealed that *MYB72* is strongly up-regulated in roots of Fe-deficient plants (Figure 8).

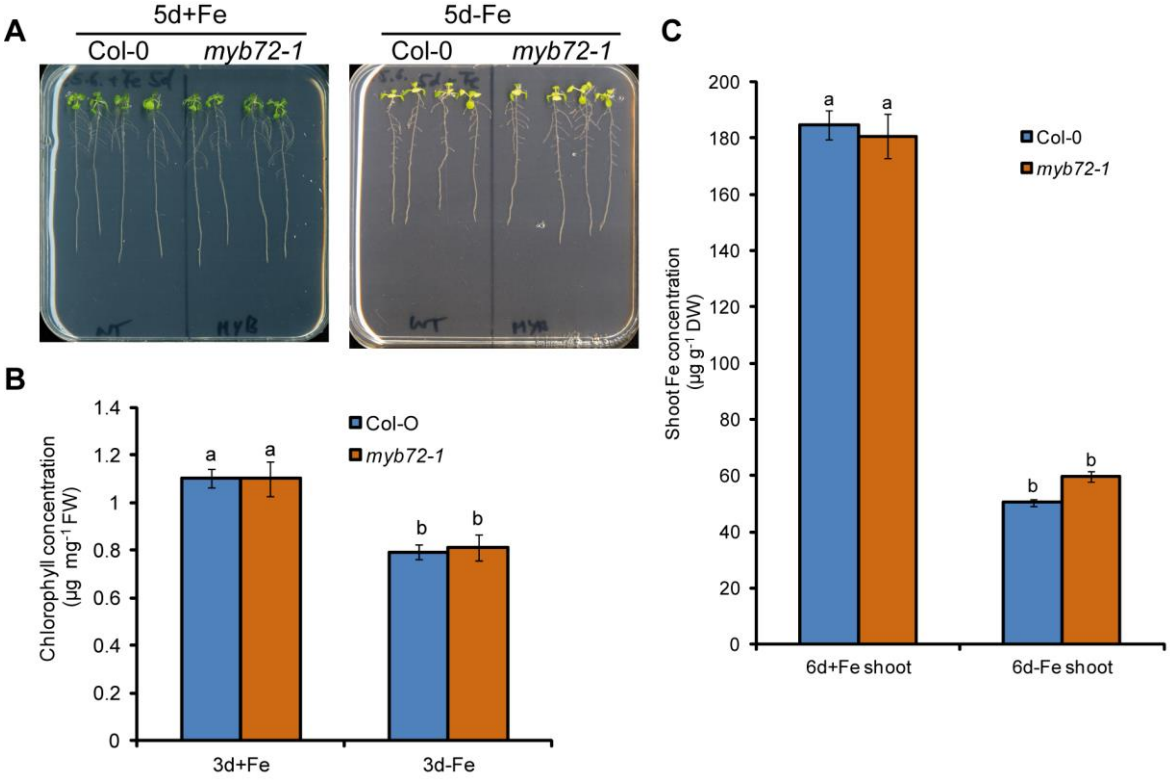

Figure 7. The phenotype of the *myb72-1* T-DNA insertion line grown on agar plates. (A) Phenotype, (B) chlorophyll and (C) shoot Fe concentrations of plants that were precultured on ½ MS agar supplemented with 75 µM Fe-EDTA for either 10 (A,B) or 12 days (C) and after transfer to Fe sufficiency (+Fe) or Fe deficiency (-Fe) for 3 (B) or 6 (C) days at pH 5.6. Bars represent means ± SE (n = 3-5 replicates). Different letters indicate significant differences according to Tukey's test ($P < 0.05$). FW and DW refer to fresh weight and dry weight, respectively.

This result is in accordance with the transcriptome study performed by (Dinneny et al., 2008). In fact, this transcriptome analysis along a time course and longitudinal root zone showed that *MYB72* is up-regulated in 5 day-old seedlings already as soon as 48 to 72 hours after transfer to Fe deficiency and that expression was highest in the mature root zone (Figure 9).

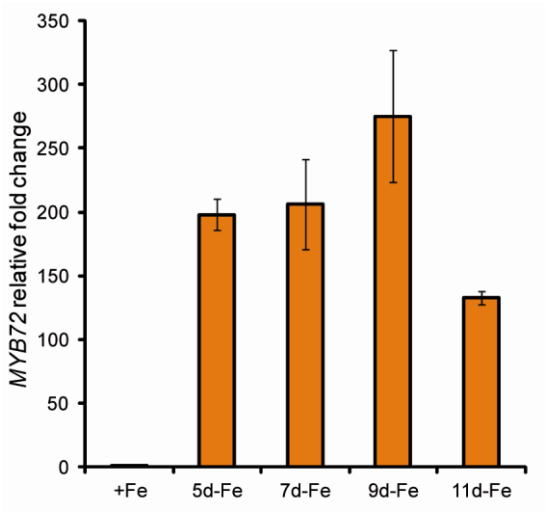

Figure 8. *MYB72* expression in response to Fe deficiency. Quantitative RT-PCR on cDNA of roots from wild-type plants precultured on ½ MS agar supplemented with 75 µM Fe-EDTA for 10 days and after transfer to Fe sufficiency (+Fe) or Fe deficiency for 5, 7, 9 or 11 days (-Fe) at pH 5.6. Bars indicate means ± SE (n = 3 biological replicates).

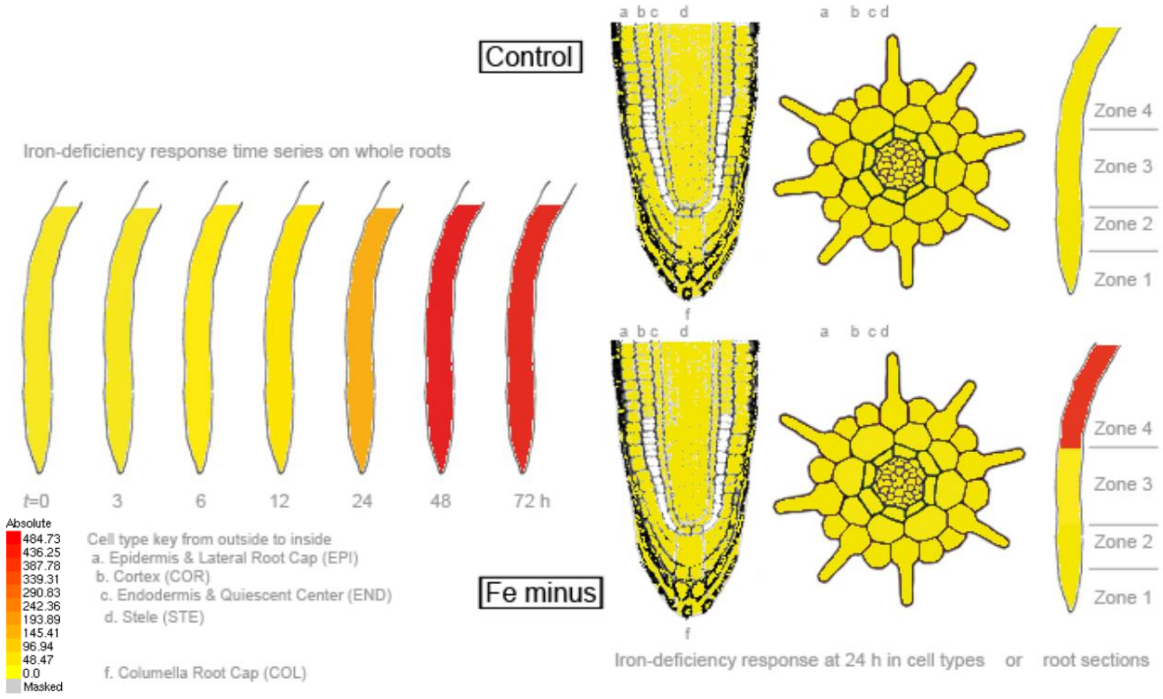

Figure 9. Response of *MYB72* to Fe deficiency according to data from the Arabidopsis eFP Browser (Dinneny, 2008) (http://bbc.botany.utoronto.ca/efp/cgi-bin/efpWeb.cgi). Whole roots from 5 day-old seedlings were deprived of Fe with ferrozine. For the spatial analyses, cell type- or section-specific data were generated by fluorescence-activated cell sorting or sectioning of roots on Fe-deficient media for 24 h.

4.3 Identification and characterization of *f6'h1* and its function in Strategy I Fe acquisition in *Arabidopsis thaliana*

4.3.1 Phenotype of *f6'h1-1* with defective expression in At3g13610 on calcareous substrate

The T-DNA insertion line *f6'h1-1* (SALK_132418C), the second mutant line that was selected during the screening due to its striking phenotype, is defective in the expression of a gene that encodes the 2-oxoglutarate-dependent dioxygenase Feruloyl-CoA 6'-Hydroxylase1 (F6'H1) (Kai et al., 2008). This line repeatedly exhibited stronger chlorosis in its youngest leaves than the wild type as a consequence of significantly lower chlorophyll and Fe concentrations in the shoot (Figure 10). Since leaf chlorosis was absent when these plants were grown on non-limed substrate at pH 5.6 and chlorophyll as well as Fe levels were recovered by supplying the pH-stable chelate Fe(III)-EDDHA, the defective gene was supposed to be involved in Fe acquisition. A second allelic insertion in the same gene (*f6'h1-2*, SALK_050137C) yielded an identical Fe-dependent phenotype (Figure 11).

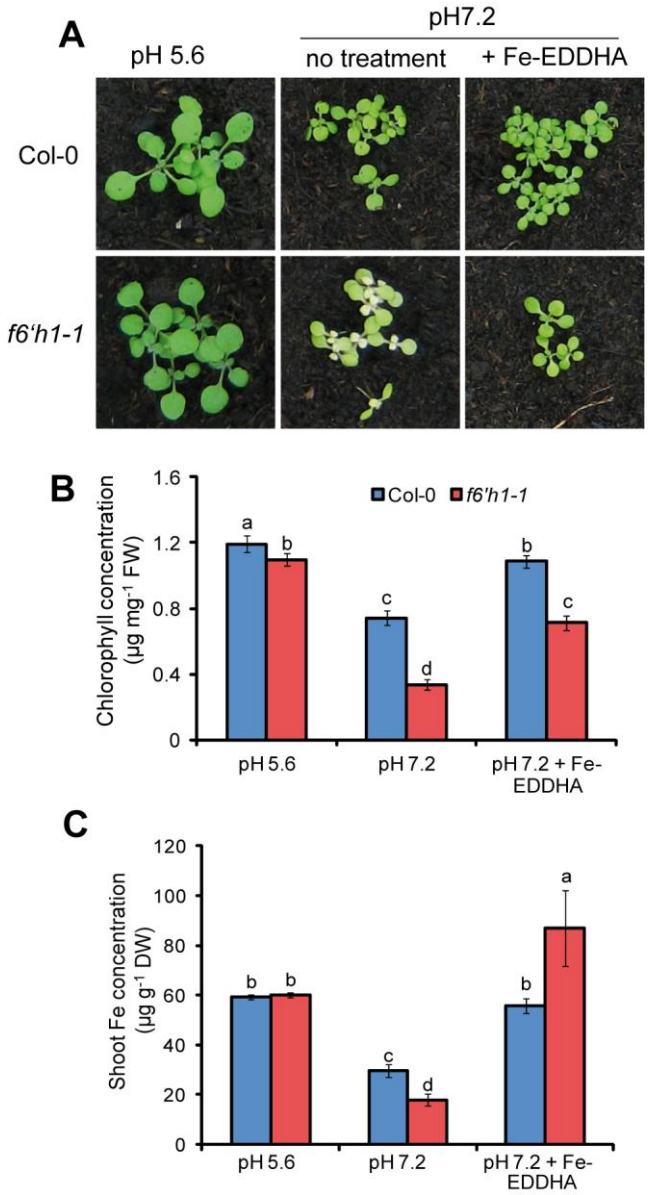

Figure 10. Phenotypic characterization of *f6'h1-1*, a T-DNA insertion line defective in the expression of the 2-oxoglutarate-dependent dioxygenase *F6'H1*. (A) Wild-type (Col-0) and *f6'h1-1* mutant plants were grown for 17 days on non-limed substrate at pH 5.6 or limed substrate at 7.2. To alleviate leaf chlorosis at pH 7.2, plants were supplied with 2.0 mL of a 0.5 g L^{-1} Fe-sequestrene (6% Fe(III)-EDDHA) solution (+Fe-EDDHA). The supplementation of Fe-EDDHA was carried out 4 days before the end of the experiment. (B) Chlorophyll and (C) Fe concentrations in shoots of wild-type and *f6'h1-1* plants grown as indicated in (A). Bars represent means ± SE (n = 3-9 replicates). Different letters indicate significant differences according to Tukey's test ($P < 0.05$). FW and DW refer to fresh weight and dry weight, respectively.

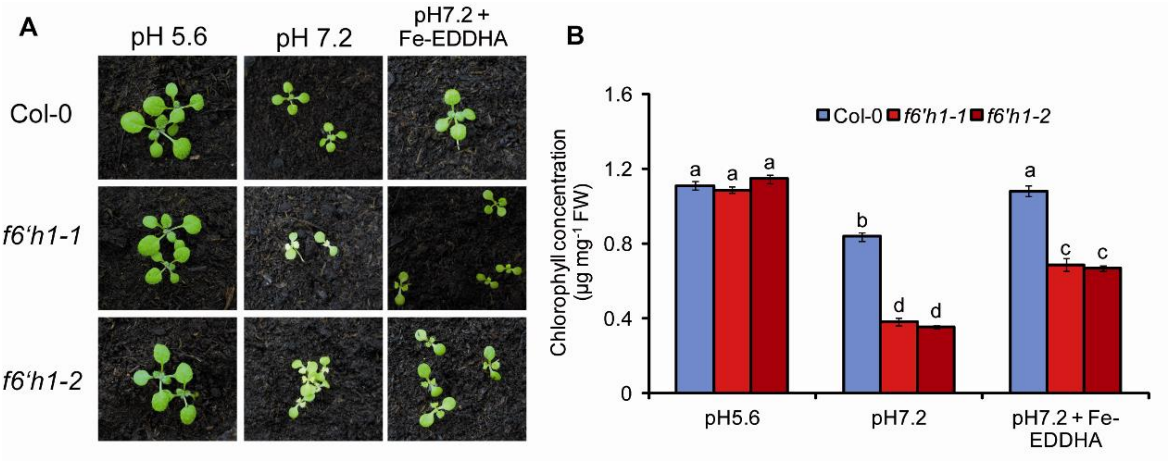

Figure 11. Phenotype of *f6'h1-1* and *f6'h1-2* on calcareous substrate. (A) Phenotype and (B) chlorophyll concentrations of whole shoots of wild type (Col-0), *f6'h1-1* and *f6'h1-2* mutant plants after growth for 17 days on non-limed (pH 5.6) or limed substrate (pH 7.2). To alleviate leaf chlorosis at pH 7.2, plants were supplied with 2.0 mL of a 0.5 g L^{-1} Fe-sequestrene (6% Fe(III)-EDDHA) solution (+Fe-EDDHA). The supplementation of Fe-EDDHA was carried out 4 days before the end of the experiment. Bars represent means ± SE (n = 5-8 biological replicates). Different letters indicate significant differences to Tukey's test ($P < 0.05$). FW refers to fresh weight.

Since the chlorotic phenotype of the *f6'h1-1* T-DNA insertion line was clearly visible as soon as 10 to 14 days after germination, it was necessary to verify whether differences in seed Fe concentrations or in ferric-chelate reductase activity could explain the strong Fe deficiency symptoms of these plants. Seed Fe concentrations of wild-type and mutant plants differed significantly (Figure 12A). However, the Fe levels recorded in *f6'h1-1* seeds can still be considered as sufficient to allow for proper germination (Waters et al., 2006). Furthermore, the ferric-chelate reductase activity in *f6'h1-1* roots was indistinguishable from wild type under both sufficient and deficient Fe conditions (Figure 12B). Thus, it was excluded that a defect in the reduction of ferric to ferrous Fe might have led to the strong chlorosis in the mutant.

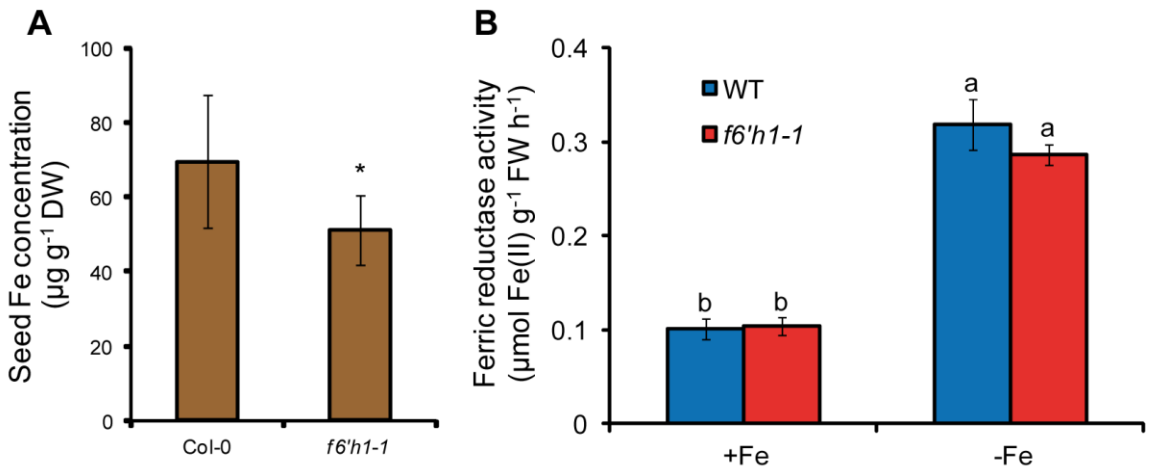

Figure 12. Seed Fe concentration and ferric-chelate reductase activity assay in roots of wild-type (Col-0) and *f6'h1-1* plants. (A) Seed Fe concentration of plants that were grown on non-limed substrate till seed maturation. Bars represent means ± SE (n = 20-30). Asterisk indicates significant differences according to Student's t-test ($P < 0.001$). (B) Ferric reductase activity. Seedlings were germinated on ½ MS agar plates supplemented with 75 µM Fe-EDTA. Ten day-old plants were then transferred for 6 days to ½ MS agar containing 75 µM Fe-EDTA (+Fe) or without Fe but 50 µM ferrozine added (-Fe) at pH 5.6. Bars represent means ± SE (n = 8 biological replicates). Different letters indicate significant differences according to Tukey's test ($P < 0.05$). FW and DW refer to fresh weight and dry weight, respectively.

In the *f6'h1-1* and *f6'h1-2* T-DNA insertion lines the defect in the expression of the 2-oxoglutarate-dependent dioxygenase *F6'H1* (Kai et al., 2008) is caused by an insertion in the first and second exon, respectively (Figure 13A). To verify whether the T-DNA insertions indeed abolished the expression of *F6'H1* in the two examined insertion lines (Figure 13A), quantitative real-time PCR (qRT-PCR) was performed. As shown in Figure 13B, *F6'H1* expression was almost completely impeded in roots of *f6'h1-1* and *f6'h1-2* plants, even when plants were precultured under Fe deficiency. The expression of *IRT1*, the major transporter for high-affinity Fe uptake under Fe deficiency (Vert et al., 2002), was used as a control for the plants Fe status. Its expression was present in both insertion lines under Fe sufficiency and was strongly increased in conditions of Fe deficiency (Figure 13C).

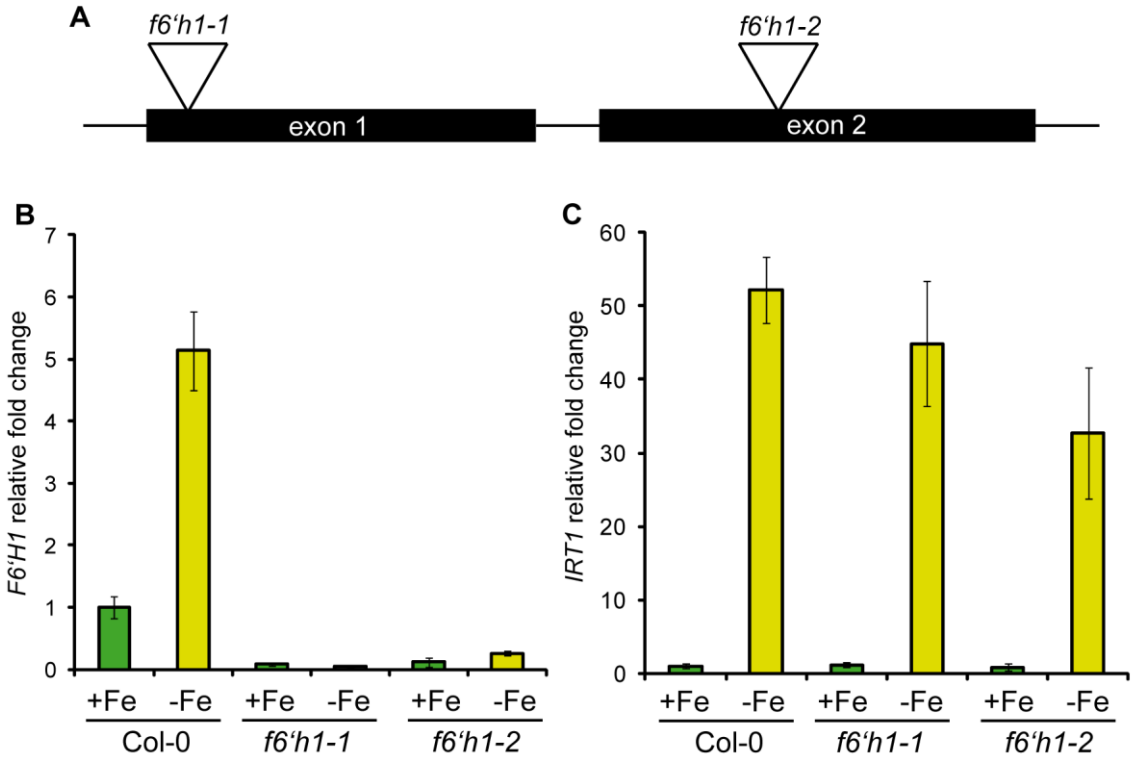

Figure 13. Gene structure of *F6'H1* and its expression under Fe deficiency. (A) Gene structure of the *2-oxoglutarate-dependent dioxygenase F6'H1* (At3g13610). According to SIGnAL (http://signal.salk.edu/) the gene has two exons, which are 511 base pairs (bp) and 573 bp long and are divided by a short intron of 84 bp. In line *f6'h1-1*, the T-DNA is inserted within the first exon 53 bp downstream of ATG, whereas in line *f6'h1-2*, the insertion is located 235 bp downstream of ATG within the second exon. (B, C) *F6'H1* and *IRT1* expression in the roots of the T-DNA insertion lines *f6'h1-1* and *f6'h1-2*. Expression levels of *F6'H1* were detected by quantitative RT-PCR in root samples of wild- type (Col-0), *f6'h1-1* and *f6'h1-2* plants grown for 4 days on Fe sufficiency (+Fe) or Fe deficiency (-Fe) at pH 5.6. Bars indicate means ± SE (n = 5-6 biological replicates).

Taken together, the phenotypic analysis of the *f6'h1* insertion lines grown on calcareous substrate revealed that a lack of *F6'H1* expression leads to the formation of severe chlorosis accompanied by reduced shoot Fe levels, which can be restored by adding generous amounts of highly plant-available Fe.

4.3.2 The expression of *F6'H1* in Fe-deficient wild-type roots

As F6'H1 is active in the phenylpropanoid pathway and phenolic substances have been proposed to be released by Fe-deficient roots to assist Fe acquisition in various plant species (Römheld and Marschner, 1983; Jin et al., 2007; Ishimaru et al., 2011b), the Fe-dependent transcriptional regulation of *F6'H1* was investigated. In agreement with data from transcriptomics and proteomics studies of

Arabidopsis roots (Dinneny et al., 2008; Buckhout et al., 2009; Lan et al., 2011), relative transcript levels of *F6'H1* increased in roots 2 to 6 days after transferring plants to Fe-deficient medium (Figure 14). Under Fe-sufficient conditions no up-regulation was observed during the same time period. A similar expression pattern was observed for *IRT1*, whose Fe deficiency-mediated up-regulation was even stronger.

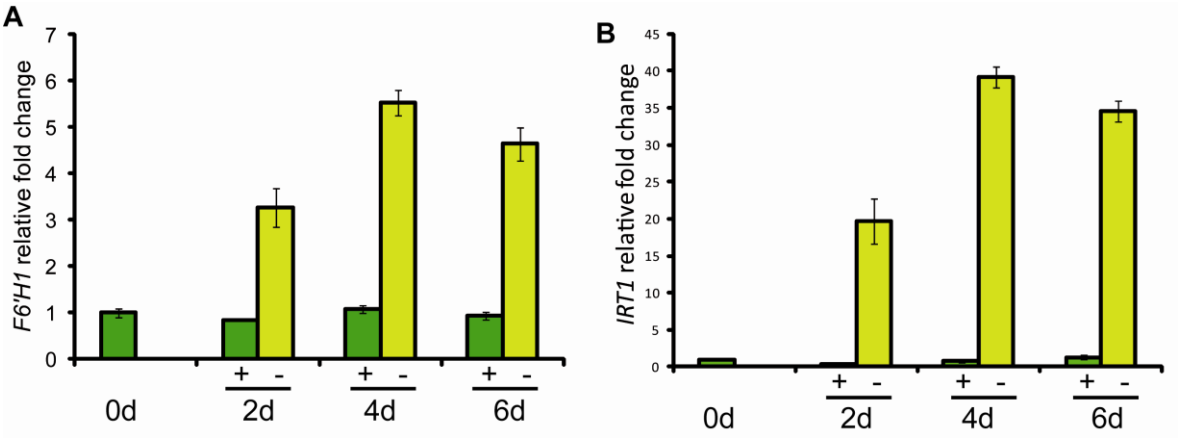

Figure 14. Expression of *F6'H1* upon Fe deficiency. Relative expression levels of (A) *F6'H1* or (B) *IRT1* as revealed by quantitative RT-PCR in roots of wild-type plants before (0 d) or after transfer to a Fe-sufficient (+) or Fe-deficient (-) medium for 2, 4 or 6 days at pH 5.6. Bars indicate means ± SE (n = 5-6 biological replicates).

In order to check the tissue-specific localization of *F6'H1*, transgenic seedlings expressing a *proF6'H1:GUS* fusion were generated. The histochemical analysis of these plants showed that *F6'H1* promoter activity was confined to roots and was up-regulated by Fe deficiency (Figure 15A). *ProF6'H1*-dependent GUS activity was detected in the mature root zone and in the root hair zone of primary and lateral roots but was absent in root tips (Figure 15B). Furthermore, a magnified picture of the mature zone of the primary root clearly revealed that *F6'H1* promoter activity was extended to the outer root cells in Fe deficient plants, namely the rhizodermal cells (Figure 15C).

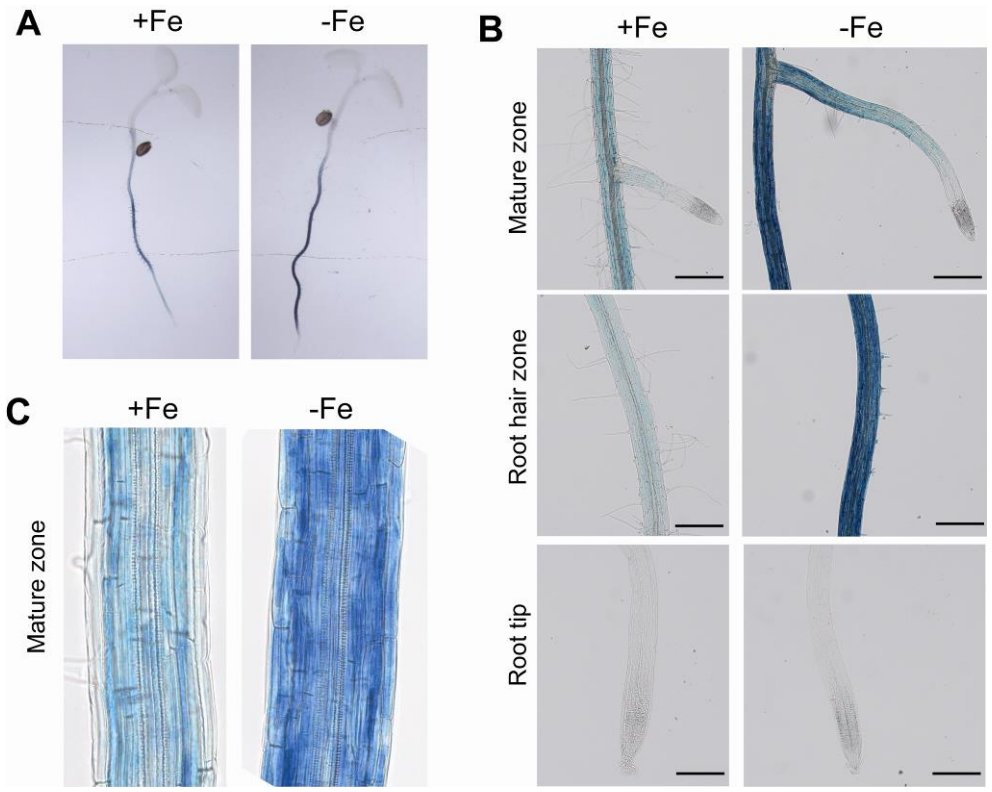

Figure 15. Tissue specific localization of *F6'H1* expression. (A) Histochemical staining of GUS activity in roots of 5 day-old seedlings transformed with a translational *proF6'H1:GUS* fusion and germinated in the presence (+Fe) or absence (-Fe) of 75 µM Fe-EDTA. Images of a representative transgenic line are shown (n = 8). (B) *proF6'H1*-dependent GUS activity in different root zones of Fe-sufficient (+Fe) or Fe-deficient plants (-Fe). GUS activity was absent in the tips of primary and lateral roots. Plants were pre-cultured in ½ MS (75 µM Fe-EDTA) for 5 days and then transferred to ½ MS with 75 µM Fe-EDTA (+Fe) or no Fe but 15 µM ferrozine added (-Fe). Shown are representative root sections (n > 10) from one representative transgenic line. Scale bars: 500 µm. (C) Close-up section of mature zone of primary root from plants as described in (B).

Confocal microscopy of Fe-deficient plants expressing a *proF6'H1:F6'H1:green fluorescence protein* (GFP) fusion further revealed highest expression levels in the basal zone of the primary root, where the protein was localized in rhizodermal and cortical cells and was almost absent in Fe-sufficient plants (Figure 16). Increased F6'H1-dependent fluorescence in cortical cells was also observed in the elongation zone of primary roots of Fe-deficient plants, whereas no F6'H1-dependent GFP fluorescence was detected in primary root tips (Figure 16).

Overall, the expression studies on F6'H1 clearly showed that its expression is induced mainly in the basal zone of the primary root under Fe deficiency and extends to cortical and rhizodermal root cells.

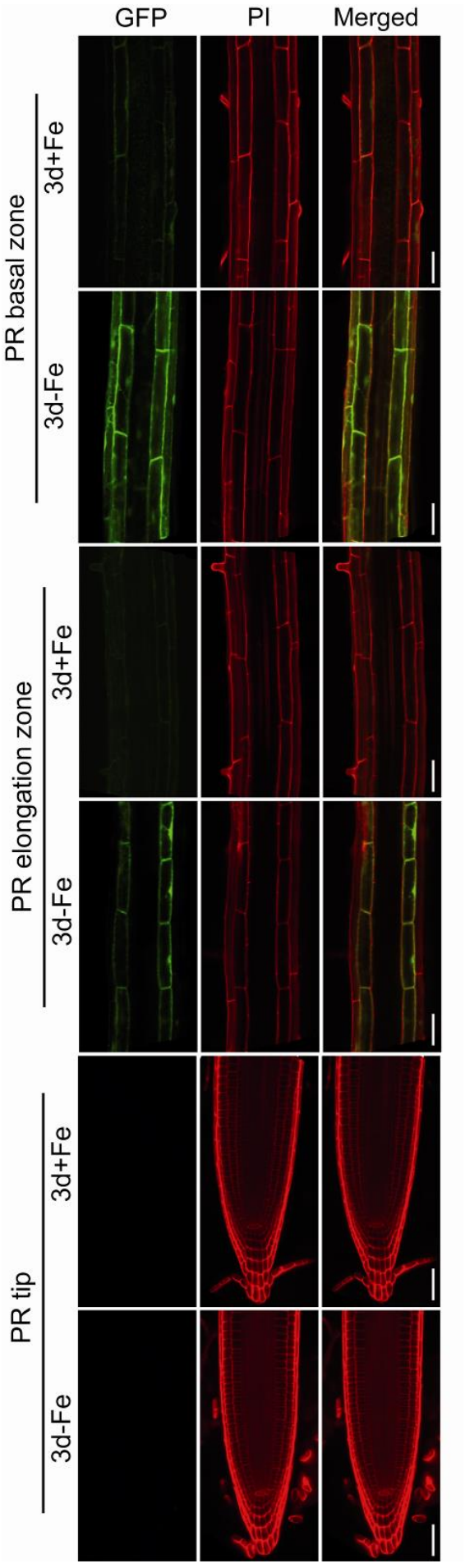

Figure 16. GFP-dependent fluorescence in the basal and elongation zone and in the root tips of primary roots (PR). Roots were obtained from Fe-deficient transgenic Arabidopsis plants expressing a translational F6'H1-GFP fusion under the control of its native promoter. Plants were precultured for 8 days on ½ MS medium containing 75 µM Fe-EDTA and then transferred for 3 days to Fe-deficient (no Fe but 15 µM ferrozine added) or Fe-sufficient medium (75 µM Fe-EDTA). Cell walls were stained with propidium iodide (PI) and imaged with a confocal microscope. GFP was excited at 488 nm and propidium iodide at 514 nm. Shown are images of representative plants from one representative transgenic line (n = 8). Scale bars = 50µm.

4.3.3 Characterization of the Fe deficiency-induced synthesis and secretion of fluorescent phenolics in dependency of F6'H1

F6'H1 utilizes molecular oxygen to catalyze the *ortho*-hydroxylation of feruloyl-CoA, which is a prerequisite for its spontaneous isomerization and lactonization in the formation of hydroxyferuloyl-CoA and the coumarin scopoletin (Kai et al., 2006; Kai et al., 2008). When exposed to UV light, coumarins characteristically exhibit blue fluorescence (Figure 17A, B).

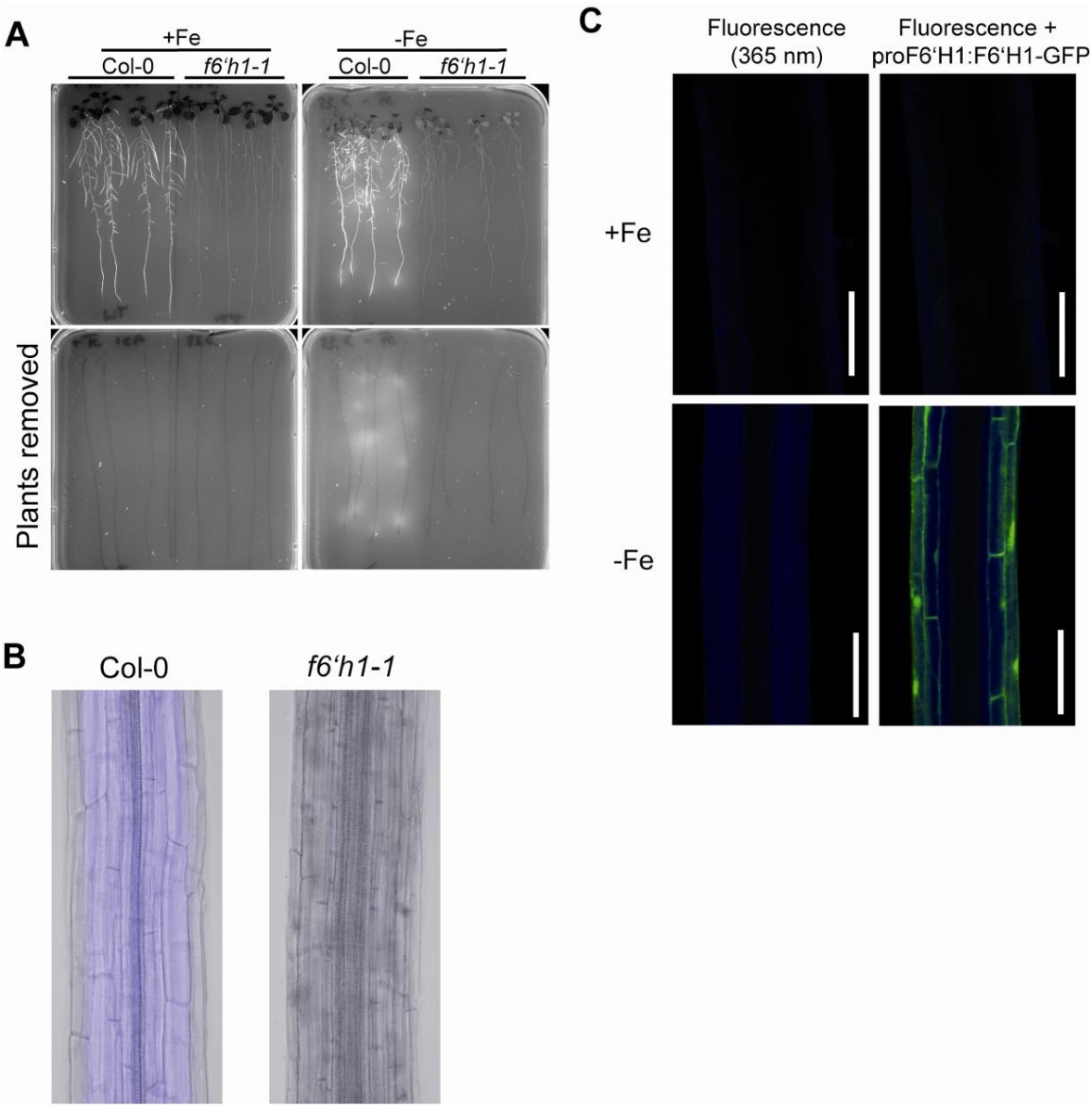

Figure 17. Accumulation of fluorescent compounds in roots and root exudates. (A, upper row) UV fluorescence (365 nm) in wild-type (Col-0) and *f6'h1-1* roots grown under adequate (+Fe) or deficient supply of Fe (-Fe) at pH 5.6. (A, lower row) Root-derived fluorescence on agar after removal of plants. (B) Close-up of UV fluorescence in primary roots of Col-0 and *f6'h1-1* mutant plants under sufficient Fe supply at pH 5.6. (C) Blue fluorescence is induced in epidermal and cortical cells of Fe-deficient (-Fe) plants and coincides with the localization of F6'H1-GFP. Scale bars: 100 µm.

The predominant coumarins occurring in roots of *Arabidopsis thaliana* are scopoletin and its glucoside scopolin, which both accumulate particularly under pathogen stress (Chong et al., 2002; Kai et al., 2008). In line with the function of F6'H1 in the synthesis of coumarins, the roots of *f6'h1-1* and *f6'h1-2* mutant plants (Figure 18A) exhibited no fluorescence under UV light at 365 nm (Figure 17A, B and Figure 18B). Importantly, root-derived fluorescence was strongly increased in wild-type plants grown under Fe deficiency. Furthermore, this fluorescence could still be detected in the agar after wild-type plants had been removed (Figure 17A and Figure 18B), suggesting that root-synthesized fluorescent coumarins were secreted into the medium. A closer inspection of the fluorescence pattern in the mature zone of roots revealed that fluorescence strongly increased in the outer root cells of Fe-deficient plants, co-localizing with the expression of *F6'H1* (Figure 17C).

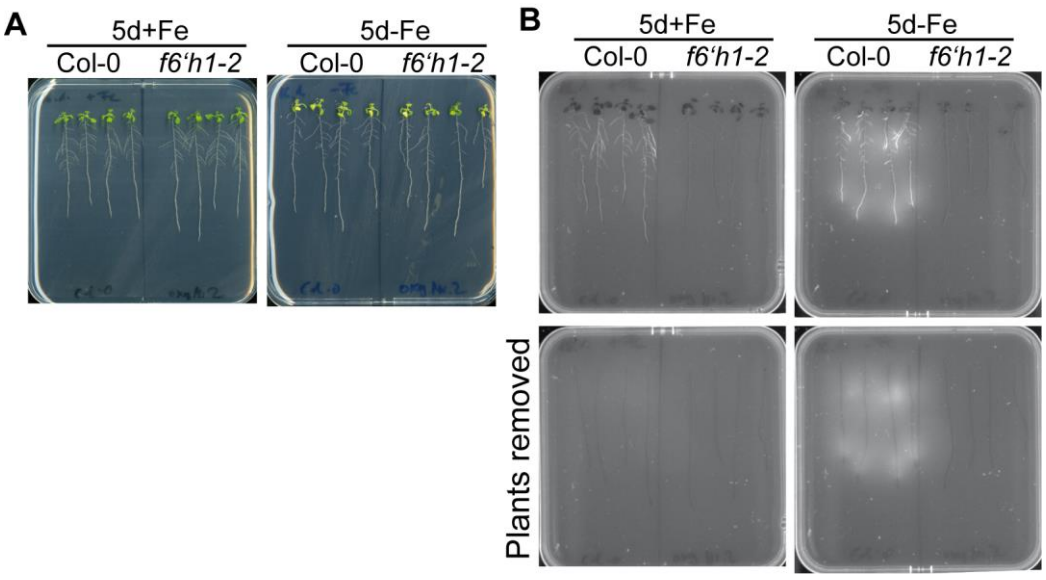

Figure 18. The insertion line *f6'h1-2* displays a similar fluorescence pattern as *f6'h1-1.* (A) Phenotype and (B) UV fluorescence of agar (lower row) and roots (upper row) of wild-type and *f6'h1-2* mutant plants grown under adequate (+Fe) or deficient supply of Fe (-Fe) for 5 days at pH 5.6.

Since *f6'h1-1* roots accumulated less fluorescent phenolic compounds, F6'H1-dependent metabolites produced in response to Fe deficiency were investigated in roots and root exudates of wild-type and mutant plants. For this purpose a system to collect root exudates was established. To collect root exudates, agar-grown

plants were cultured in the presence or absence of Fe for 4 days and then placed for 6 hours in 12-well plates containing ultrapure water (Figure 19B). After 6 hours, a considerable amount of the fluorescent compounds was released (Figure 19A). Furthermore, fluorescence in the collected exudates was strongest in samples obtained from Fe-deficient wild-type plants and was completely absent in root exudates collected from mutant plants or in the water control (Figure 19C).

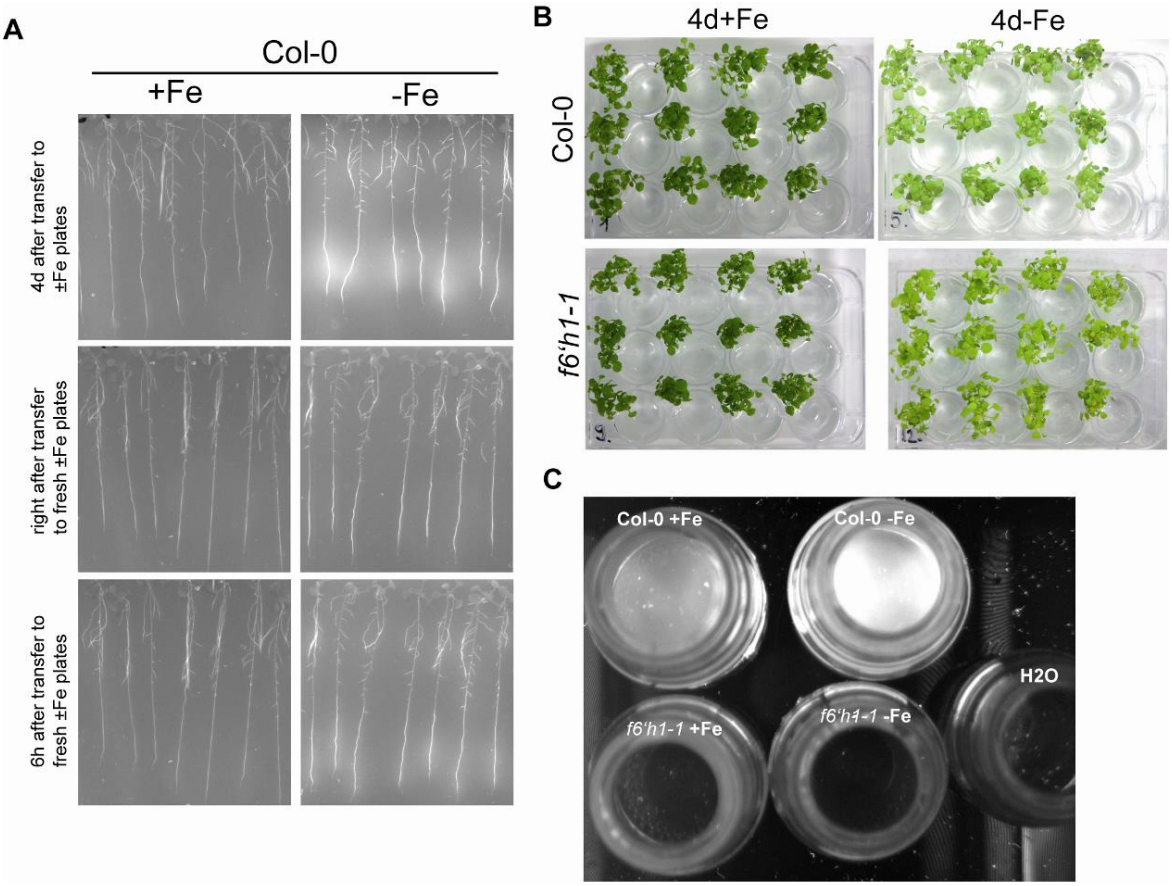

Figure 19. Procedure for the collection of root exudates. (A, upper row) UV fluorescence of wild-type roots on agar plates is strongly enhanced in Fe deficient plants (-Fe) and (A, middle row) not yet visible on agar plates shortly after transfer of the plants to fresh agar plates. (A, lower row) After 6 hours, UV fluorescence on the agar plates is again visibly increased in Fe deficient plants (-Fe). (B) Root exudates were collected from plant roots incubated in ultrapure water for 6 hours on 24 well plates. (C) UV fluorescence of the collected root exudates in 60 ml Schott bottles.

Subsequently, root extracts and exudates of wild-type and *f6'h1-1* plants were compared by ultra performance liquid chromatography coupled with a fluorescence detector (UPLC-FLD). When compared to wild-type root extracts, several fluorescent phenolic compounds belonging to the coumarins were

decreased or not detected in *f6'h1-1* extracts (Figure 20A). In these samples, scopolin was identified as the predominant fluorescent compound in wild-type roots. Since it was observed that some coumarin standards exhibit poor fluorescence under the acidic conditions used during the UPLC separation (data not shown), the chemical analysis was extended by using liquid chromatography coupled to electrospray ionization-mass spectrometry (LC-ESI-MS). This approach allowed the identification of several metabolites that exhibited at least 75% reduction in *f6'h1-1* root exudates as compared to the wild type under sufficient and/or deficient Fe conditions (Table 2, except for esculin). Although some of these metabolites could currently not yet be identified by the analytical approach used here, nine compounds were identified based on their mass and retention times, which are scopolin, scopoletin, esculin, esculetin, fraxetin, isofraxetin, glucoside of dihydroxyscopoletin and isofraxidin/methoxyscopoletin (Table 2). The root extract concentrations of scopolin were quantified by LC-ESI-MS and found to be increased by approximately 40% under Fe deficiency (Figure 20C). In root extracts, the concentrations of scopolin were much higher than those of its aglycon scopoletin (Figure 20E). However, the exudation rate of scopoletin was much more pronounced than that of scopolin, exceeding it by twofold under Fe deficiency (Figure 20B, D and F). Another prominent coumarin detected in root extracts was esculin (Figure 20A and G), even though it accumulated to a 500-fold lower extent than scopolin (Figure 20C and G). The concentration of esculin in root extracts was significantly lower in *f6'h1-1* than in wild-type roots but also decreased in wild-type plants grown under Fe deficiency (Figure 20G). Relative to scopolin and scopoletin, the amount of released esculin was low, irrespective of the Fe nutritional status of the plants (Figure 20H). In quantitative terms esculetin, the aglycon of esculin, was detected in very low amounts in roots (Figure 20I). However, compared to its glycosylated form esculin, root exudation of esculetin was higher, increasing by fourfold under Fe deficiency (Figure 20H and J). Nevertheless, the release of esculetin was by far lower than that of scopoletin (Figure 20F and 5J). In addition, the accumulation in root exudates of fraxetin, isofraxetin, of coumarins tentatively identified as isofraxidin/methoxyscopoletin and eleven unknown metabolites was also increased in Fe-deficient wild-type but not in *f6'h1-1* plants (Table 2). A similar metabolite exudation pattern was also found in the second independent T-DNA insertion line, *f6'h1-2* (Figure 21). Thus, F6'H1 is

required for the synthesis of several fluorescent coumarins under Fe deficiency, several of which also appear in root exudates.

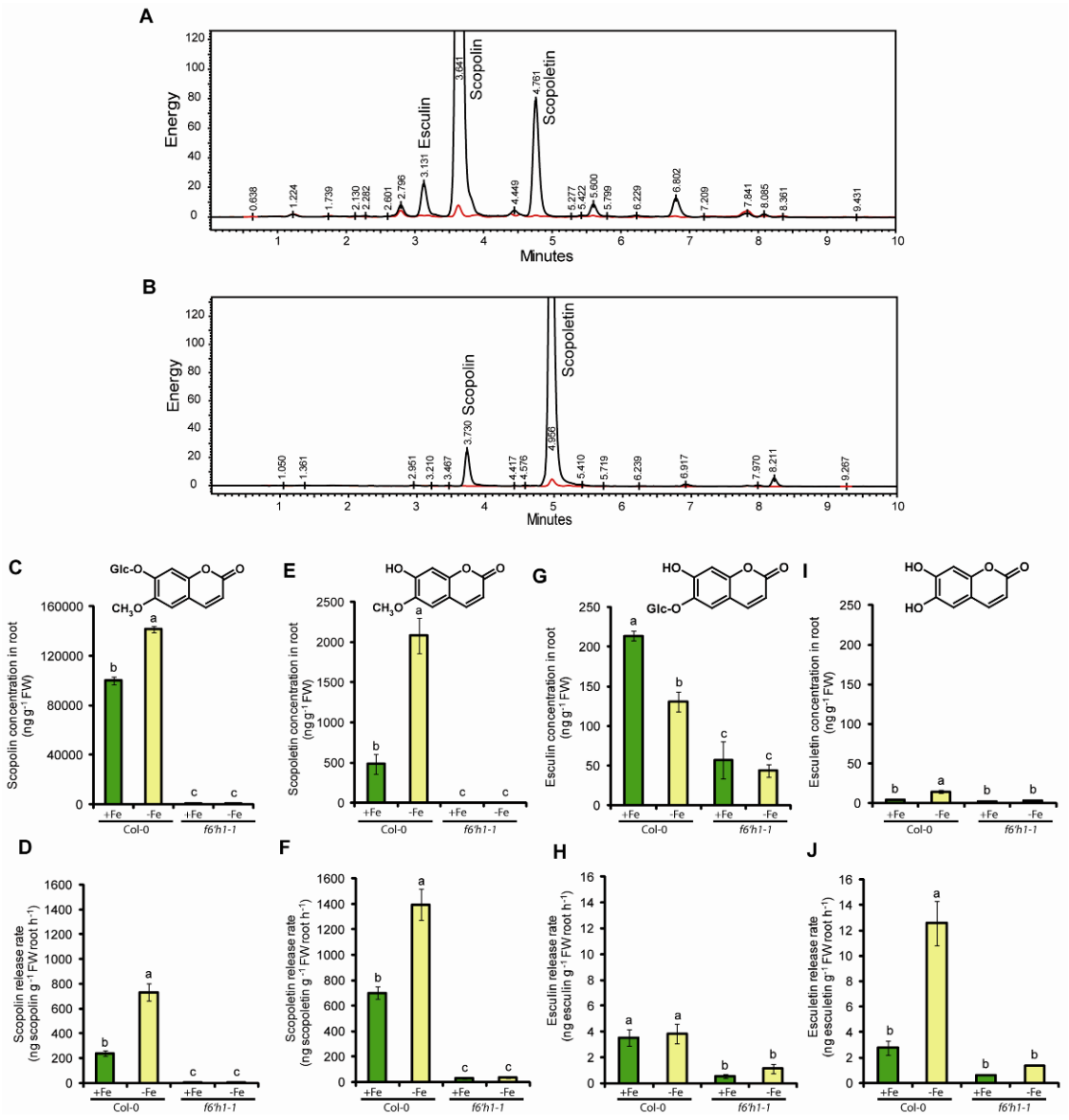

Figure 20. The accumulation of coumarins in root extracts and exudates of *f6'h1-1* plants. UPLC-FLD chromatograms of (A) root extracts or (B) root exudates from wild-type and *f6'h1-1* plants. Black lines indicate wild type and red lines *f6'h1-1* samples. Accumulation of (C, D) scopolin, (E, F) scopoletin, (G, H) esculin and (I, J) esculetin in (C, E, G and I) root extracts or (D, F, H and J) root exudates of wild- type and *f6'h1-1* plants grown under adequate (+Fe) or deficient supply of Fe (-Fe) for 4 days at pH 5.6. Bars indicate means ± SE (n = 3 biological replicates). Different letters indicate significant differences according to Tukey's test ($P < 0.05$). FW refers to fresh weight. Data obtained in cooperation with Dr. Döll, IPK Gatersleben.

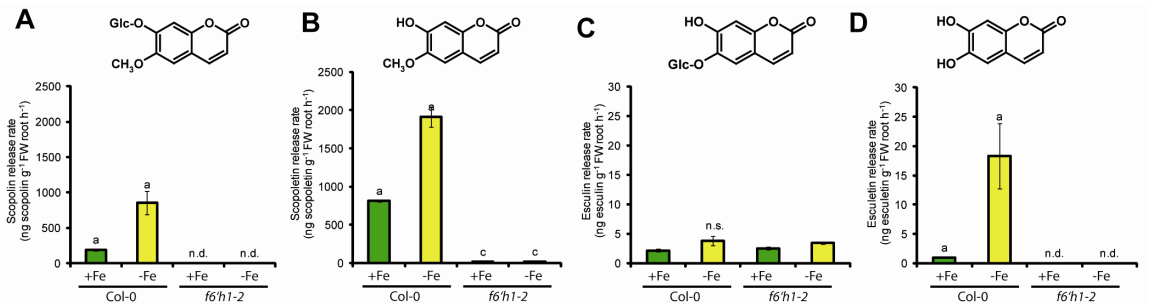

Figure 21. The accumulation of coumarins in root exudates of *f6'h1-2* plants. Accumulation of (A) scopolin, (B) scopoletin, (C) esculin and (D) esculetin in root exudates of wild-type and *f6'h1-2* plants grown under adequate (+Fe) or deficient supply of Fe (-Fe) for 4 days at pH 5.6. Bars indicate means ± SE (n = 3 biological replicates). Different letters indicate significant differences according to Tukey's test ($P < 0.05$). FW refers to fresh weight. Data obtained in cooperation with Dr. Döll, IPK Gatersleben.

Table 2. Compounds identified in the root exudates of wild-type (Col-0) and *f6'h1-1* plants. Plants were grown on sufficient (+Fe) or deficient Fe (-Fe) supplies for 4 days at pH 5.6. The retention times, *m/z* ratios and peak areas were determined by the LC-ESI-MS analysis of the indicated root exudates. Shown are means and ± SE (n = 3 biological replicates). Data obtained in cooperation with Dr. Döll, IPK Gatersleben.

Name	RT	Measured	Calculated	Predicted molecular	Peak areas			
					Col-0		*f6'h1 -1*	
	(min)	*m/z*	*m/z*	formula	+Fe	-Fe	+Fe	-Fe
Esculin*	3.31	341.0874	341.0867	$C_{15}H_{17}O_9^+$	18069 ± 1441	12805 ± 2272	11440 ± 3542	14864 ± 2543
Glycoside of dihydroxyscopoletin**	3.73	M1=225.0395	225.0394 Mother ion = 387.0922	$C_{10}H_9O_6^+$	79301 ± 11365	2641901 ± 117733	3062 ± 696	3377 ± 808
Unknown	3.75	223.0234	223.0237	$C_{10}H_7O_6^+$	18013 ± 3357	101426 ± 2307	4930 ± 79	6258 ± 538
Esculetin*	3.78	179.0332	179.0339	$C_9H_7O_4^+$	15733 ± 3062	49565 ± 5273	10490 ± 5430	8227 ± 831
Scopolin*	3.91	M1=193.0490	193.0495	$C_{10}H_9O_4^+$	226235 ± 19171	571775 ± 16979	5591 ± 861	7379 ± 1093
		M2=355.1027	355.1024	$C_{16}H_{19}O_9^+$	64507 ± 8084	148863 ± 11317	10035 ± 1202	13422 ± 2260
Fraxetin*	4.49	209.0441	209.0444	$C_{10}H_9O_5^+$	25305 ± 5286	225031 ± 117013	8372 ± 975	6299 ± 1240
Unknown	4.54	223.0236	223.0237	$C_{10}H_7O_6^+$	16854 ± 2229	515206 ± 31278	3162 ± 837	4633 ± 1449
Isofraxetin**	4.82	209.0442	209.0444	$C_{10}H_9O_5^+$	53507 ± 12849	1010147 ± 86942	8856 ± 2617	8609 ± 2142
Unknown	5.1	441.1023	441.1028	$C_{19}H_{21}O_{12}^+$	95883 ± 3995	150762 ± 13777	7214 ± 502	5994 ± 1378
Scopoletin*	5.22	193.0492	193.0495	$C_{10}H_9O_4^+$	1996137 ± 77912	3320083 ± 204047	77485 ± 4889	74366 ± 2679
Isofraxidin/Methoxyscopoletin**	5.52	223.0599	223.0601	$C_{11}H_{11}O_5^+$	11777 ± 1904	119054 ± 7690	9529 ± 1778	12124 ± 5768
Isofraxidin/Methoxyscopoletin**	5.89	223.0599	223.0601	$C_{11}H_{11}O_5^+$	14752 ± 2759	115354 ± 6731	6985 ± 2924	7478 ± 3103
Unknown	6.12	248.0554			7528 ± 2316	208094 ± 45482	14483 ± 985	7092 ± 1111
Unknown	7.48	403.1027	403.1024	$C_{20}H_{19}O_9^+$	7178 ± 493	158811 ± 34853	7333 ± 3116	9216 ± 1458
Unknown	7.8	387.1078	387.1074	$C_{20}H_{19}O_8^+$	12018 ± 4139	61725 ± 11846	6042 ± 2716	4739 ± 1430
Unknown	7.96	387.1078	387.1074	$C_{20}H_{19}O_8^+$	16075 ± 4428	158465 ± 24537	8185 ± 1510	9632 ± 1892
Unknown	8.12	387.1078	387.1074	$C_{20}H_{19}O_8^+$	33011 ± 4774	254127 ± 3392	29217 ± 3821	10616 ± 2260
Unknown	8.26	417.1179	417.118	$C_{21}H_{21}O_9^+$	34151 ± 5932	187640 ± 13781	6010 ± 1290	10272 ± 3620
Unknown	8.33	387.1078	387.1074	$C_{20}H_{19}O_8^+$	41095 ± 5026	1074268 ± 18071	8124 ± 2685	5902 ± 987
Unknown	8.55	M1=193.049 M2=335.1005	M1=193.0495	$C_{10}H_9O_4^+$	96864 ± 6764	164994 ± 16606	2018 ± 575	5911 ± 2362

* Identification based on standard.
** Predicted based on literature search.

4.3.4 The Fe(III) mobilization capacity of root exudates from Fe-deficient Arabidopsis plants

Several studies have already shown that Fe deficiency leads to the exudation of various organic compounds in Strategy I plants (Römheld and Marschner, 1983; Welkie, 2000; Jin et al., 2007; Rodriguez-Celma et al., 2011), some of which might possess Fe-mobilizing abilities. A lower secretion of fluorescent compounds, especially upon Fe deficiency, was a very distinctive difference between wild-type and mutant plants (chapter 4.3.3). In order to verify whether this also entails the poor ability of *f6'h1* mutants in accessing Fe under calcareous conditions (Figure 10) the following experiment was performed. Root exudates were collected from wild-type and *f6'h1-1* plants grown axenically with or without Fe. Then, the ability of these root exudates in mobilizing Fe(III) from freshly prepared Fe hydroxide at alkaline conditions was compared. The Fe mobilization capacity of exudates did not differ significantly between the two genotypes grown under sufficient Fe supply (Figure 22 and Figure 23A). However, the root exudates collected from Fe-deficient wild-type plants were able to mobilize 17-fold more Fe than the exudates collected from Fe-sufficient plants (Figure 23A). Importantly, the Fe mobilization capacity of root exudates of *f6'h1-1* and *f6'h1-2* plants grown under Fe deficiency remained low (Figure 22 and Figure 23A).

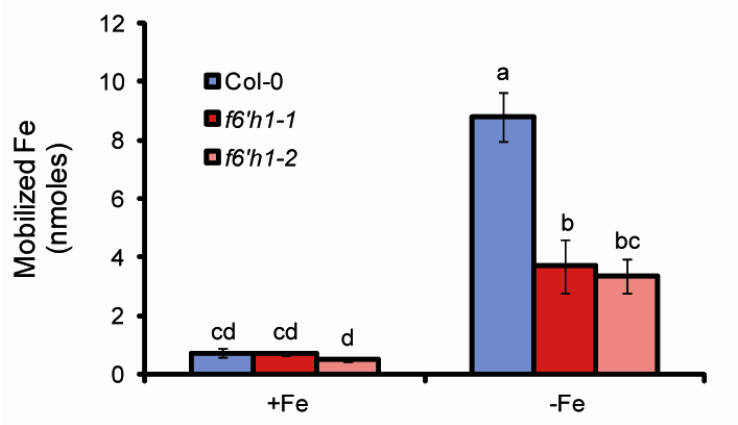

Figure 22. Fe(III) mobilization capacity of exudates collected from wild-type, *f6'h1-1* and *f6'h1-2* roots. Fe(III) mobilization capacity of root exudates from plants grown for 4 days in the presence (+Fe) or absence of Fe (-Fe). During the assay, 0.05 ml exudates were incubated with 1.95 ml of 0.1 mM precipitated Fe(III)-hydroxide at pH 7.2 and the amount of solubilized Fe was detected by HR-ICP-MS. Bars indicate means ± SE (n = 3 replicates). Different letters indicate significant differences according to Tukey's test ($P < 0.05$).

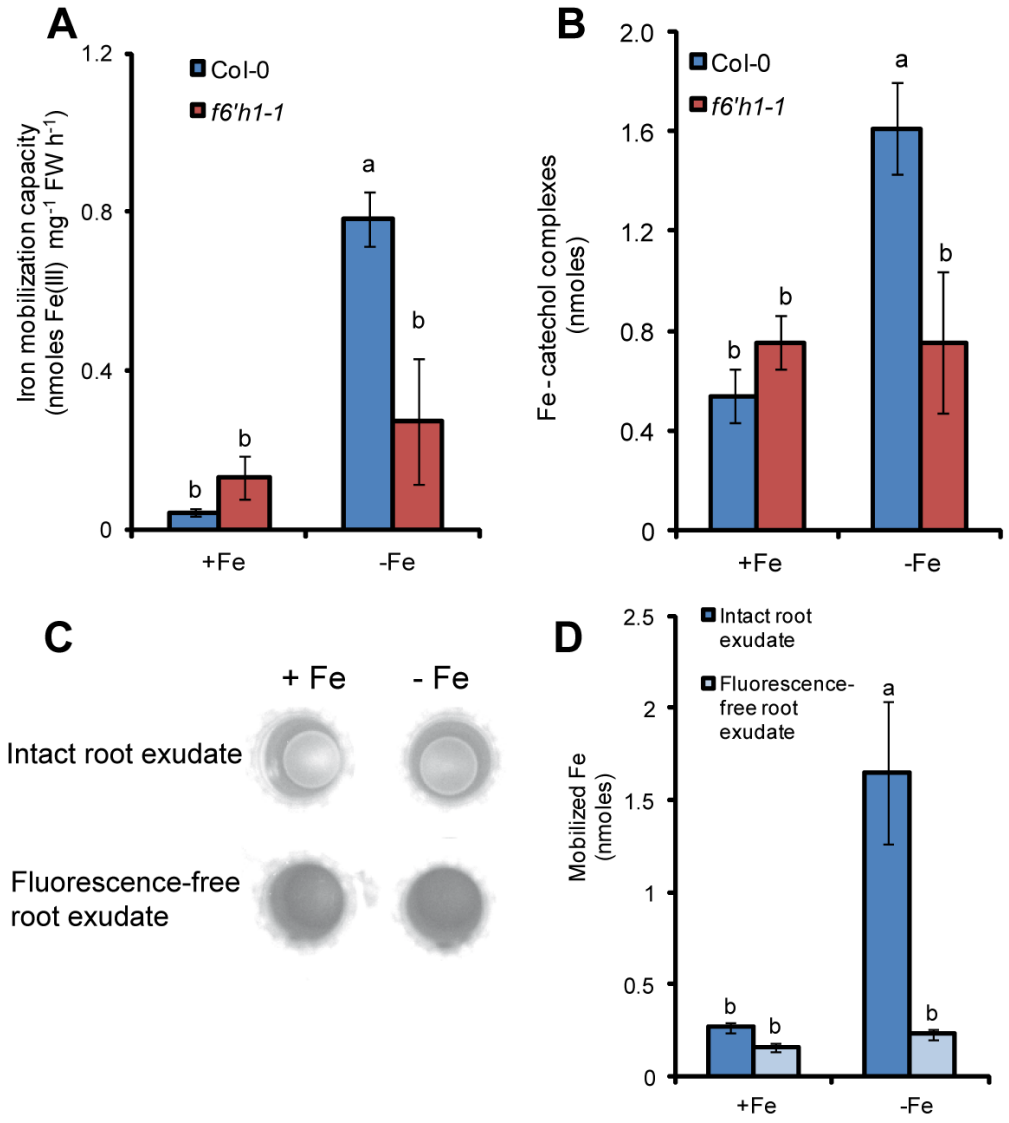

Figure 23. Fe(III) mobilization capacity of root exudates. (A) Fe(III) mobilization capacity of root exudates from wild-type (Col-0) or *f6'h1-1* plants grown for 4 days in the presence (+Fe) or absence of Fe (-Fe). During the assay, 0.05ml of exudates were incubated with 1.95 ml of 0.1 mM precipitated Fe hydroxide at pH 7.2 and the amount of solubilized Fe was detected by HR-ICP-MS. (B) Accumulation of Fe-catechol complexes detected at 460 nm after the incubation of root exudates with Fe hydroxide. (C) Fluorescent compounds were removed from root exudates of Fe-sufficient (+Fe) or Fe-deficient (-Fe) wild-type (Col-0) plants by passing through a Sep-Pak C18 column and (D) their Fe(III) mobilization capacity at pH 7.2 was assessed as described in (A). Bars indicate means ± SE (n = 3 replicates). Different letters indicate significant differences according to Tukey's test ($P < 0.05$). FW refers to fresh weight.

In order to determine whether the Fe(III) mobilization capacity of root exudates was related to the formation of Fe complexes with catechols, their formation was measured spectrophotometrically at 460 nm which is indicative for the formation of Fe(III)-catechol complexes (McBryde, 1964; Salama et al., 1978; Ormö et al., 1992). When exudates from Fe-deficient wild-type plants were mixed with Fe

hydroxide, significantly more Fe(III)-catechol complexes were detected (Figure 23B). However, it is noteworthy that the formation of Fe-catechol complexes did not completely mirror the difference in Fe(III) mobilization capacity observed when growing plants under adequate versus deficient Fe supply (Figure 23A and B). This suggested either that other components of the root exudates contributed to the overall Fe(III) mobilization capacity or that the absorption at 460 nm also detected other Fe complexes. As an approach to determine the contribution of the fluorescent compounds in the Fe(III) mobilization capacity of root exudates, these compounds were removed from the root exudates of wild-type plants by using a Sep-Pak C18 column. In fact, passing the root exudates through this column removed almost completely UV fluorescence from the exudate samples (Figure 23C). The withdrawal of fluorescent and maybe further C18-immobilized compounds from the root exudates of Fe-deficient roots decreased significantly the Fe(III) mobilization capacity of these exudates (Figure 23D). Altogether, these results show that the increased secretion of fluorescent phenolic compounds by Fe-deficient plants enhances the capacity for the mobilization of Fe(III) from Fe hydroxide precipitates under alkaline conditions.

4.3.5 Addition of coumarins to Fe-deficient chlorotic *f6'h1-1* and *f6'h1-2* mutant plants

Among the identified F6'H1-dependent coumarins, esculetin was of particular interest because it accumulated in root exudates (Figure 20J) and because it represents a dihydroxy-coumarin with two adjacent hydroxy groups (Figure 20I) thus resembling catechol-type siderophores (Hider and Kong, 2010). It is noteworthy that esculin and scopoletin also exhibit such a moiety, but in these compounds the 6'-hydroxy position is made inaccessible by the conjugation of a glucoside or a methyl group, respectively (Figure 20E and G). To test whether these compounds could prevent Fe deficiency-induced chlorosis in *f6'h1-1* plants, they were supplied exogenously to plants grown under conditions where Fe availability was decreased. In the presence of exogenous esculetin, *f6'h1-1* shoots remained green and had leaf chlorophyll and Fe concentrations comparable to wild-type plants and to *f6'h1-1* plants supplied with EDTA (Figure 24A, B and C).

Interestingly, also esculin and scopoletin prevented *f6'h1-1* plants from chlorosis and from falling below critical deficiency levels for Fe. These effects were also obtained when the plants were grown on agar plates at pH 7.2, i.e. under conditions of increased Fe insolubility (Figure 25). On calcareous substrate, both esculin and esculetin were also able to rescue the chlorotic phenotype of *f6'h1-1* and *f6'h1-2* mutant plants (Figure 27). However, when coumarins were supplied to *f6'h1-1* plants in the absence of an additional external source of Fe, they were not able to prevent the development of severe Fe deficiency symptoms in these plants (Figure 26). Accordingly, these results suggest that the coumarins released by Fe-deficient plants are able to mobilize Fe from otherwise unavailable sources.

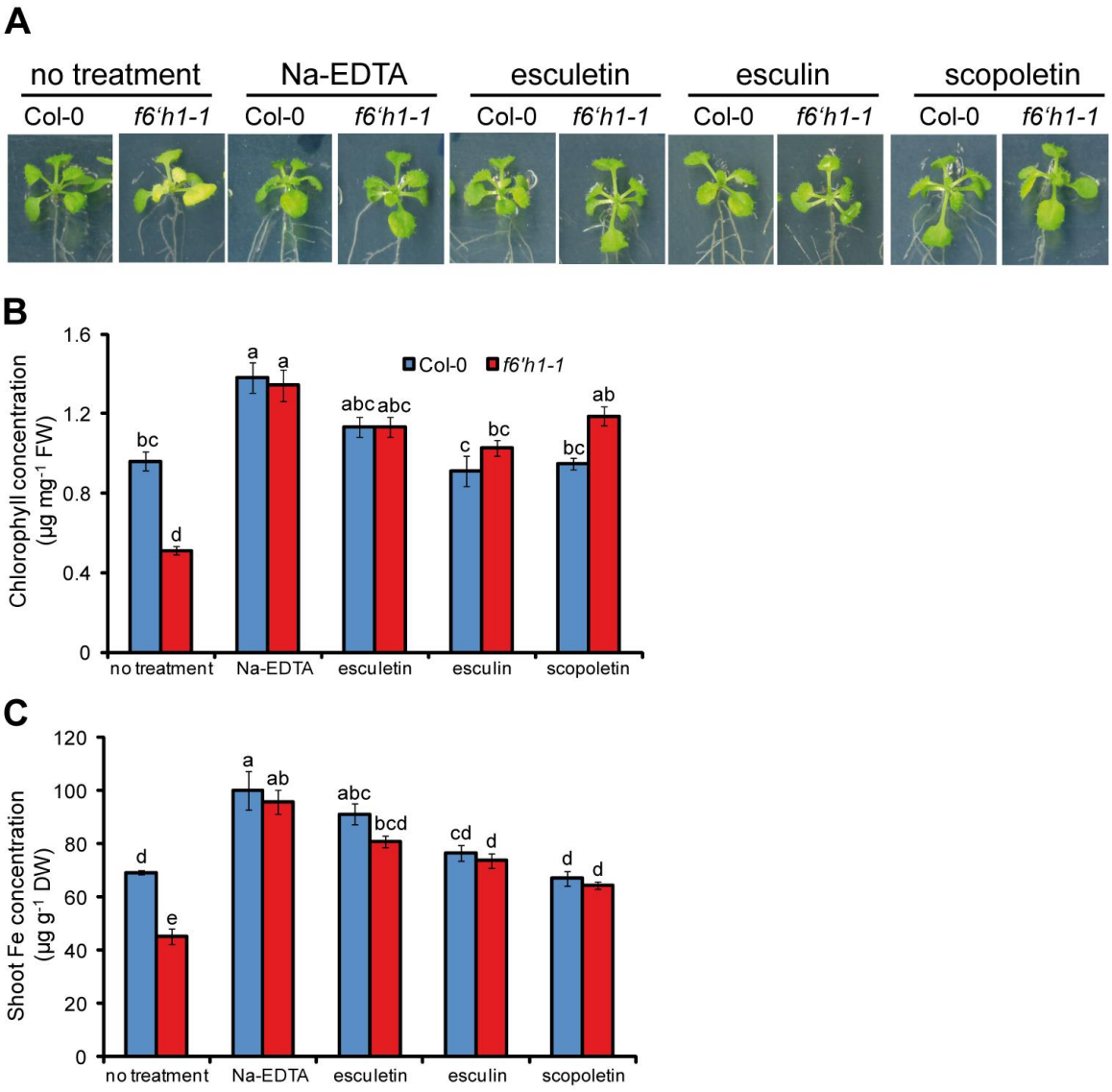

Figure 24. Effect of several coumarins on Fe deficiency-induced chlorosis in *f6'h1-1* plants under low Fe availability at pH 5.6. (A) Phenotype, (B) chlorophyll and (C) shoot Fe concentrations of wild-type (Col-0) and mutant (*f6'h1-1*) plants grown on agar plates at pH 5.6. Plants were grown for 10 days on ½ MS agar at pH 5.6 before transfer for 6 days onto ½ MS agar supplemented with 50 µM $FeCl_3$ (no treatment) or additionally 160 µM Na-EDTA, 500 µM esculetin, 500 µM esculin or 500 µM scopoletin at pH 5.6. Bars represent means ± SE (n = 5 biological replicates). Different letters indicate significant differences according to Tukey's test ($P < 0.05$). FW and DW refer to fresh weight and dry weight, respectively.

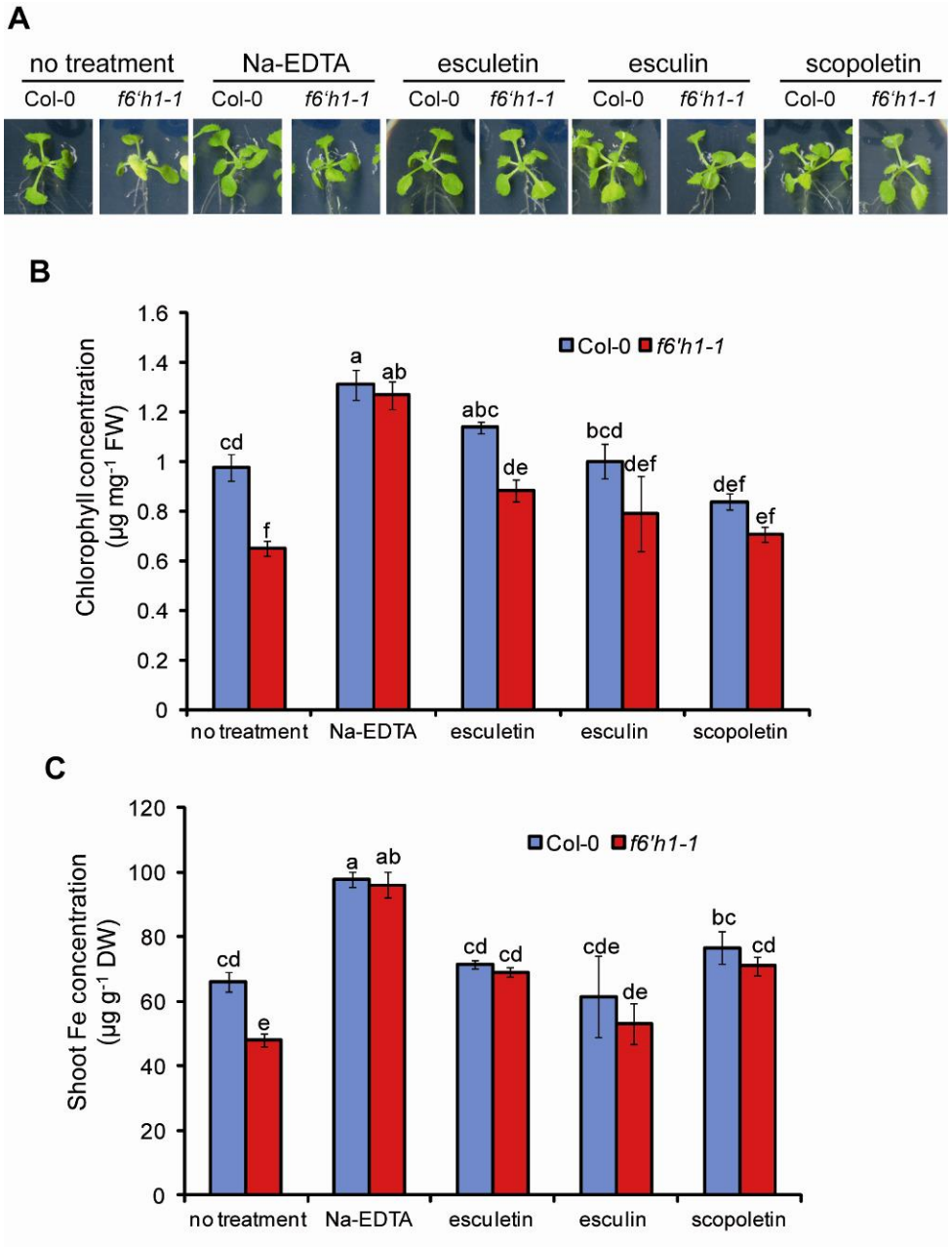

Figure 25. Effect of several coumarins on Fe deficiency-induced chlorosis in *f6'h1-1* plants under low Fe availability at pH 7.2. (A) Phenotype, (B) chlorophyll and (C) shoot Fe concentrations of wild-type (Col-0) and mutant (*f6'h1-1*) plants grown on agar plates at pH 7.2. Plants were grown for 10 days on ½ MS agar at pH 5.6 before transfer for 6 days onto ½ MS agar supplemented with 50 µM $FeCl_3$ (no treatment) or additionally 160 µM Na-EDTA, 500 µM esculetin, 500 µM esculin or 500 µM scopoletin at pH 7.2. Bars represent means ± SE (n = 4-9 biological replicates). Different letters indicate significant differences according to Tukey's test ($P < 0.05$). FW and DW refer to fresh weight and dry weight, respectively.

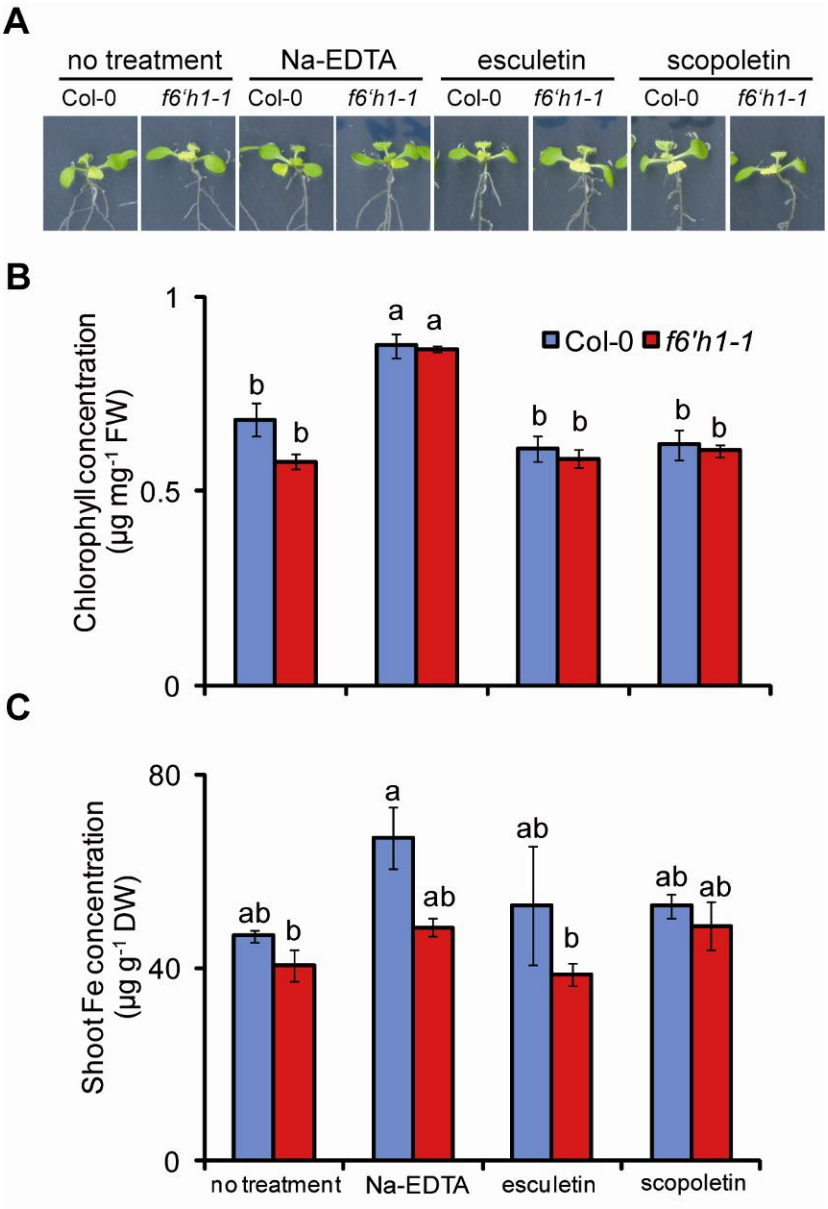

Figure 26. Effect of esculetin and scopoletin on Fe deficiency-induced chlorosis in *f6'h1-1* plants in the absence of an external Fe source at pH 5.6. (A) Phenotype, (B) chlorophyll and (C) shoot Fe concentrations of wild-type (Col-0) and mutant (*f6'h1-1*) plants grown for 8 days on ½ MS agar at pH 5.6 before transfer for 5 days onto ½ MS agar in the absence of an external Fe source (no treatment) or additionally 160 µM Na-EDTA, 500 µM esculetin, 500 µM esculin or 500 µM scopoletin at pH 5.6. Bars represent means ± SE (n = 5 biological replicates). Different letters indicate significant differences according to Tukey's test ($P < 0.05$). FW and DW refer to fresh weight and dry weight, respectively.

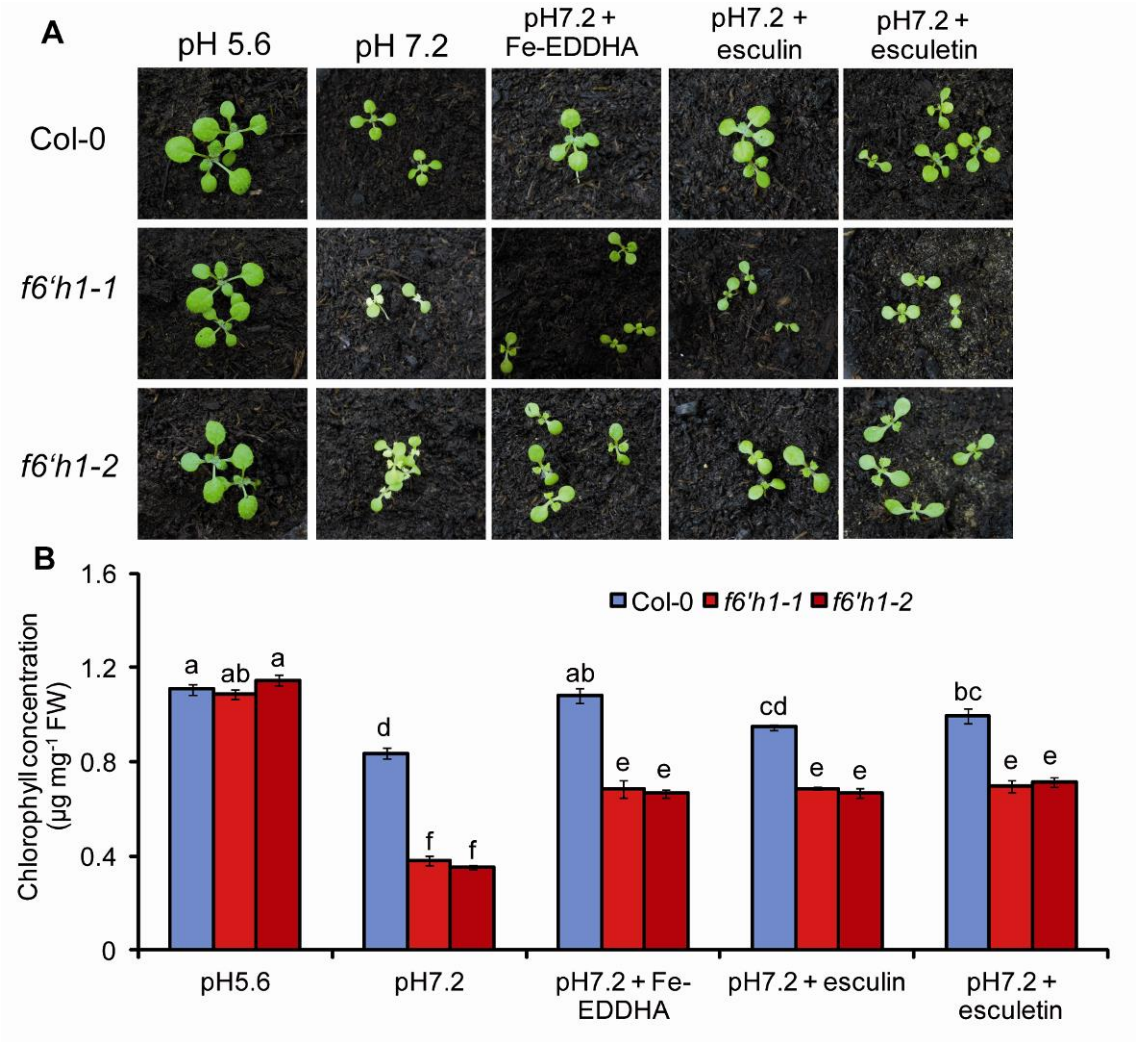

Figure 27. Addition of esculin or esculetin to chlorotic *f6'h1-1,* and *f6'h1-2* plants grown on calcareous substrate. (A) Phenotype and (B) chlorophyll concentrations of whole shoots of wild-type (Col-0), *f6'h1-1* and *f6'h1-2* mutant plants after growing for 17 days on non-limed (pH 5.6) or limed substrate (pH 7.2). To alleviate leaf chlorosis at pH 7.2, plants were supplied with 2.0 mL of a 0.5 g L^{-1} Fe-sequestrene (6% Fe(III)-EDDHA) solution (+Fe-EDDHA), 29 mM esculin or 34 mM esculetin solution for 4 days before the end of the experiment. Bars represent means ± SE (n = 5-8 biological replicates). Different letters indicate significant differences to Tukey's test ($P < 0.05$). FW refers to fresh weight.

4.3.6 Performance of *F6'H1* overexpressing lines in comparison to wild-type and *f6'h1-1* mutant plants

The results presented before showed that an increased release of *F6'H1*-dependent coumarins, as occurring under conditions of Fe deficiency, also led to an increased ability to mobilize Fe(III) (Figure 22 and Figure 23A). Furthermore, the addition of some of these F6'H1-dependent coumarins to chlorotic mutant plants increased their Fe acquisition (Figure 24, Figure 25 and Figure 27). In an effort to increase the Fe(III) mobilizing capacity of wild-type plants under

conditions where Fe is sparingly available, transgenic lines overexpressing *F6'H1* under control of the cauliflower mosaic virus *35S* promoter were generated. Six lines exhibiting at least 100-fold higher *F6'H1* expression than wild-type plants (Figure 28) were selected for further analysis.

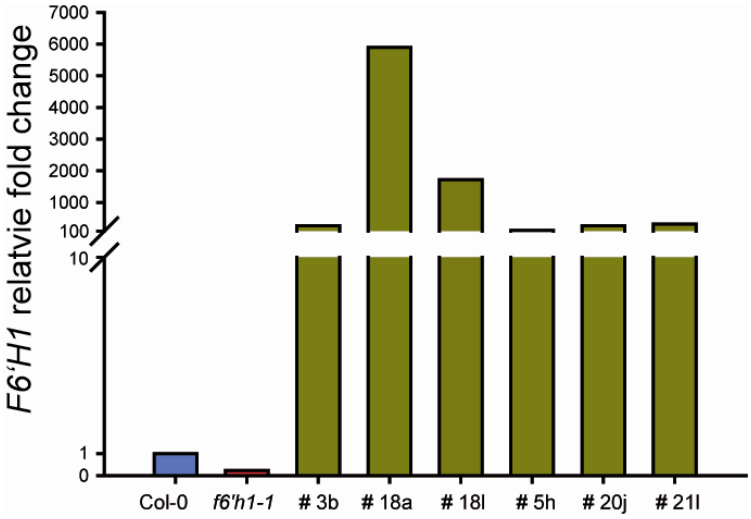

Figure 28. Relative expression level of *F6'H1*. The expression level of *F6'H1* was determined by quantitative RT-PCR on cDNA from pooled shoot samples of 25-30 single plants respectively, of wild type (Col-0), *f6'h1-1* and the transgenic lines after growth for 14 days on ½ MS medium at pH 5.6.

First the growth of the six *35S:F6'H1* lines (line 3b, line 18a, line 18l, line 5h, line 20j and line 21l) was assessed on limed substrate to investigate whether they may perform better than the chlorotic wild type. For comparison, the lines were also grown on non-limed substrate where they did not differ visibly from wild-type or *f6'h1-1* mutant plants. On limed substrate all 6 transgenic lines developed chlorosis similar to wild-type plants, but not as strong as the *f6'h1-1* mutant plants (Figure 29A). Solely line 18l appeared a bit bigger in terms of shoot size, but both shoot fresh and dry weight did not differ from wild-type values (Figure 29C and E). This was also the case for chlorophyll concentrations, suggesting that the nutritional status of the transgenic lines was not superior (Figure 29B). Moreover, the transgenic lines failed to accumulate more shoot Fe (Figure 29D). Some transgenic lines (line 18a and 5h) had even lower shoot Fe contents than wild-type plants.

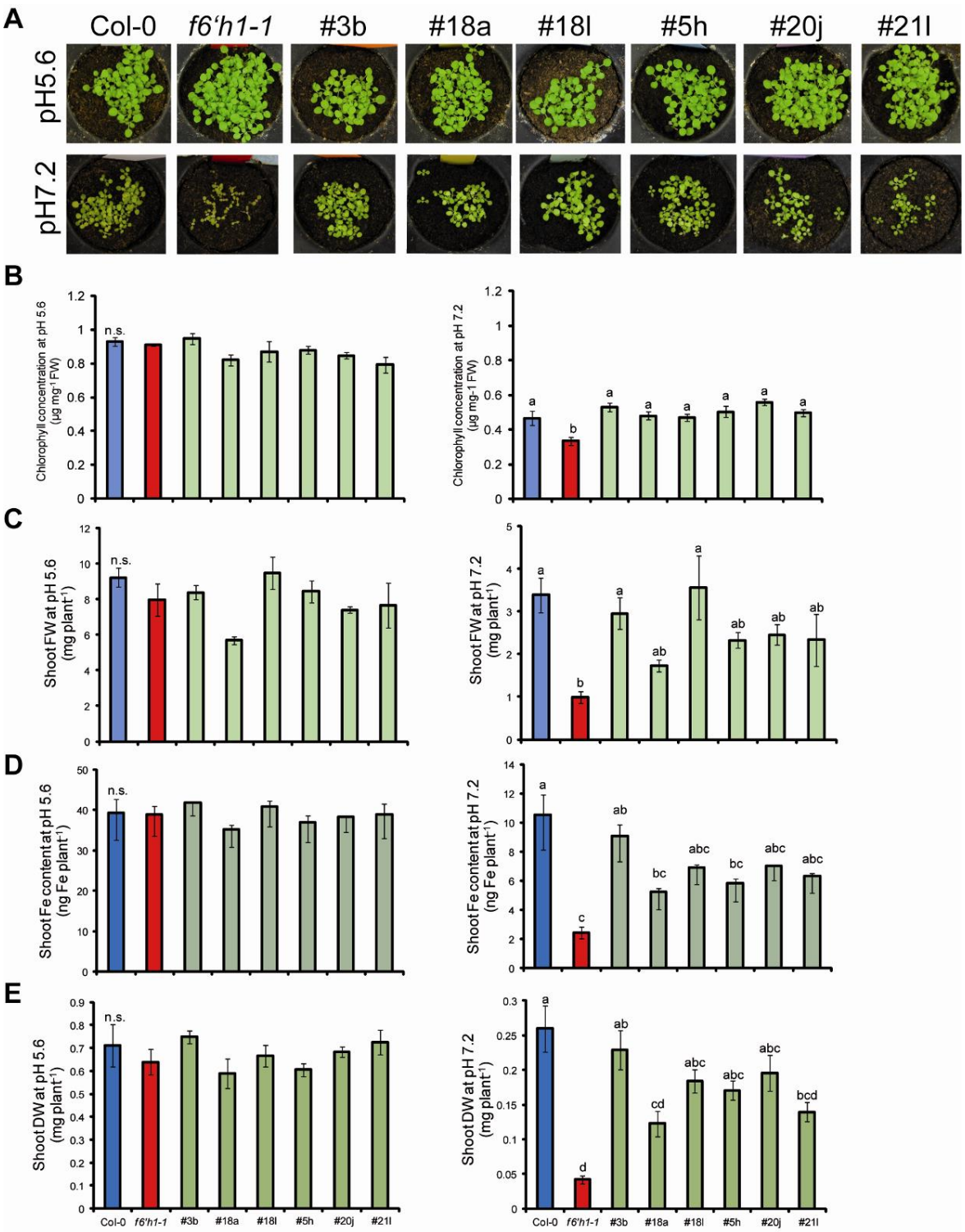

Figure 29. Phenotypic characterization of *F6'H1*-overexpression lines. (A) Wild type (Col-0), *f6'h1-1* insertion and F6'H1-overepressing lines were grown for 17 days on non-limed substrate at pH 5.6 or limed substrate at pH 7.2 (21g kg^{-1} $CaCO_3$ and 13g kg^{-1} $NaHCO_3$). (B) Chlorophyll concentrations and (D) Fe content in shoots as well as (C) shoot FW and (E) shoot DW of lines grown as indicated in (A). Bars represent means ± SE (n = 3-7 replicates). Different letters indicate significant differences according to Tukey's test ($P < 0.05$). FW and DW refer to fresh weight and dry weight, respectively.

Additionally, all 6 transgenic lines were also tested on agar plates. At this stage of the investigations these lines were grown under conditions where Fe was highly available (provided as Fe-EDTA) or omitted completely from the medium (no Fe but 50 µM ferrozine added), to be able to study the root fluorescence pattern just as described in Figure 17A. Under Fe sufficiency, none of the 6 transgenic lines displayed stronger fluorescence than the wild type. Moreover, only lines 5h, 20j and, to a lower extent also line 3b, showed consistently stronger root fluorescence under Fe deficiency which achieved a similar level as in wild-type roots (Figure 30B). None of the transgenic lines exhibited stronger fluorescence than the wild type. As to be expected, when Fe was readily available, there was no significant difference in shoot Fe concentrations between the transgenic lines and the wild type (Figure 30C).

Taken together, the transgenic lines did not perform better in terms of tolerance to Fe deficiency-induced chlorosis or of Fe and chlorophyll levels under the growth conditions tested so far.

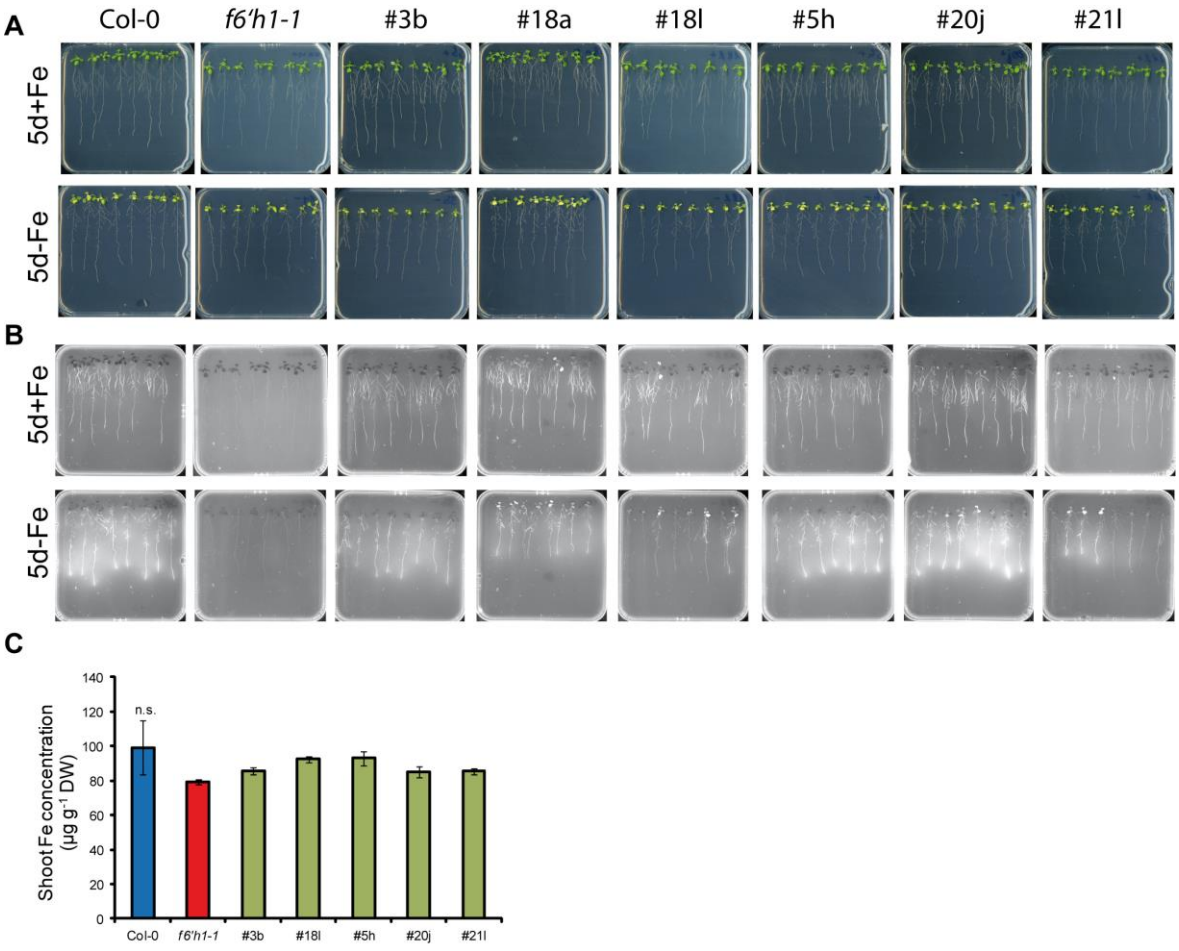

Figure 30. Phenotypic characterization of *F6'H1*-overexpression lines in dependence of Fe supply. (A-C) Growth phenotype, root fluorescence and shoot Fe concentrations from plants pre-cultured for 10 days on 40 µM Fe-EDTA before transfer to agar medium supplemented with 40 µM Fe-EDTA (+Fe) or without Fe (-Fe) for 5 days at pH 5.6. Bars represent means ± SE (n = 3 biological replicates). Different letters indicate significant differences according to Tukey's test ($P < 0.05$). DW refers to dry weight.

4.3.7 The interplay of several Fe acquisition genes in the secretion of F6'H1-dependent fluorescent phenolics

The Fe-dependent and cell type-specific expression pattern of *F6'H1* (Figure 14, Figure 15 and Figure 16) is reminiscent to that of other genes involved in Fe acquisition, such as *IRT1* and *FRO2*, which are regulated by the bHLH-type transcription factor FIT (Colangelo and Guerinot, 2004). Thus, the transcriptional regulation of *F6'H1* as well as its role amongst the well-known Fe acquisition genes has been investigated.

4.3.7.1 Involvement of the transcription factor FIT in *F6'H1* expression and the secretion of fluorescent compounds

Firstly, to study whether *F6'H1* is also under the control of FIT, quantitative real-time PCR on cDNA obtained from roots of Fe-sufficient or –deficient *fit* mutants was performed. Just as *IRT1* up-regulation in response to Fe deficiency requires a functional FIT (Figure 31B), also *F6'H1* does (Figure 31A). Consistent with the de-regulated *F6'H1* expression in the *fit* mutant, *fit* roots failed to exhibit an increased accumulation and release of fluorescent compounds when grown under Fe deficiency (Figure 32A). Moreover, overexpression of *FIT* led to an increase of fluorescence only under Fe deficiency and remained normal in Fe sufficient roots, just as observed for the wild type (Figure 32B).

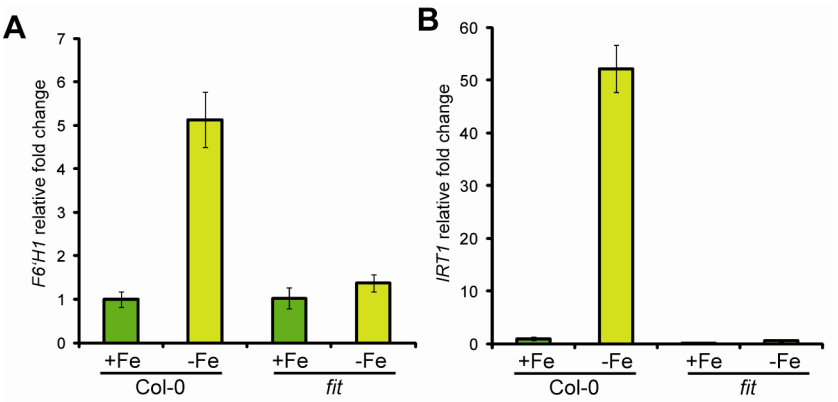

Figure 31. *F6'H1* expression in roots of the *fit* mutant. (A) *F6'H1* and (B) *IRT1* expression was determined in wild-type and *fit* roots 4 days after transfer to Fe-sufficient (+Fe) or -deficient (-Fe) conditions at pH 5.6. Bars indicate means ± SE (n = 5-6 replicates).

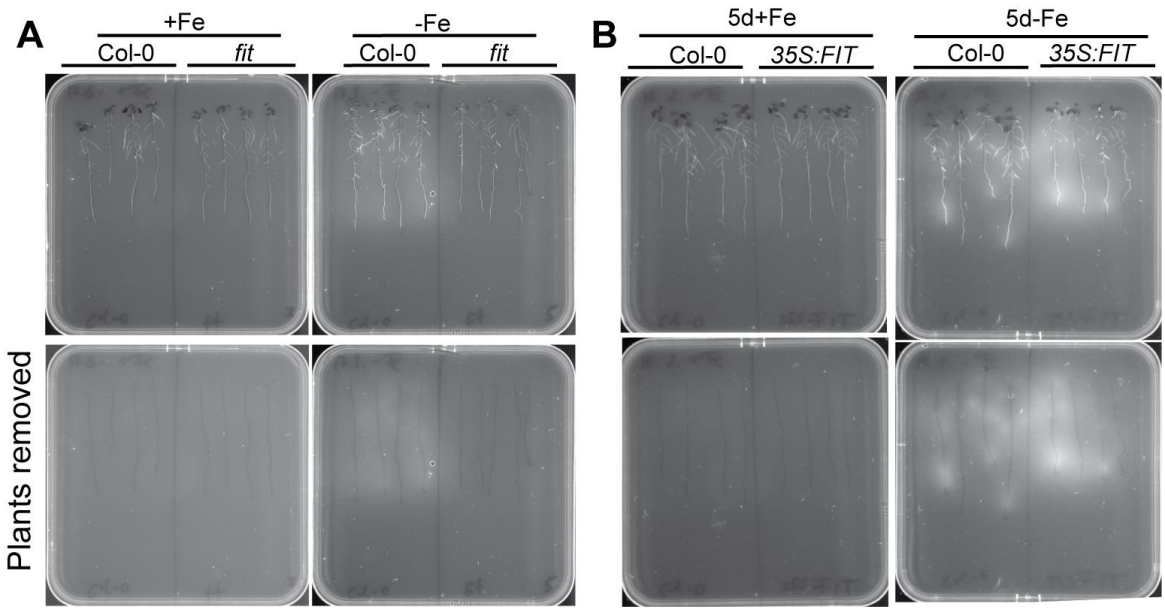

Figure 32. Fluorescence of roots and root exudates of Fe-deficient *fit* and *35S:FIT* plants. (Upper row) UV fluorescence (365 nm) in wild type (Col-0), *fit* (A) or *35S:FIT* (B) roots grown under adequate (+Fe) or deficient supply of Fe (-Fe). (Lower row) Root-derived fluorescence on agar after removal of plants. Wild-type (Col-0) and *fit* plants were germinated and grown on ½ MS (75 µM Fe-EDTA) for 10 days. Plants were then transferred to ½ MS without Fe but 50 µM ferrozine added (-Fe) or supplemented with 75 µM Fe-EDTA (+Fe) at pH 5.6. Fluorescence was detected in roots and in the agar under UV light (365 nm).

The *fit* mutant is defective in the expression of the main Fe acquisition genes (Colangelo and Guerinot, 2004) and is barely able to survive even on non-limed substrate (Figure 33A). As this mutant obviously failed secreting fluorescent compounds under Fe deficiency (Figure 32), the question arose to which extent this shortcoming accounts for its chlorotic phenotype. When treated with generous amounts of Fe it slowly recovered from its strong chlorosis even on pH 7.2 (Figure 33A and C). On the contrary, the addition of esculin failed to regreen this mutant on either non-limed or limed substrate, and shoot chlorophyll concentrations remained low (Figure 33B and C). Altogether, these results suggest that *F6'H1* belongs to the FIT-regulated Fe acquisition machinery in Arabidopsis roots and that a Fe-deficient release of fluorescent compounds requires the full function of this transcription factor.

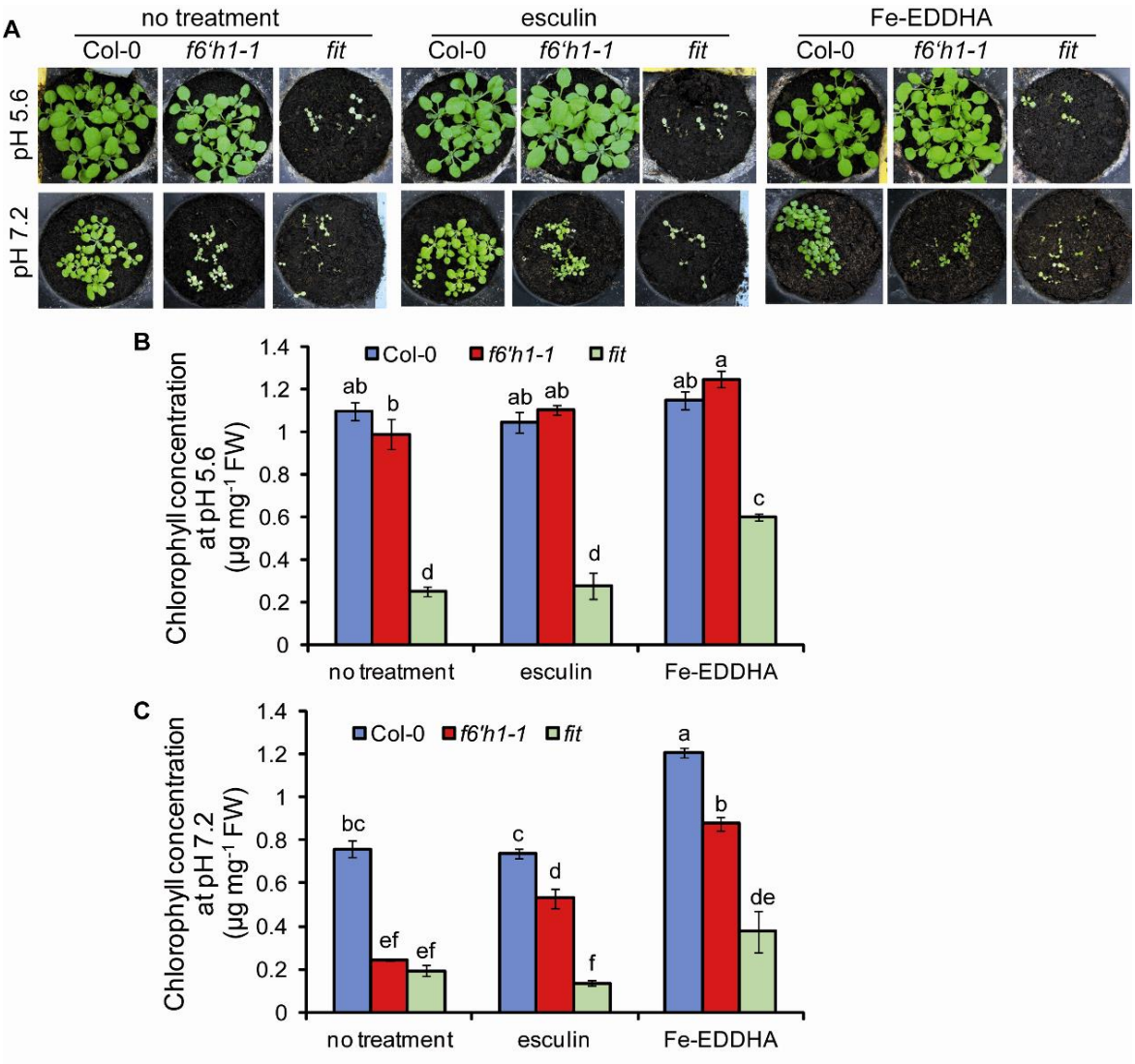

Figure 33. Phenotypic analysis of the *fit* mutant after addition of esculin. (A) Wild-type (Col-0), *f6'h1-1* and *fit* plants were grown for 19 days on non-limed substrate at pH 5.6 or limed substrate at pH 7.2. Plants were supplied with 2.0 mL of a 0.5 g L^{-1} Fe-sequestrene (6% Fe(III)-EDDHA) solution (+Fe-EDDHA) or 29 mM esculin solution for 6 days before the end of the experiment. (B, C) Chlorophyll concentrations in shoots of wild-type, *f6'h1-1* and *fit* mutant plants grown as indicated in (A) at pH 5.6 (B) or pH 7.2 (C). Bars represent means ± SE (n = 3-5 replicates). Different letters indicate significant differences according to Tukey's test ($P < 0.05$). FW refers to fresh weight.

4.3.7.2 Investigation of root fluorescence in the *myb72* insertion line and the *MYB72*-overexpressor line under Fe deficiency

According to the microarray study of Colangelo and Guerinot (2004), the Fe deficiency-mediated up-regulation of *MYB72* depends at least partially on a functional FIT. This is reminiscent of *F6'H1*, whose Fe regulation mainly depends on this transcription factor (Colangelo and Guerinot, 2004; Figure 31). As shown in Figure 8, *MYB72* expression increased upon Fe deficiency and according to

Figure 6A, the *myb72* T-DNA insertion line developed a strong chlorosis in alkaline substrate, that could be reverted by adding a highly available Fe source (Figure 6B). These data suggest an involvement of *MYB72* in Fe homeostasis and in particular Fe acquisition. Thus, root fluorescence under conditions of Fe deficiency was also observed in *myb72*. Under sufficient Fe supply, the root fluorescence in the mutant did not differ from that of wild-type plants. But when plants were grown in the absence of Fe, conditions in which the wild type showed increased root fluorescence, *myb72* root fluorescence remained low and did not increase further (Figure 34A, B). This was similar as observed for the *fit* mutant (Figure 32). In transgenic lines that constitutively overexpress *MYB72* (Van der Ent et al., 2008) a strong increase in root fluorescence was observed in plants even when grown with adequate supply of Fe (Figure 34C). In the absence of Fe, root fluorescence remained high, even to a higher extent than observed in Fe-deficient wild-type plants (Figure 34C).

These results indicate that *MYB72* expression is required for the characteristic release of fluorescent metabolites by Fe-deficient roots.

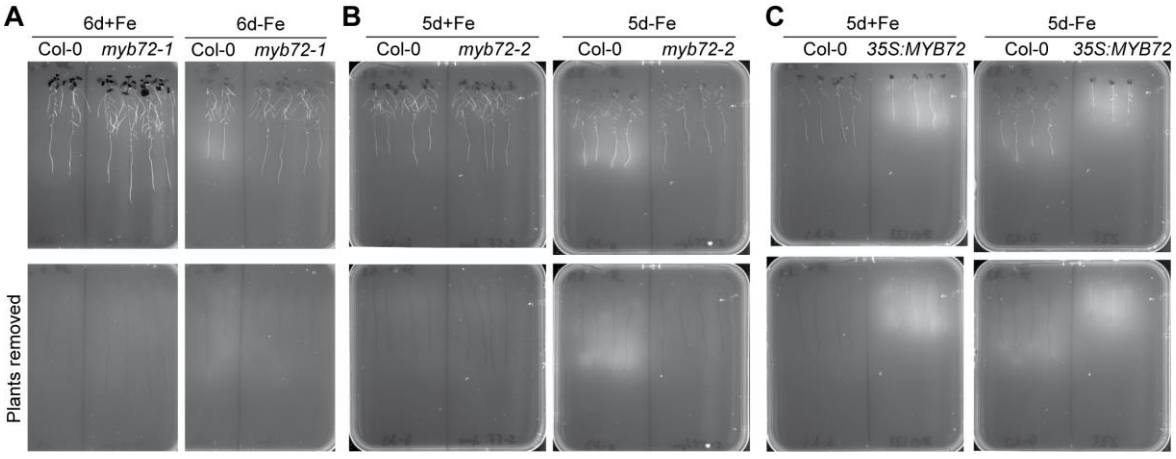

Figure 34. Fluorescence of roots and root exudates of *myb72* and *35S:MYB72* plants. UV fluorescence (365 nm) in wild type (Col-0), *myb72-1*, *myb72-2* and *35S:MYB72* roots grown under sufficient (+Fe; 75 µM Fe-EDTA) or deficient supply of Fe (-Fe, 50 µM ferrozine added) for 5 or 6 days at pH 5.6. Plants were pre-cultured on ½ MS 75 µM Fe-EDTA for 10 days.

4.3.7.3 Growth performance of the *irt1* mutant after addition of F6'H1-dependent coumarins in dependence of Fe availability

F6'H1-dependent fluorescent metabolites are able to mobilize and chelate Fe(III) (Figure 23). In an attempt to study whether IRT1, the major transporter required for high-affinity Fe uptake under Fe deficiency (Vert et al., 2002), can be bypassed when plants are provided with coumarin-chelated Fe(III), chlorotic *irt1* plants were supplied with esculetin, esculin or scopoletin. When grown on non-limed or limed substrate, only Fe-EDDHA was able to regreen the *irt1* mutant, whereas the addition of esculetin and esculin failed to correct the chlorosis that even developed on a non-limed substrate (Figure 35).

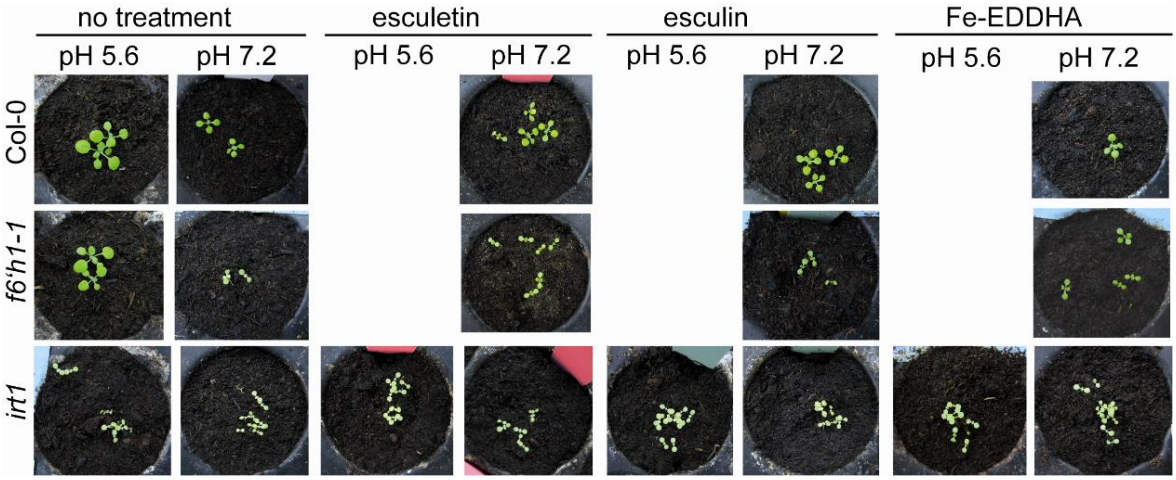

Figure 35. Iron deficiency-induced chlorosis of the Fe(II) uptake-defective mutant *irt1* after the supply of esculetin or esculin. Representative images of wild-type (Col-0), *f6'h1-1* and *irt1* mutant plants after growth for 17 days on non-limed (pH 5.6) or limed substrate (pH 7.2). Plants were supplied with 2.0 mL of a 0.5 g L^{-1} Fe-sequestrene (6% Fe(III)-EDDHA) (+Fe-EDDHA), 34 mM esculetin or 29 mM esculin solution for 4 days before the end of the experiment.

The chlorotic phenotype of *irt1* could also not be alleviated by the addition of esculetin and scopoletin when plants were grown on agar plates. Solely the treatment with Fe-EDTA and Na-EDTA was able to restore chlorosis and increase shoot chlorophyll and Fe shoot concentrations significantly (Figure 36). The increased secretion of fluorescent metabolites under Fe deficiency as observed in wild-type plants was also obvious in *irt1* mutants (Figure 37), implying that *F6'H1* and *IRT1* rather act in concert to accomplish successful Fe acquisition.

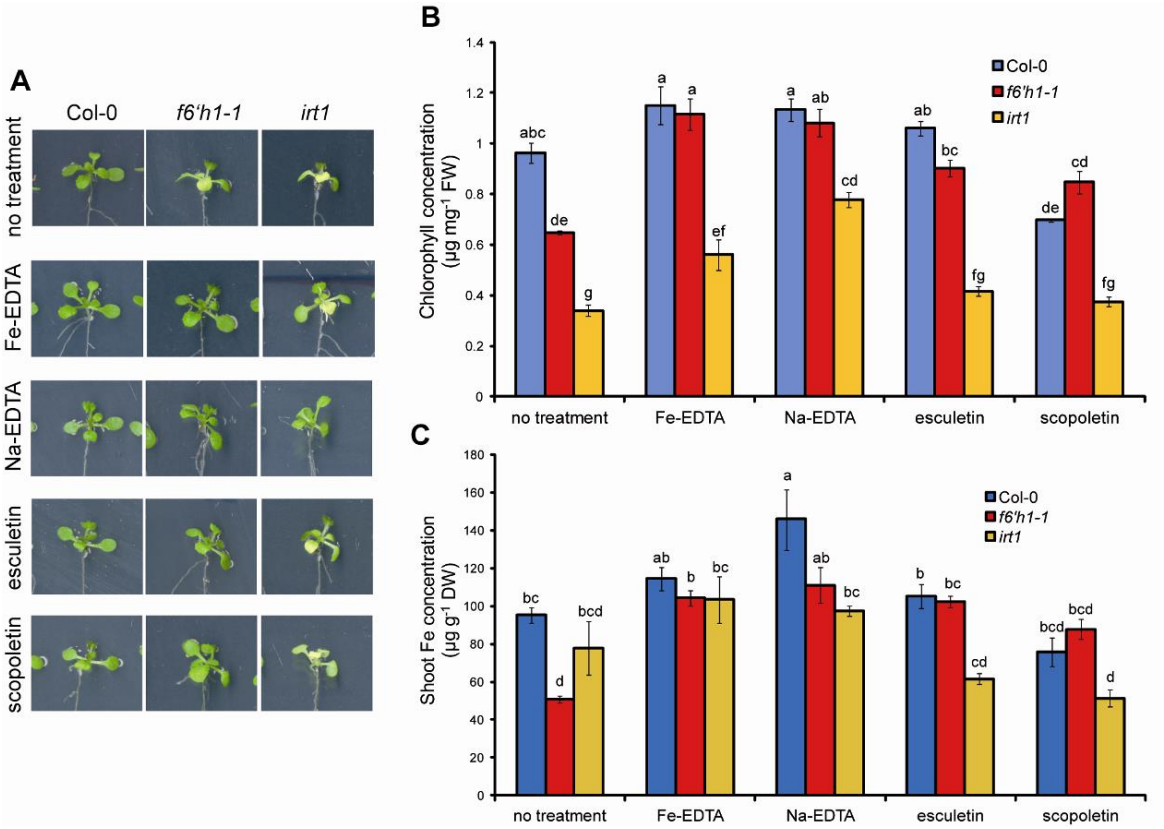

Figure 36. Iron deficiency-induced chlorosis of the Fe(II) uptake-defective mutant *irt1* after the supply of esculetin or scopoletin. (A) Phenotype, (B) chlorophyll and (C) Fe concentrations of whole shoots of wild-type (Col-0), *f6'h1-1* and *irt1* mutant plants precultured for 10 days on 40 µM Fe-EDTA and then treated as indicated for 6 days at pH 5.6 with either 50 µM Fe-EDTA or 50 µM $FeCl_3$ (no treatment) and additionally with 160 µM Na-EDTA, 500 µM esculetin or 50 µM scopoletin. Bars represent means ± SE (n = 4-5 biological replicates). Letters indicate a significant difference according to Tukey's test ($P < 0.05$). FW and DW refer to fresh weight and dry weight, respectively.

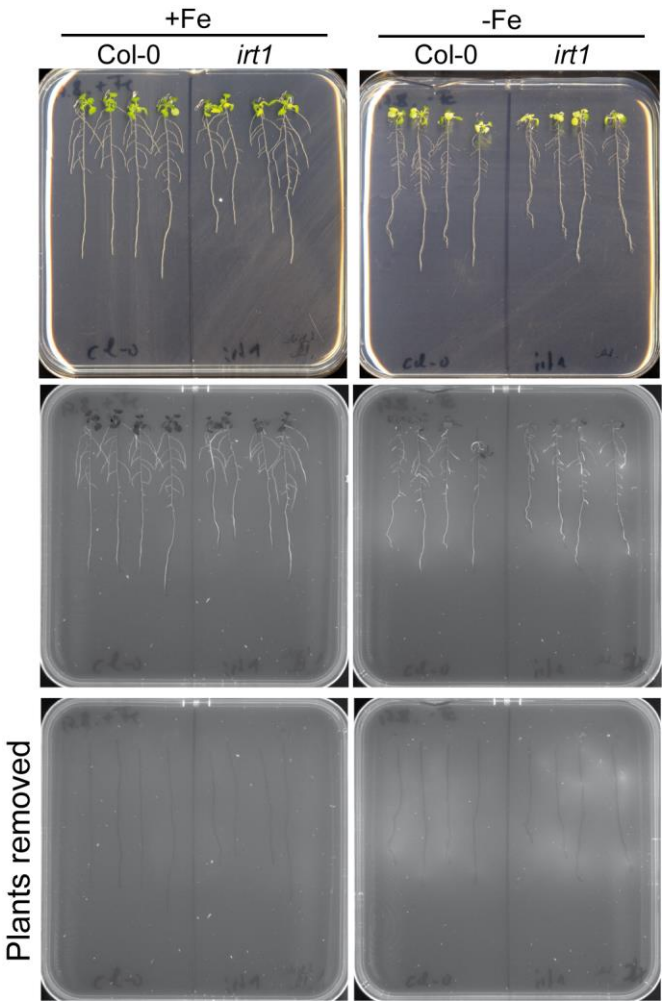

Figure 37. Fluorescence of roots and root exudates of the *irt1* mutant . (Upper row) Wild-type (Col-0) and *irt1* plants were germinated and grown on ½ MS (75 µM Fe-EDTA) for 10 days. Plants were then transferred to ½ MS without added Fe but including 50 µM ferrozine (-Fe) or supplemented with 75 µM Fe-EDTA (+Fe) at pH 5.6. Fluorescence was detected in roots (middle row) and in the agar (lower row) under UV light (365 nm).

4.3.7.4 The importance of a functional reduction step in coumarin-dependent Fe acquisition under alkaline conditions

Arabidopsis thaliana is able to reduce e.g. EDTA-chelated Fe(III) by the Fe-regulated ferric-chelate reductase (FRO2) (Robinson et al., 1999), prior to uptake via IRT1. Therefore it was examined whether coumarin-chelated Fe(III) also needs to be reduced by FRO2 or whether coumarin-chelated Fe(III) can be reduced by alternative mechanisms (Harrington and Crumbliss, 2009). At pH 5.6 the lack of FRO2 function in the *fro2* mutant had no adverse effect on the plant growth or chlorosis development (Figure 38A, B). On the contrary, at a higher pH of 7.2 loss of FRO2 expression led to severely reduced Fe uptake as reflected in lower chlorophyll concentrations (Figure 38A, C). Furthermore, in the *f6'h1-1* mutant but

not in *fro2* plants, addition of esculin alleviated shoots from Fe deficiency-induced chlorosis and increased chlorophyll levels, even though with weaker efficacy as Fe-EDDHA (Figure 38), indicating that the utilization of coumarin-bound Fe(III) depends on FRO2-mediated Fe(III) reduction.

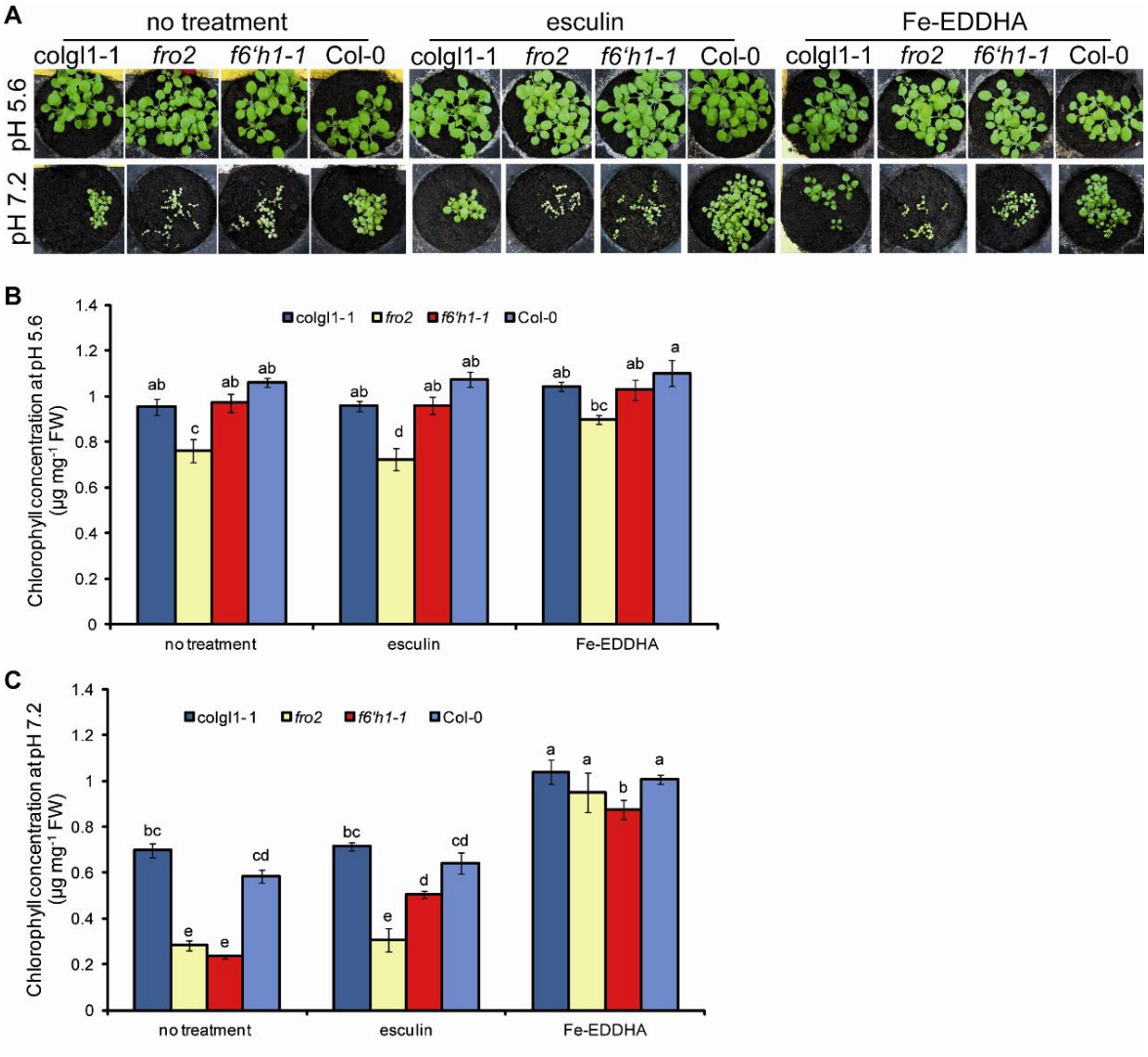

Figure 38. Influence of esculin supply on growth performance and chlorophyll concentrations of *fro2* mutant plants in dependence of Fe availability. (A) Phenotype of 19 day-old plants grown on either non-limed (pH 5.6) or limed (pH 7.2) substrate and supplied with 2.0 mL of a 0.5 g L^{-1} Fe-sequestrene (6% Fe(III)-EDDHA) (+Fe-EDDHA) or 29 mM esculin solution for 6 days before the end of the experiment. (B, C) Chlorophyll concentrations in shoots of wild-type, *f6'h1-1* and *fro2* mutant plants grown as indicated in (A) at pH 5.6 (B) or pH 7.2(C). Bars represent means ± SE (n = 3-4 replicates). Different letters indicate significant differences according to Tukey's test ($P < 0.05$). FW refers to fresh weight.

On agar plates at pH 7.2, the *fro2* mutant also remained chlorotic after being treated with esculetin (Figure 39). Since it was provided as $FeCl_3$, Fe was hardly

available to plants on agar plates already at pH 5.6 which caused chlorosis of the mutant. Therefore, the substantially improved recovery of *fro2* mutant plants by esculetin at pH 5.6 relative to pH 7.2, suggested that the lack of FRO2 can be partially compensated by esculetin itself (Figure 39).

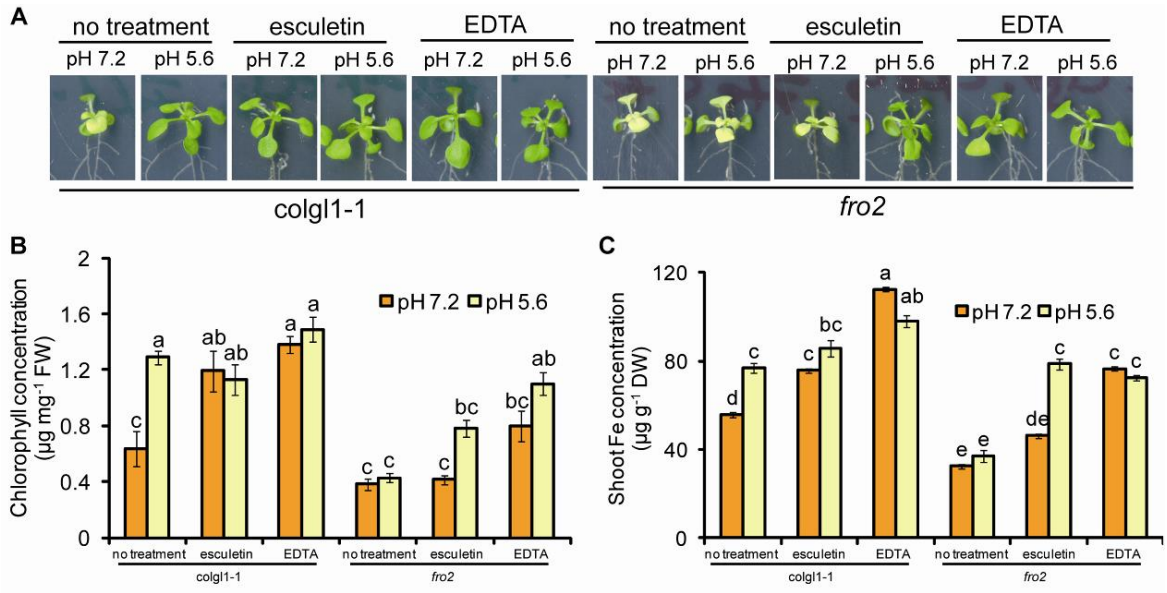

Figure 39. Phenotype, chlorophyll and Fe concentrations in leaves of the Fe reductase-defective mutant *fro2* after treatment with esculetin and EDTA. (A) Phenotype, (B) chlorophyll and (C) Fe concentrations of whole shoots of wild-type (colgl1-1), and *fro2* mutant plants precultured for 10 days on 40 µM Fe-EDTA and then treated as indicated for 6 days at pH 5.6 or 7.2 with either 50 µM $FeCl_3$ (no treatment) or additionally with 500 µM esculetin or 160 µM Na-EDTA. Bars represent means ± SE (n = 5 biological replicates). Letters indicate a significant difference according to Tukey's test ($P < 0.05$). FW and DW refer to fresh weight and dry weight, respectively.

Furthermore, *fro2* mutants displayed the same fluorescent pattern as wild-type plants (Figure 40) thus making it likely that the released metabolites not only support the plants to mobilize Fe(III) but also assist to reduce Fe(III) prior to uptake via IRT1.

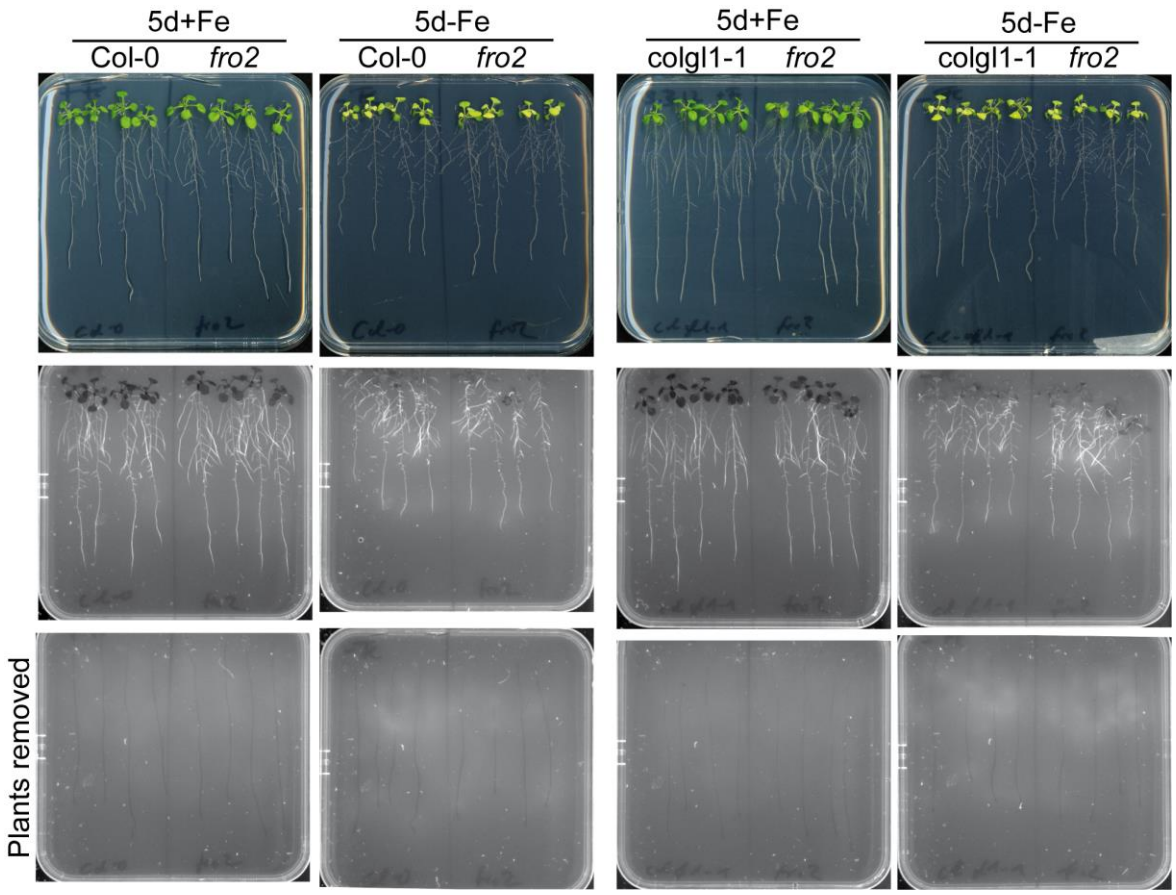

Figure 40. Iron deficiency-induced root fluorescence of *fro2* mutant and wild-type plants. (Upper row) Wild-type (Col-0 or colgl1-1) and *fro2* plants were germinated and grown on ½ MS (75 µM Fe-EDTA) for 10 days. Plants were then transferred to ½ MS without Fe but 50 µM ferrozine added (-Fe) or supplemented with 75 µM Fe-EDTA (+Fe) at pH 5.6. Fluorescence was detected in roots (middle row) and in the agar (lower row) under UV light (365 nm).

4.4 Characterization of coumarins as potential Fe(III)-chelators

4.4.1 Fe-mobilizing and –reducing ability of esculetin and other coumarins

Given the occurrence of scopoletin, esculetin and esculin in root exudates (Figure 20) and a comparable efficacy of esculetin, esculin and scopoletin in alleviating *f6'h1-1* from Fe deficiency under low Fe availability (Figure 24, Figure 25 and Figure 27), the ability of these compounds to mobilize Fe(III) from Fe hydroxide at pH 7.2 was compared. As to be expected from the inaccessibility of the 6'-hydroxy group for Fe(III) chelation, scopoletin and esculin were incapable of mobilizing Fe(III). Only esculetin was able to chelate and mobilize Fe(III) in this *in vitro* assay (Figure 41A). The Fe(III) mobilization capacity of esculetin was even comparable to that of EDTA, a potent synthetic Fe chelator. As indicated by a concentration-

dependent mobilization assay, the detection limit of this assay was 10 to 100 nmol of esculetin. Lower amounts of this compound were not able to mobilize any Fe(III) in this assay (Figure 41B).

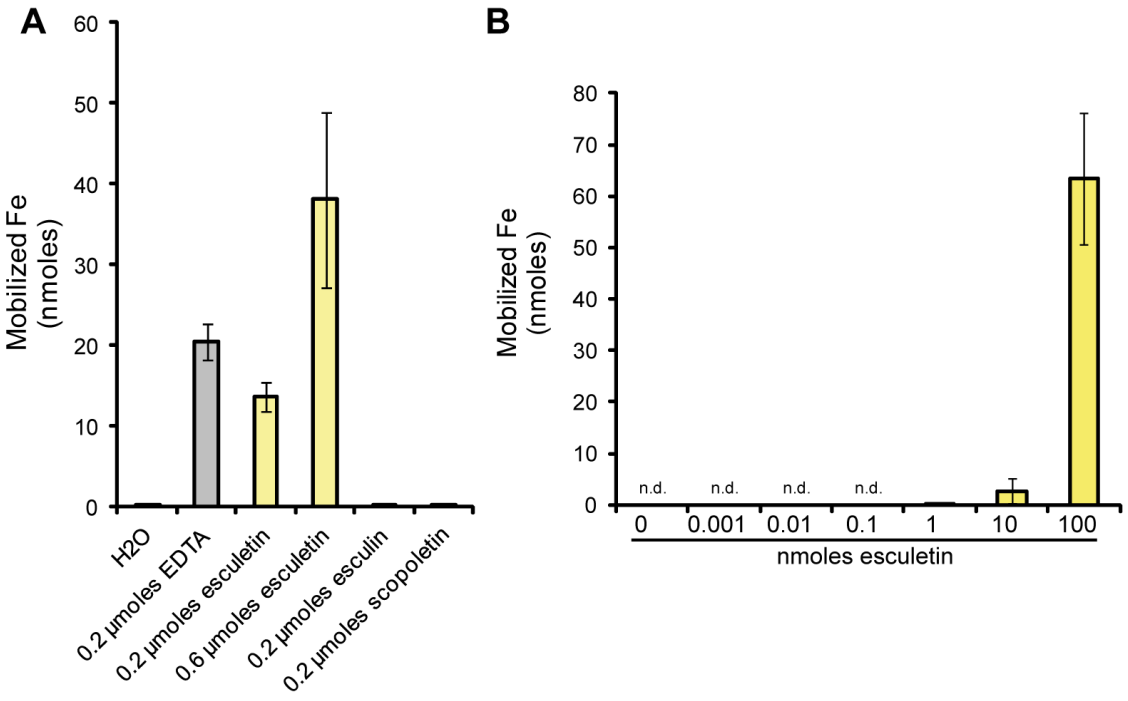

Figure 41. Iron-mobilizing capacity of esculetin and other coumarins. (A, B) The amount of mobilized Fe(III) from an Fe hydroxide precipitate. 0.05 ml of the indicated compounds were incubated with 1.95 ml of 0.1 mM Fe hydroxide (pH 7.2) and the amount of solubilized Fe was detected by HR-ICP-MS. Bars indicate means ± SE (n = 3); n.d. = not detected.

The difference in the amount of esculetin measured in wild-type exudates from Fe-sufficient versus -deficient plants was about 2.81 pmol in 0.05 ml of exudate (Figure 20J). In an attempt to define the contribution of released esculetin to the total Fe(III)-mobilizing capacity of wild-type exudates, this differing amount of esculetin was added to the exudates and the Fe(III)-mobilizing capacity was re-determined. However, the addition of esculetin to exudates collected from Fe-sufficient wild-type or mutant plants did not increase their capacity to mobilize Fe(III) (Figure 42).

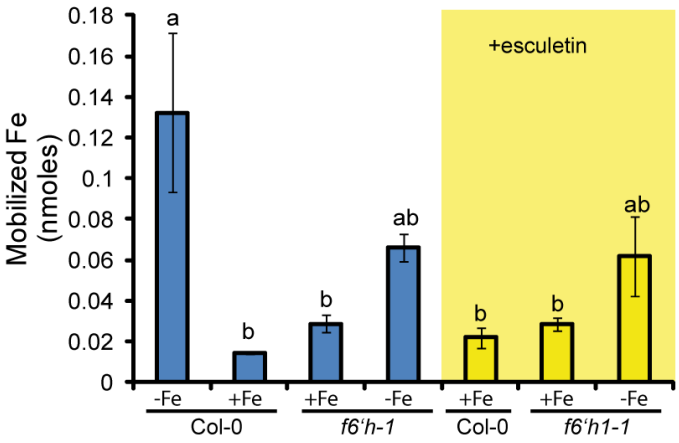

Figure 42. Fe(III) mobilization capacity of root exudates from wild-type (Col-0) or *f6'h1-1* plants and of root exudates spiked with esculetin. Plants were grown for 4 days in the presence (+Fe) or absence of Fe (-Fe). 0.05 ml of exudates were incubated with 1.95 ml of 0.1 mM precipitated Fe hydroxide at pH 7.2 and the amount of solubilized Fe was detected by HR-ICP-MS. In the case of exudates spiked with esculetin, the same exudate samples were supplemented with 2.81 pmol esculetin (yellow background), corresponding to the Fe deficiency-induced increase in the release of esculetin in wild-type plants, and subjected to the same treatment. Bars indicate means ± SE (n = 3 replicates). Different letters indicate significant differences according to Tukey's test ($P < 0.05$).

The affinity of a ligand towards Fe can be regarded as a measure for the physiological significance of the resulting Fe-ligand complex (von Wirén et al., 1999). In order to assess if esculetin, as a potential Fe(III)-chelator in the rhizosphere, has a comparable affinity for Fe(III) to other plant-borne chelators, the affinity constant of esculetin towards Fe(III) was determined. A logK_f value of 17.1 ± 0.2 was measured. This is close to the affinity constant of Fe(III)-phytosiderophores (log K_f = 17.7-18.4) but eight log K units lower than that of Fe(III)-EDTA (log K_f = 25.1) (Table 3).

Table 3. Comparison of the affinity constants (log K) for Fe(III) complexes with esculetin, ethylenediamintetraacetic (EDTA) or the phytosiderophores 2'-deoxymugineic acid (DMA) and mugineic acid (MA).

Ligand	log K_f for Fe(III)
Esculetin	17.1 ± 0.2 [a]
EDTA	25.1[b]
MA	17.7[c]
DMA	18.4[c]

[a] Data obtained in cooperation with Prof. Dr. Hider, King's College, London

[b] Data from Smith and Martell (1989) or [c] from Murakami et al. (1989)

As catechols are bidentate ligands chelating Fe(III) at different stochiometries (Hider and Kong, 2010), complex formation in dependence of pH was modeled and revealed that the 1:1 esculetin:Fe complex formed in a pH range of 4 to 5 is not competitive against the formation of hydroxyl complexes (Figure 43A). However, the 2:1 complex formed above pH 6 and especially the 3:1 complex prevailing above pH 7.5 outcompete any of the Fe(III)-hydroxy complexes that usually represent highly competitive ligands at alkaline pH (Scheffer and Schachtschabel, 2002).

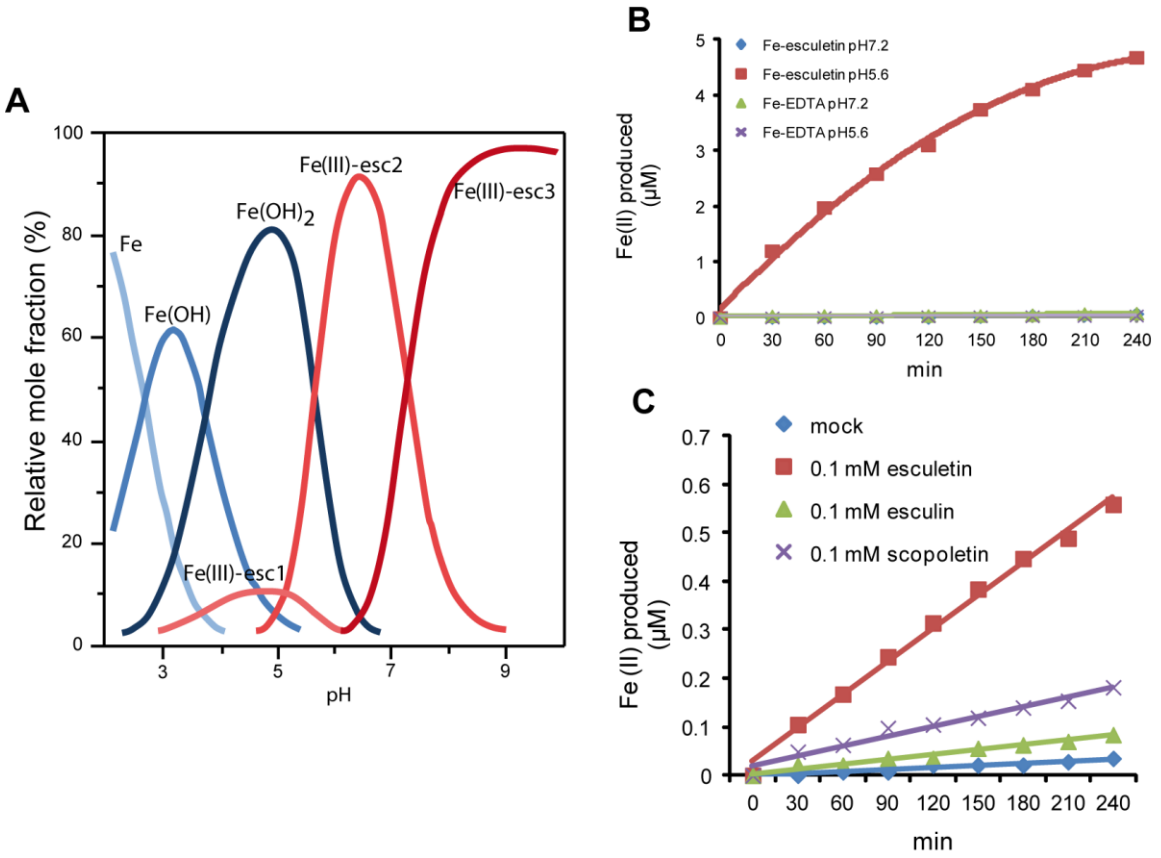

Figure 43. Fe(III)-chelating and Fe(III)-reducing properties of esculetin. (A) Speciation plot of Fe(III)-hydroxide and Fe(III)-esculetin complexes in dependence of pH. Data obtained in cooperation with Prof. Dr. Hider, King's College, London. (B) In vitro assay for Fe(III) reduction. Time-course of Fe(II)-ferrozine formation due to Fe(III) reduction from 0.05 mM Fe(III)-EDTA or 0.05 mM Fe(III)-esculetin at pH 5.6 or pH 7.2. Values of Fe(II)-ferrozine formation from Fe-EDTA at pH 5.6 and 7.2 and from Fe-esculetin at pH 7.2 are below 0.08 µM. (C) In vitro assay of Fe(III) reduction from Fe(III)-EDTA (mock) by the supplementation of 0.1 mM esculetin, esculin or scopoletin. Reactions were carried out in darkness at room temperature and measurements (absorbance at 562 nm) were taken at the indicated times. Mock: no additional compound was added to the reaction solution containing 0.1 mM Fe(III)-EDTA buffered with 1 mM MES at pH 5.6.

In a subsequent experiment the released coumarins were investigated for their ability to reduce ferric Fe from an Fe(III)-EDTA complex. At pH 5.6 Fe(III) was reduced only from an Fe(III)-esculetin complex but not from an Fe(III)-EDTA complex, indicating that esculetin itself facilitated the reduction of its bound Fe(III). At pH 7.2 the Fe(III)-reducing capacity of esculetin was lost, similar to what was observed for EDTA (Figure 43B). By comparing the Fe(III)-reducing capacity of esculetin, esculin and scopoletin from Fe(III)-EDTA at pH 5.6, esculetin clearly outcompeted the other coumarins (Figure 43C) pointing to a likely involvement only of esculetin in Fe(III) reduction processes.

Since the addition of esculetin led to increased Fe levels in the *f6'h1-1* mutant (Figure 24 and Figure 25), it was assumed that plants were actually able to utilize esculetin-chelated Fe(III). Measuring Fe(II)-ferrozine production from Fe(III)-EDTA is an established method to account for plasma membrane-dependent ferric-chelate reductase activity (Waters et al., 2006). Indeed, plant roots incubated with either EDTA- or esculetin-complexed Fe(III) showed substantial ferric-chelate reductase activity which significantly increased under -Fe (Figure 44A), independent of the provided Fe(III) ligand. The influence of the Fe preculture was clearly weaker when the assay was performed at pH 7.2 (Figure 44B).

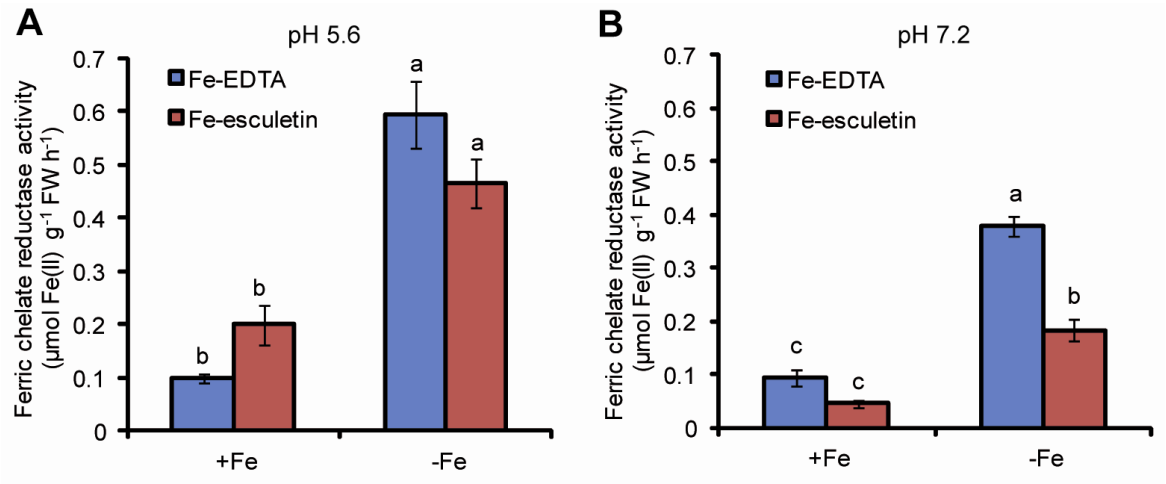

Figure 44. Fe(III) reducing capacity of wild-type plants either supplied with Fe(III)-EDTA or Fe(III)-esculetin. The reaction solution was buffered with 1mM MES to (A) pH 5.6 or (B) pH 7.2. Plants were precultured for 5 days in the absence or presence of Fe. Bars indicate means ± SE (n = 3). Different letters indicate significant differences according to Tukey's test ($P < 0.05$). FW refers to fresh weight.

Altogether, these results indicate that esculetin forms plant-available complexes with Fe(III), especially at high pH, with affinities comparable to other potent Fe-chelators. Interestingly, at low pH, esculetin also displays Fe(III)-reducing capacity.

4.4.2 Structural modifications of coumarins in the rhizosphere

As esculin and scopoletin have no Fe(III) chelation capacity on their own (Figure 41A) due to the inaccessibility of the 6'-hydroxy group in the catechol moiety, their efficacy in Fe acquisition (Figure 24, Figure 25 and Figure 27) suggested their conversion to esculetin in the rhizosphere. It was therefore hypothesized that Arabidopsis roots are able to de-glycosylate esculin and to de-methylate scopoletin to yield in both cases esculetin. First, Arabidopsis roots were incubated with esculin and Fe(III)-citrate as a readily available Fe source and the formation of a dark brown Fe(III)-esculetin complex (Trepeta and Edberg, 1987) was monitored. In the presence of esculin, wild-type and *f6'h1-1* roots formed Fe(III)-esculetin complexes to a similar extent, indicating esculin de-glycosylation and confirming that the assay was not affected by an endogenous release of esculetin (Figure 45A, B). Moreover, complex formation was even more effective at pH 7.2 than at pH 5.6 (Figure 45B), supporting the view of an increasing efficacy of esculetin to chelate Fe(III) at alkaline pH (Figure 43A). Furthermore, Fe supply during the preculture of either genotype did not affect the rate of Fe(III)-esculetin complex formation (Figure 45B).

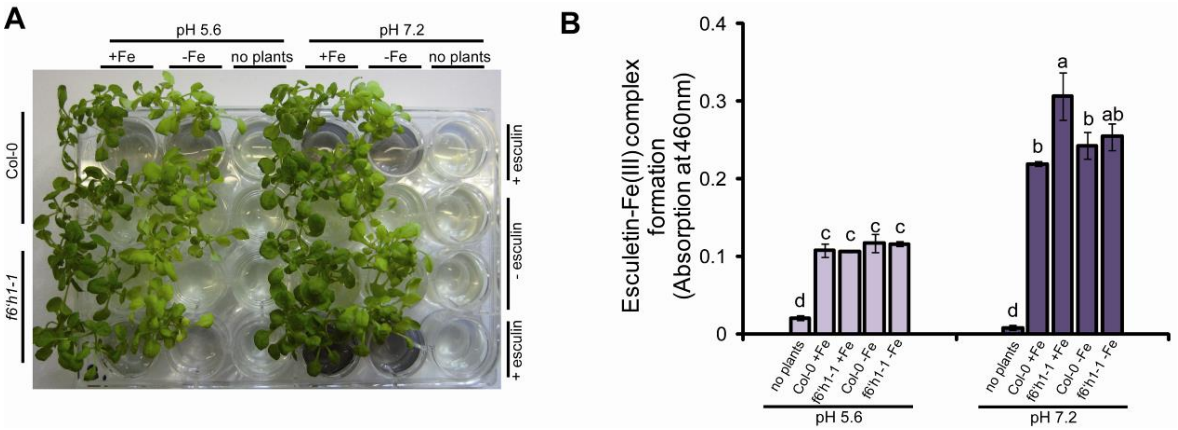

Figure 45. Assay for the de-glycosylation of esculin to esculetin. (A and B) Fe-sufficient or Fe-deficient wild-type (Col-0) or *f6'h1-1* plants were incubated in solution containing esculin and ammonium Fe citrate. The formation of esculetin was detected by the appearance of the dark-brown Fe(III)-esculetin complex. (B) Quantification of Fe(III)-esculetin complex formation at pH 5.6 or pH 7.2. Bars represent means ± SE (n = 3). Different letters indicate significant differences according to Tukey's test ($P < 0.05$). Blank = respective values without esculin added were subtracted.

Then, Arabidopsis roots were incubated with Fe(III)-citrate and scopoletin. It was hypothesized that root-borne de-methylases might be able to de-methylate scopoletin to generate esculetin and thus realizing the formation of a dark Fe(III)-esculetin complex. In contrast to the expectation, the typical dark brown color formation in the medium was not observed, irrespective of Fe preculture and genotype (Figure 46A to D). However, a closer look to the roots revealed the formation of a blue coloration in the roots, especially at pH 7.2, but independently of genotype or nutritional Fe status of the plants (Figure 46E). It remains unclear how this staining represents Fe(III)-esculetin precipitation and to what extent it interferes with the quantification of the complex.

Taken together, these results indicated that roots can mediate an extracellular de-glycosylation of esculin, whereas in the case of scopoletin, roots appeared having the potential for its de-methylation, however, a quantitative assessment was not yet possible.

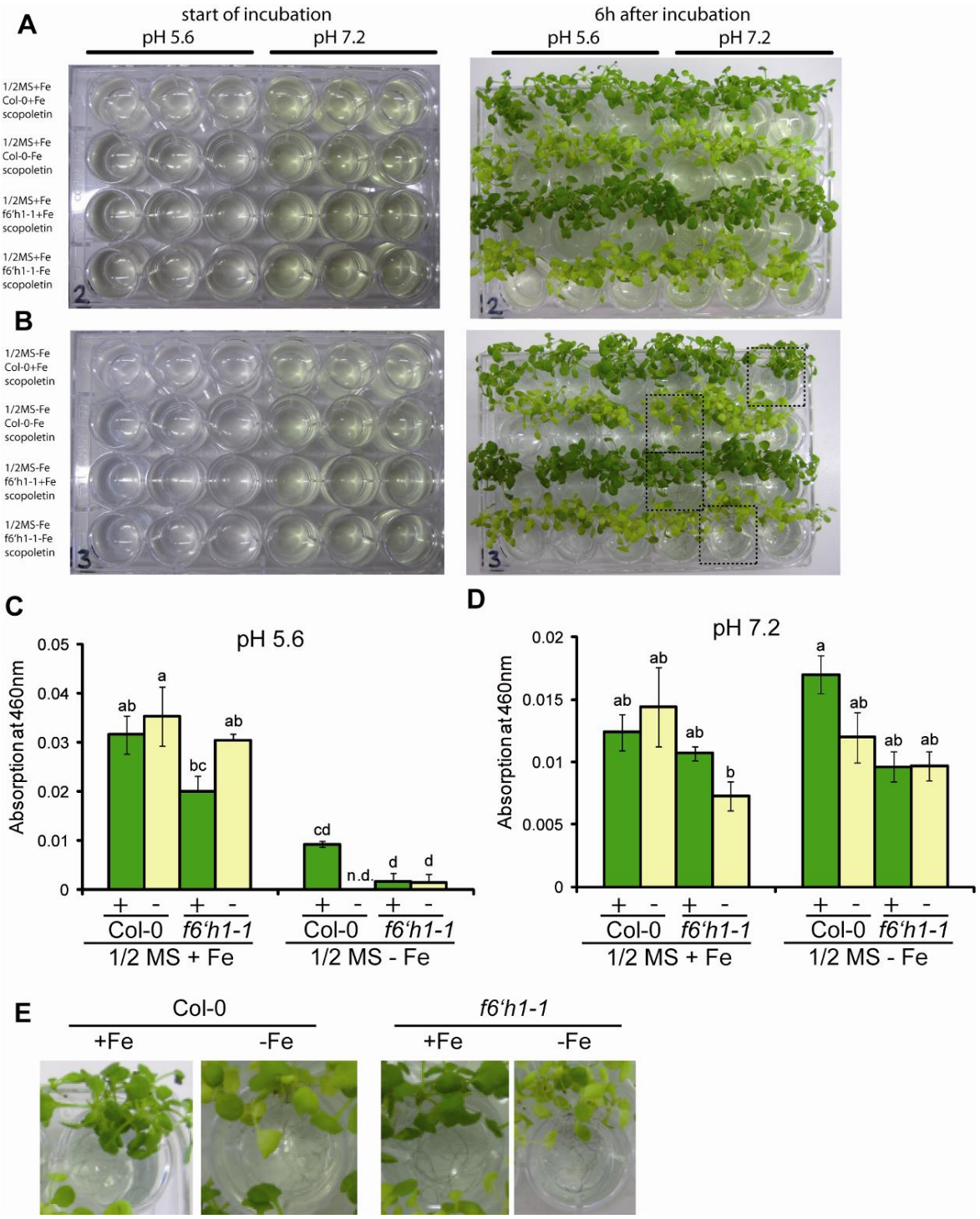

Figure 46. Assay to test for de-methylation of scopoletin. (A and B) Fe-sufficient (+Fe) or Fe-deficient (-Fe) wild-type (Col-0) or *f6'h1-1* plants were incubated in a ½ MS (without Fe) scopoletin solution either (A) containing or (B) not containing ammonium Fe citrate. (C and D) Quantification of Fe(III)-esculetin complex formation at pH 5.6 or pH 7.2. Bars represent means ± SE (n = 3); n.d. = not detected. Different letters indicate significant differences according to Tukey's test ($P < 0.05$). Blank = respective values without scopoletin added were subtracted. (E) Representative close-up images of plants from (B).

5 Discussion

The occurrence of Fe deficiency is a persistent problem in agricultural soils that exhibit high pH and/or high concentrations of bicarbonate, which lower the availability of this micronutrient (Marschner, 2012). Whilst the chelator-based Fe acquisition strategy used by grasses is relatively pH-insensitive, these plants can efficiently acquire Fe under calcareous conditions, the reduction-based strategy of non-graminaceous plants is strongly compromised (Ohwaki and Sugahara, 1997; Schmidt, 1999; Susin et al., 1996). Early studies indicated that Fe-deficient Strategy I plants like Arabidopsis not only release protons and induce a ferric chelate reductase, but also release organic compounds in the rhizosphere (Römheld and Marschner, 1983; Römheld and Marschner, 1981; Susin et al., 1993; Welkie, 2000). However, the importance, the mechanism of action as well as the molecular identity of these compounds have remained largely unknown.

By unraveling the identity and the mechanism of action of some root metabolites that are secreted in response to Fe deficiency, the work presented here extends the knowledge of Strategy I-type Fe acquisition by a mechanism that becomes especially crucial in conditions of low Fe availability. It could be shown that Arabidopsis plants release fluorescent coumarins into the rhizosphere that can chelate and mobilize Fe(III) and thus make it available for the reduction and uptake at the plasma membrane of rhizodermal and cortical cells.

Several lines of evidence led to these conclusions. First of all, strong Fe deficiency symptoms developed in a mutant that is defective in the phenylpropanoid pathway and lacks the synthesis of F6'H1-dependent coumarins. Secondly, a comparative biochemical analysis of root exudates of wild-type and *f6'h1* mutant plants led to the identification of several catechol-type coumarins that exhibit Fe(III) chelating and reducing abilities. Thirdly, the external supply of some of these F6'H1-dependent coumarins can successfully revert the chlorotic phenotype of *f6'h1* plants. Finally, the significance of the released compounds became most crucial in conditions of low Fe availability, as the *f6'h1* mutant did not exhibit any impaired growth when the pH is low or Fe offered in a highly available source. In the following sections these aspects are elucidated in more detail.

5.1 The identification of two genes involved in Fe efficiency in Arabidopsis by screening for tolerance to Fe deficiency-induced chlorosis

The basis for the discovery of two mutants with impaired tolerance to Fe deficiency-induced chlorosis was the development of a solid substrate with low Fe availability. By addition of calcium carbonate and bicarbonate to a peat-based substrate, the pH of the substrate was elevated to pH 7.5 thereby mimicking highly buffered pH values that are typically found in calcareous soils (Lucena et al., 2007). Furthermore, this approach was considered promising, since for the first time Arabidopsis mutants were screened under conditions of an intact rhizosphere. Compared to more artificial Arabidopsis growth systems like agar plates or hydroponic cultures (Chaney et al., 1992; Alcantara et al., 2000), this newly established 'close-to-nature' system bears the advantage that (i) Fe is not completely absent nor fully available, but rather hardly available, (ii) it allows plants to establish functional rhizosphere gradients, (iii) plants grow in non-axenic conditions, thus resembling more ‘natural’ conditions, (iv) it allows high throughput screening since it does not require special equipment and (v) it enables quick and easy detection of mutants by screening for visible changes in leaf chlorosis (Norvell and Adams, 2006). For this forward genetic approach, a collection of about 7,000 homozygous T-DNA insertion lines of *Arabidopsis thaliana* (Alonso et al., 2003) were chosen to serve as screening material. Consequently, about one quarter of the currently annotated 27,029 protein-coding Arabidopsis genes (Swarbreck et al., 2008) were covered by this collection. These T-DNA insertion lines are homozygous and the precise genomic localization of the T-DNA insertion, and hence the identity of the interrupted gene, is known (Alonso et al., 2003). Furthermore, gene knockouts provide a very good direct causality between the sequence and the function of a gene (Krysan et al., 1999).

The established screening system led to the isolation of the T-DNA insertion lines *f6’h1-1* and *myb72-1*. Compared to wild-type plants, the *f6’h1-1* T-DNA insertion line showed stronger leaf chlorosis and growth retardation on calcareous substrate, mainly as a consequence of reduced Fe uptake (Figure 10). A first indication that the chlorosis was indeed caused by Fe deficiency derived from the fact that the addition of generous amounts of Fe-EDDHA led to a regreening of the

mutant (Figure 10). Importantly, the inability of the *f6'h1-1* mutant to acquire sparingly soluble Fe was not obvious when Fe availability was high, as on substrate at pH 5.6 (Figure 10). Thus it seems that the F6'H1-dependent contribution to Fe mobilization can be partially "by-passed" by naturally-occurring chelates or by the acidification of the rhizosphere since secreted protons were not further neutralized due to the absence of bicarbonate (Norvell and Adams, 2006; Ohwaki and Sugahara, 1997; Römheld and Marschner, 1983; Römheld and Marschner, 1981; Susin et al., 1993; Welkie, 2000). In *f6'h1* plants, the T-DNA insertion disrupts the expression of *F6'H1* (Figure 13), a gene which encodes an enzyme previously shown to be involved in the synthesis of coumarins within the phenylpropanoid pathway (Kai et al., 2008). To verify that indeed a mutation in this gene is responsible for the chlorotic phenotype of *f6'h1-1* plants, several experiments carried out with this insertion line were successfully repeated with an independent second allelic insertion mutant, named *f6'h1-2* (Kai et al., 2008; Krysan et al., 1999) (Figure 13).

Furthermore, *f6'h1-1* plants developed strong chlorosis not only when grown on alkaline substrate, but also on agar plates at pH 5.6, if Fe was provided in an insoluble form as $FeCl_3$ (Figure 10 and Figure 24). This was very important, because this agar-based plant culture system is bicarbonate-free and growth occurs in non-alkaline conditions. That means that any potential secondary influences on Fe uptake mechanisms caused by the addition of $CaCO_3$ or $NaHCO_3$ to the substrate or simply the use of substrate that is manually arranged and watered (Norvell and Adams, 2006; García et al., 2014; Lucena et al., 2007; Santi and Schmidt, 2009) can be neglected. In fact, in high pH calcareous soils the protons released by Fe-deficient plants are buffered by bicarbonate (Norvell and Adams, 2006; Ohwaki and Sugahara, 1997) and the activity of the ferric chelate reductase can be largely repressed (Romera et al., 1997; Alcantara et al., 2000; Lucena et al., 2007). Under these conditions, the reduction-based mechanism can stall and thus contribute to cause the formation of a chlorotic phenotype.

The other T-DNA insertion line that was identified in the screening is disrupted in the expression of *MYB72*, a member of a transcription factor family characterized by a R2 and R3 MYB helix-turn-helix DNA-binding domain (Kranz et al., 1998). This gene has been previously described to play a role in pathogen resistance and

is required for induced systemic resistance (Van der Ent et al., 2008). The *myb72-1* T-DNA insertion line exhibited a chlorotic phenotype when grown on alkaline substrate (Figure 6A). The chlorosis could be recovered by the addition of generous amounts of Fe-EDDHA (Figure 6B), indicating that the chlorosis was indeed caused by Fe deficiency.

The growth performance of *myb72-1* plants on agar plates was not yet tested in conditions where Fe availability is decreased. In the experiments carried out so far, Fe was either provided in a readily accessible form (as Fe-EDTA) or was completely absent, as any possibly remaining traces of this metal were kept immobile by the addition of ferrozine (Stookey, 1970) (Figure 7). Actually, plants are able to acquire Fe from Fe-EDTA under many circumstances, even when expression of Fe uptake-related genes is impaired (Vert et al., 2003). Accordingly, the phenotype of *myb72-1* plants did not differ from the wild type, remaining green when supplied with Fe-EDTA or similarly chlorotic when Fe was absent (Figure 7). Since this was also observed in initial experiments with *f6'h1-1* plants on agar plates supplied with Fe-EDTA, even when the conditions were alkaline (data not shown), it can be expected that the *myb72* plants may develop stronger Fe deficiency symptoms than wild-type plants when grown on agar plates where Fe availability is decreased, as it was shown for the *f6'h1-1* mutant (Figure 24). This would support the hypothesis that the loss of *MYB72* expression only becomes detrimental when *MYB72*-regulated processes are crucial in acquiring Fe when this micronutrient is less available.

The simultaneous identification of two T-DNA insertion lines in the same screening procedure, that exhibit similar phenotypes and whose disrupted genes seems to influence in both cases a proper function of the phenylpropanoid pathway (Figure 17 and Figure 34) strongly argues for the significance of this pathway in Fe efficiency. Based on these findings it can be expected that other genes whose disruption leads to a significant impairment of this pathway or to a reduced ability to mobilize scarcely available Fe through other mechanisms, might as well be identified in screening conditions as presented herein.

5.2 The synthesis and release of coumarins is induced by Fe deficiency

All genes that have so far been described to be involved in Fe acquisition are tightly regulated at the transcriptional level by the plant's Fe nutritional status (Jakoby et al., 2004; Colangelo and Guerinot, 2004; Vert et al., 2002; Connolly et al., 2003). Indeed, in agreement with early transcriptome analyses (Colangelo and Guerinot, 2004; Dinneny et al., 2008; Yang et al., 2010; Rodriguez-Celma et al., 2013), quantitative RT-PCR showed that *F6'H1* expression was strongly up-regulated in response to Fe deficiency (Figure 14) in a FIT-dependent manner (Figure 31). Since plants grown on alkaline substrate exhibited severe symptoms of Fe deficiency (Figure 10), it can be concluded that also other FIT-dependent genes were up-regulated under these conditions. Nevertheless, the loss of *F6'H1* expression could not be compensated for by increased expression of FIT regulated Fe acquisition genes (Figure 10).

F6'H1 is not the only enzyme of the phenylpropanoid pathway that is regulated by Fe. In fact, according to the proteome study of Lan et al. (2011), Fe deficiency also induces the accumulation of other enzymes acting upstream of *F6'H1* within the phenylpropanoid pathway, such as PHENYLALANINE AMMONIA-LYASE2 (PAL2) and CAFFEOYL COENZYME A ESTER O-METHYLTRANSFERASE (CCoAOMT1) (Figure 47). Furthermore, the expression of another enzyme of the phenylpropanoid pathway, TRANS-CAFFEOYL-COA 3-O-METHYLTRANSFERASE1 (CCoAMT1), is also up-regulated by Fe deficiency (Fourcroy et al., 2014). These findings indicated that compounds downstream of these enzymes in the phenylpropanoid pathway, including coumarins, play an important role for the adaptation of plants to sparingly soluble Fe. This held true whenever the Fe nutritional status of a plant is low, irrespective of whether Fe deficiency was the consequence (i) of low Fe availability in an alkaline medium (Figure 10), (ii) of supplying an unstable Fe source at neutral or slightly acid pH (Figure 25) or (iii) of omitting this micronutrient from the growth medium (Figure 17). In the latter case, the complete absence of this element led to chlorosis also in the wild type (Figure 18A).

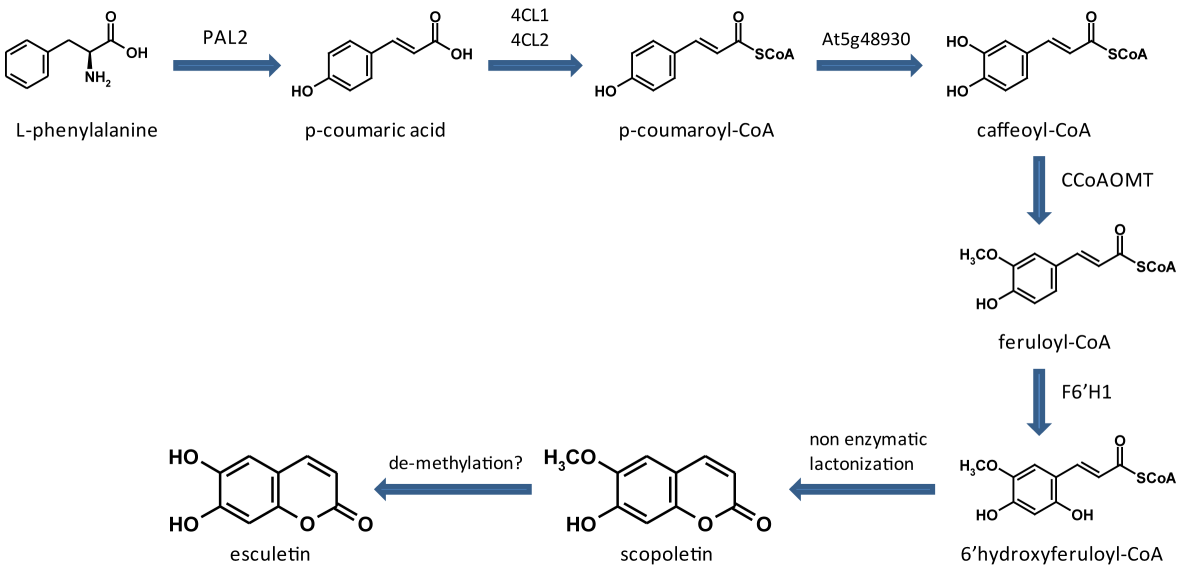

Figure 47. Proposed scheme of the phenylpropanoid pathway in *Arabidopsis thaliana*. Coumarins, such as scopoletin or esculetin, are synthesized via the phenylpropanoid pathway, using phenylalanine as precursor. In subsequent reactions, feruloyl-CoA is synthesized. The enzyme F6'H1 is responsible for the o*rtho*-hydroxylation of feruloyl-CoA, a reaction that is followed by *trans/cis* isomerization and lactonization steps to yield scopoletin. This metabolite, in turn, is most likely de-methylated to form esculetin. According to the proteome study of Lan et al. (2011) the abundance of all enzymes depicted in the present figure is increased upon Fe deficiency. PAL2, Phe ammonia-lyase; 4CL1 and 2, 4-coumarate:CoA ligases; CCoAOMT, caffeoyl-CoA O-methyltransferase; F6'H1, 2-oxoglutarate-dependent dioxygenase. Depiction modified from Lan et al. (2011), Kai et al. (2008), Bourgaud et al. (2006) and Döll (2013).

The cell type-specific localization of *F6'H1* gene expression further indicated an involvement of this gene in Strategy I Fe acquisition. *F6'H1* promoter activity was confined to roots (Figure 15A) and was up-regulated by Fe deficiency especially in the basal zone of the primary root (Figure 15 and Figure 16), where it mainly localized to rhizodermal and cortical cells (Figure 16). This Fe-dependent and cell type-specific expression pattern of *F6'H1* is reminiscent to that of other genes involved in Fe acquisition, such as *FIT* (Jakoby et al., 2004; Colangelo and Guerinot, 2004), *IRT1* (Vert et al., 2002) and *FRO2* (Connolly et al., 2003). In fact, as shown by network analysis, many genes encoding enzymes of the phenylpropanoid pathway, including *F6'H1*, share a similar Fe-dependent expression pattern with *FIT*, *IRT1*, *FRO2* and *AHA2* (Rodríguez-Celma et al., 2013).

As revealed by gene expression studies in wild-type roots, *MYB72* was also strongly up-regulated under conditions of Fe deficiency (Figure 8). This observation is consistent with the results of transcriptome studies performed by Colangelo and Guerinot (2004), Dinneny et al. (2008) and Buckhout et al. (2009)

on this root-specific transcription factor (Van De Mortel et al., 2008; Zamioudis, 2012). Interestingly, the work of Colangelo and Guerinot (2004) and Sivitz et al. (2012) further indicated that *MYB72* is regulated by FIT, just as the Fe acquisition genes *IRT1*, *FRO2* and *F6'H1*. Nevertheless, using expression data from Genevestigator (Zimmermann et al., 2004) none of the typical Fe acquisition genes were co-expressed with *MYB72* in datasets from experiments with various Fe deficiency treatments (data not shown).

Altogether, these results indicate that both *F6'H1* and *MYB72* are transcriptionally activated in roots by Fe deficiency in a FIT-dependent manner and that *F6'H1* is expressed in the same root zones and cell types as other major Strategy I components.

5.3 F6'H1 is required for the synthesis of root released coumarins with Fe mobilization ability

The enzyme F6'H1 is responsible for the conversion of feruloyl-CoA to 6'-hydroxyferuloyl-CoA (Figure 47 and Kai et al., 2008). This metabolite, in turn, serves as precursor for the synthesis of coumarins, such as scopoletin and its ß-glucoside scopolin (Figure 47 and Kai et al., 2008). Coumarins are plant-derived phenylpropanoids that originate from the precursor phenylalanine (Bourgaud et al., 2006). The presence of these compounds in roots can be easily assessed, since many coumarins exhibit fluorescence when excited with UV light (365 nm) (Chong et al., 2002). When the appearance of root-derived fluorescence was observed in wild-type plants, it was found that fluorescence strongly increased in response to Fe deficiency (Figure 17A) in a FIT-dependent manner (Figure 32A). In contrast, almost no fluorescence was detected in *f6'h1-1* roots (Figure 17A and B).

Furthermore, it could be shown that the increased accumulation of fluorescent compounds under Fe deficiency coincides with an increased expression of *F6'H1* in epidermal cells (Figure 17C). Importantly, the majority of the fluorescent compounds produced under Fe deficiency was secreted by wild-type plants (Figure 17A), but are not yet known. However, knowledge about the identity of the released compounds might help to explain the chlorotic phenotype of *f6'h1* plants

(Figure 10). Thus, the nature of the fluorescent metabolites accumulating downstream of F6'H1 under Fe deficiency was investigated. UPLC-FLD and a more exploratory UPLC-ESI-MS analysis on root extracts showed that the accumulation not only of scopoletin and scopolin but also of esculin and esculetin was significantly decreased in *f6'h1-1* roots (Figure 20A, C, E, G, I). Furthermore, UPLC-ESI-MS analysis on root exudates revealed that scopolin, scopoletin, esculetin, fraxetin, isofraxetin, glycoside of dihydroxyscopoletin, coumarins tentatively identified as isofraxidin/methoxyscopoletin and eleven unknown metabolites were increased in wild-type exudates under Fe deficiency, but remained relatively low in *f6'h1-1* exudates (Figure 20D, F, H, J and Table 2). These results indicated that F6'H1 is a key enzyme not only for the synthesis of scopolin and scopoletin as shown by Kai et al. (2008), but also for coumarins, such as esculetin, fraxetin or isofraxidin (Table 2). The minor remaining amounts of some metabolites in the *f6'h1* mutant might be explained by alternative routes for the synthesis of coumarins that bypass F6'H1, as proposed by Bourgaud et al., (2006). However this is still speculative, since the phenylpropanoid pathway is not completely elucidated to date (Döll, 2013). Yet, the remaining amounts of metabolites in *f6'h1* is small compared to wild type and barely differs in response to Fe deficiency. Their synthesis seems therefore not to be regulated by Fe deficiency (Table 2) and can thus be neglected.

Generally, the exudation of root metabolites is suggested to occur via efflux by MATE (MULTIDRUG AND TOXIN EXTRUSION) or ABC (ATP-binding cassette) transporters (Walker et al., 2003; Martinoia et al., 2002; Neumann and Römheld, 2007). Recently it was reported by Fourcroy et al. (2014) that the release of fluorescent compounds under Fe deficiency is mainly mediated by the ATP-binding cassette (ABC) transporter ABCG37/ PLEIOTROPIC DRUG RESISTANCE 9 (PDR9). Interestingly, ABCG37/PDR9, just as *F6'H1,* is transcriptionally regulated by FIT (Colangelo and Guerinot, 2004). Furthermore, the expression of this transporter is also induced by Fe deficiency (Rodriguez-Celma et al., 2013; Fourcroy et al., 2014), particularly in rhizodermal cells (Dinneny et al., 2008; http://bbc.botany.utoronto.ca/efp). Interestingly, some of the released compounds that were highly increased under Fe deficiency in the wild type but occurred in very low amounts in *f6'h1-1* root exudates, namely scopoletin, isofraxidin and methoxyscopoletin, were also absent in *pdr9* exudates (Table 2

and Fourcroy et al., 2014). Thus, it is very likely that F6'H1 and ABCG37/PDR9 work in concert to enhance the synthesis and release of fluorescent coumarins under Fe deficiency.

Since most of the F6'H1-dependent coumarins were released into the growth medium under Fe deficiency (Table 2), it is likely that they play a functional role outside the root cells. Even though the recent works of Rodríguez-Celma et al. (2013) and Fourcroy et al. (2014) have also shown that Fe deficiency induces the exudation of coumarins in Arabidopsis, the function and mode of action of these compounds during the adaptation of plants to limited Fe conditions was not experimentally addressed in these studies. Employing mobilization assays that reflect a chelator-dependent dissolution of Fe hydroxide, it was observed that Fe deficiency increased the Fe(III) mobilization capacity of root exudates from wild-type plants, whereas such an increase was almost completely absent when the assay was carried out with *f6'h1-1* root exudates (Figure 22 and Figure 23A). Furthermore, when fluorescent compounds were removed from root exudates of Fe-deficient wild-type plants (Figure 23C), the Fe(III) mobilization capacity of these exudates strongly decreased (Figure 23D). Since the Sep-Pak C18 resin was washed three times with 10% (v/v) methanol, it can be assumed that most organic acids that could also chelate Fe(III) (Dakora and Phillips, 2002) were separated from the fluorescent compounds and did not substantially contribute to Fe mobilization (Figure 23C and D). Thus, one or more of the coumarins synthesized in an F6'H1-dependent manner must be able to chelate and solubilize Fe from Fe-hydroxide precipitates.

Since the F6'H1-dependent coumarins help plants mobilizing hardly available Fe (Figure 22 and Figure 23A), it was reasonable to assume that an increased synthesis of these compounds could be beneficial to plants growing under harsh calcareous conditions. Thus, transgenic lines overexpressing *F6'H1* were generated. In all 35S:*F6'H1* plants tested so far no obvious increase in the root synthesis or release of fluorescent compounds could be detected (Figure 30B). Moreover, none of the *F6'H1* overexpression lines tested did show better growth on limed substrate (Figure 29). Also in initial experiments on agar plates, where Fe was sparingly available and the medium pH elevated, the *F6'H1* overexpression lines did not perform any better than the wild type (data not shown). Besides

testing further different Fe regimes to assess the performance of the *F6'H1* overexpression lines compared to wild type, it would also be essential to quantify the Fe(III) mobilizing capacity of exudates from *F6'H1* overexpression lines. In addition, it remains to be measured if coumarin concentrations inside roots were increased by *F6'H1* overexpression or if an increased release of these substances requires the simultaneous up-regulation of an efflux transporter, such as ABCG37/PDR9 (Fourcroy et al., 2014).

The regulation of the synthesis of root-released coumarins that function in Fe(III) mobilization may, at least partially, be accomplished by MYB72. This assumption finds support on the fact that root fluorescence was not increased in *myb72* plants grown in conditions of Fe deficiency (Figure 34A and B). In addition, it has already been described that MYB transcription factors are involved in regulating branches of the phenylpropanoid pathway (Kranz et al., 1998; Van De Mortel et al., 2008; Mehrtens et al., 2005). More recently, Zamioudis (2012) showed that the overexpression of *MYB72* leads to transcriptional up-regulation of genes encoding key enzymes in the shikimate and phenylpropanoid pathway, such as phenylalanine ammonia-lyase (PAL) or 4-coumarate:CoA ligase (4CL). Interestingly, the overexpression of *MYB72* was able to induce the appearance of strong root fluorescence and release of fluorescent compounds already under Fe sufficient conditions (Figure 34C). In contrast, *FIT* overexpression lines did not show increased root fluorescence under Fe sufficiency (Figure 32B). This might be explained by the post-transcriptional regulation of FIT. FIT can only activate the expression of its target genes when 'active' and this transcription factor is in this state only when an Fe deficiency signal is present (Meiser et al., 2011). However, MYB72 seems to regulate F6'H1, as MYB72 is required for the characteristic release of fluorescent metabolites (Figure 34A, B), and might thus also regulate their exudation via PDR9 (Fourcroy et al., 2014). Interestingly, in a different context it has been shown that *PDR9* induction requires a functional MYB72 (Zamioudis, 2012). In this study a microarray analysis carried out to identify *Pseudomonas fluorescens* WCS417 bacteria-responsive genes revealed, that *PDR9* was de-regulated in the *myb72-2* mutant background (Zamioudis, 2012). Future studies should be carried out to test if root exudates of *MYB72* overexpression lines exhibit a higher Fe mobilization capacity, if these exudates

resemble those found in wild-type exudates regarding their type and proportion and if these lines are thus able to better cope with conditions of low Fe availability.

5.4 Esculetin as a prototype for Fe(III)-mobilizing catechols secreted by Fe-deficient Arabidopsis roots

Several coumarins were absent or remained in low quantities in the root exudates of the *f6'h1-1* mutant (Figure 20 and Table 2). Thus the development of Fe deficiency-mediated chlorosis in *f6'h1-1* plants was most likely linked to the impaired synthesis and release of coumarin by roots of these plants. In fact, when substrate-grown *f6'h1-1* mutants were supplemented with esculetin or esculin, the chlorotic phenotype of these plants could be largely recovered (Figure 27). Importantly, the substrate pH remained constant at around pH 7.2 after these treatments (data not shown), thus excluding the possibility that increased Fe uptake was facilitated through substrate acidification. This is of relevance, because soil acidification has been described as a concomitant effect of the release of some organic acids which simultaneously leads to increased proton release into the rhizosphere (Dakora and Phillips, 2002; Sugiyama and Yazaki, 2012). In fact, the supply of scopoletin, esculin and esculetin to agar-grown *f6'h1-1* plants prevented the development of Fe deficiency symptoms in these plants, irrespective of the ambient pH (Figure 24 and Figure 25). This indicates that the abovementioned coumarins, which were amongst those identified in root exudates (Figure 20 and Table 2), are effective in preventing plants from developing Fe deficiency symptoms when grown under low Fe availability. Noteworthy, an indirect mode of action of these coumarins, such as via the involvement of microbial Fe(III) dissolution (Marschner et al., 2011), can be excluded because plants grown in agar culture were kept under axenic conditions (Figure 24). Since the chlorotic phenotype of *f6'h1-1* plants could not be rescued in absence of Fe from the growth medium (Figure 26), the supplied coumarins did apparently not remobilize Fe from the root apoplast or another plant-endogenous pool, as it was shown in rice for some phenols (Ishimaru et al., 2011). Instead, their effectiveness depended on the presence of an external Fe source, supporting a crucial role of the released coumarins in Fe mobilization from the rhizosphere. A similar effect was demonstrated for root-released phenolics in red clover, which are essential in

preventing these plants from Fe deficiency by reutilization of Fe from the root apoplast (Jin et al., 2007). Furthermore, the results presented here show that a successful regreening of the chlorotic *f6'h1* mutant in calcareous substrate depends on intact *FIT*, *IRT1* and *FRO2* activity. In fact, the chlorotic phenotypes of *fit, irt1 and fro2* mutants grown on calcareous substrate could not be prevented by the application of esculin or esculetin (Figure 33, Figure 35 and Figure 38Figure 39).

Amongst the coumarins that prevented *f6'h1-1* plants from Fe deficiency-induced chlorosis (Figure 24), only esculetin was able to mobilize Fe(III) from precipitated Fe hydroxide *in vitro* (Figure 41A). This implies a direct involvement of esculetin in Fe chelation and delivery to plants. So far the chemical identity of the root exudate compounds conferring Fe mobilization could not yet be completely resolved, but a part of the resulting Fe(III) complexes formed in the mobilization assay showed absorption at 460 nm (Figure 23B), which is indicative for Fe(III)-catechol complexes (McBryde, 1964; Salama et al., 1978; Ormö et al., 1992). In fact, not only coumarins, but also phenols have been shown to chelate Fe(III) *in vitro*, if they contain two adjacent hydroxy groups (Andjelkovic et al., 2006; Mladenka et al., 2010). The fact that scopoletin and esculin were incapable of mobilizing any Fe(III) provides further support to the notion that the two adjacent hydroxyl groups of the coumarin must be accessible for Fe(III) chelation (Mladenka et al., 2010). Esculetin (6,7-dihydroxycoumarin) and fraxetin (7,8-dihydroxy-6-methoxycoumarin) are the only coumarins identified in the present study to harbor such two adjacent hydroxy groups (Figure 20I and Harborne and Baxter, 1993). In the other identified coumarins the hydroxy group is not accessible as it is for example methylated (scopoletin; Figure 20E) or engaged in a glycosidic linkage (esculin; Figure 20G). Importantly, a structure with two adjacent hydroxy groups resembles that of catechol-type siderophores produced and released by bacteria or fungi to mobilize and chelate Fe (Table 1 and Hider and Kong, 2010).

In general, Fe(III) complexation by catechols occurs over a wide pH range up to 9 (Powell and Taylor, 1982) and thus catechol-mediated Fe(III) chelation can occur in alkaline soils. This was supported by the mobilization assays of the present study, which were performed at high pH (Figure 22 and Figure 23A), indicating that Fe(III) mobilization and chelation by coumarins is not sensitive to alkaline pH.

In fact, also the Fe(III) mobilization assay with esculetin was performed at alkaline pH (Figure 41A). Furthermore, by modeling Fe(III)-esculetin complex formation in dependence of pH (Figure 43A), it was revealed that at high pH an excess amount of the ligand compared to the metal is needed to form a stable complex that would be able to outcompete other Fe-complexes. Complex formation of catechol ligands with Fe(III) is particularly very sensitive to pH, as protons compete with Fe(III) for binding to the ligand. As shown in the speciation plot of Fe(III)-hydroxide and Fe(III)-esculetin complexes in Figure 43A, at high pH, esculetin is de-protonated and stably binds Fe(III) in a 3:1 ratio. However, at low pH, the hydroxy groups of esculetin become protonated and bind Fe in a 2:1 or 1:1 ratio, which are rather unstable complexes (Mladenka et al., 2010) or are no longer available for Fe(III) binding. In contrast to bidentate coumarins like esculetin, phytosiderophores like mugineic acid are hexadentate ligands and their six binding ligands are carboxy-, amino- and hydroxyl-groups (Table 1; Hider and Kong, 2010; Sugiura and Nomoto, 1984). A hexadentate chelation is more effective than chelation of Fe(III) mediated by individual ligands, which is the case when esculetin forms a 3:1 complex with Fe(III). Interestingly, the affinity of esculetin to bind Fe(III) is similar to phytosiderophores such as 2'-deoxymugineic acid (DMA) and mugineic acid (MA) (Table 3 and Murakami et al., 1989). Nevertheless, due to the different nature of their binding ligands these complexes differ regarding their pH stability. The hexadentate ligands, like those found in phytosiderophores, are less quickly protonated at low pH than catecholates like e.g. esculetin, especially when such hexadentate ligands are hydroxylated (von Wirén et al., 1999; von Wirén et al., 2000).

The mobilization assays (Figure 22 and Figure 23A) showed also that coumarins form a complex with Fe(III), as they were performed at high pH. In the case of phytosiderophores, Fe(III) is complexed with higher affinity than Fe(II) (von Wirén et al., 1999). However, investigations on the metal specificity of esculetin have not been the subject of this study. It might be that esculetin is also able to bind divalent cations like zinc(II), as it is known for phytosiderophores (Treeby et al., 1989; Shenker et al., 2001). However, literature data supporting this assumption were not found. Nevertheless, under high pH conditions the ferric form generally dominates over ferrous Fe (Scheffer and Schachtschabel, 2002) which makes it unlikely that the chelation of ferrous Fe is relevant in the soil.

Furthermore, it was attempted to quantify to what extent the Fe(III) mobilization capacity of root exudates from Fe-deficient Arabidopsis plants was caused by esculetin (Figure 42). Therefore it was calculated how much of the esculetin present in the exudates employed in the Fe(III) mobilization assay was able to mobilize the amount of measured Fe. Unfortunately, this contribution turned out to be very small. Nevertheless, this question was also addressed experimentally. Esculetin was therefore added in amounts that reflected the increased level in exudates obtained from Fe-deficient wild type, to exudates collected from Fe-sufficient wild-type or from mutant plants. The Fe(III) mobilization capacity of these exudates could not be increased (Figure 42). This result might be related to the low sensitivity of this assay (Figure 41B). Furthermore, since the identity of many of the coumarins detected in the root exudates still remains to be resolved (Table 2), it cannot be excluded that other exudate compounds or a combination of them contributed to Fe(III) mobilization. It is therefore a future challenge to determine the nature of the remaining unknown coumarins (Table 2), which could not yet be identified by the LC-ESI-MS method, and to develop approaches for a direct comparison of the Fe(III) mobilization capacity of individual root exudate components. The separation of individual components of root exudates from Fe-deficient wild-type plants can be achieved by e.g. HPLC fractionation and subsequent annotation by LC-MS (Döll, 2013). Fractions of interest could also be 'preselected' according to their possible Fe(III) chelating ability and for this reason be subjected to colorimetric assays as introduced by Schwyn and Neilands (1987) and refined by Milagres et al. (1999) and Shin et al. (2001). This assay is able to detect catechol-type siderophores by their interaction with Fe(III) that was formerly bound to chrome azurol S (CAS) (Terano et al., 2002; Radzki et al., 2013; Alexander and Zuberer, 1991). In order to directly measure the proportion and speciation of Fe(III)-esculetin complexes in root exudates, samples could be spiked with Fe(III) and analyzed by hydrophilic interaction chromatography/Fourier transform ion cyclotron resonance coupled to high-resolution MS (HILIC-FTICR/MS) (Weber et al., 2006; Köster et al., 2011).

Interestingly, coumarins not only display Fe(III)-chelating, but also Fe(III)-reducing abilities. In this regard, even when ferric-chelate reductase is severely inhibited, as it is the case in the *fro2* mutant (Robinson et al., 1999), Fe deficiency-mediated

chlorosis could nonetheless be restored through coumarin supply (Figure 39). However, this strongly depended on the ambient pH (Figure 39) and was not the case on calcareous substrate (Figure 38). In order to see whether plants are able to reduce Fe(III) chelated by esculetin, an assay was designed that measures the amount of produced Fe(II) when plant roots were incubated with an Fe(III)-esculetin solution. As shown in Figure 44, this was indeed the case in wild-type plants where ferric-chelate reductase activity, mainly mediated by FRO2, was fully functional. Yet, most likely due to the decreased ferric-chelate reductase activity at alkaline pH (Romera et al., 1997; Alcantara et al., 2000; Lucena et al., 2007; Santi and Schmidt, 2009), this ability was clearly lower when the assay was performed at pH 7.2 (Figure 44B). Obviously in the case of the successful restoration of the chlorotic *fro2* mutant by esculetin supply (Figure 39), processes other than root ferric-chelate reductase activity must have been able to assist Fe reduction at pH 5.6. As shown in Figure 43B and C, esculetin acted as a reductant and facilitated Fe(III) reduction from Fe(III)-esculetin or other Fe(III)-complexes as soon as the pH turned slightly acidic. Therefore it can be concluded that esculetin contributes to the reduction of ferric Fe whenever it enters acidic environments, such as the root apoplast, whereas under alkaline conditions Fe(III) reduction by coumarins may not be relevant (Figure 39). This is in accordance with studies from Mladenka et al. (2010), who showed that some coumarins are able to reduce Fe(III), even though the efficiency of this reaction is significantly decreased under high pH.

The ability of esculetin to reduce Fe(III) might be explained by the nature of the catecholate ligand of esculetin. In general, hexadentate Fe(III) complexes like those of phytosiderophores have a more negative redox potential than bidentate complexes like Fe(III)-esculetin (Hider and Kong, 2010). In cooperation with the group of Robert C. Hider (King's College, London) the redox potential of esculetin-Fe(III) was determined to be approximately +270 mV, while that of mugineic acid-Fe(III) is approximately -102 mV (Sugiura and Nomoto, 1984). A highly negative redox potential renders a complex more redox-stable (Hider and Kong, 2010). Interestingly, in low pH conditions the value of the redox potential can increase and in complexes where catechol-type ligands are involved, this might even lead to internal redox reactions with Fe(III), thus enabling reduction of Fe(III) (Hider and Kong, 2010; Mladenka et al., 2010).

Overall, these findings indicate that the F6'H1-dependent coumarin esculetin is a potent chelator in high pH environments, that is able to assist plants Fe acquisition. Esculetin is able to mobilize and chelate Fe(III) with affinities comparable to phytosiderophores like mugineic acid. At low pH, Fe(III)-esculetin complexes become less redox-stable and thus facilitate Fe(III) reduction. However, the contribution of esculetin and other exudate compounds to the total Fe(III) chelation capacity of root exudates remains to be elucidated.

5.5 Structural modifications and additional roles of F6'H1-dependent metabolites in the rhizosphere

One surprising observation in the present study was that although scopolin was the most abundant coumarin in roots, its aglycon scopoletin was the prevailing compound in root exudates (Figure 20). However, the higher accumulation of scopolin in roots may possibly help to overcome the low solubility of its aglycon scopoletin and protects it from intracellular oxidation (Chong et al., 1999). In addition, because scopoletin was more abundant in root exudates, it is likely that scopolin undergoes de-glycosylation just before or right after being exported across the root plasma membrane. This assumption is in agreement with the existence of root-expressed ß-glucosidases that have the capacity to hydrolyze scopolin (Ahn et al., 2010). Interestingly, such a modification is not restricted to the pair scopolin-scopoletin, but may also apply to esculin and its aglycon esculetin. While esculin was more abundant in roots, esculetin was mainly detected in root exudates (Figure 20G to J). Similar to scopoletin, further chemical modifications in the root apoplast may be involved in the enrichment of esculetin in root exudates, since esculin can also serve as substrate for root-expressed ß-glucosidases (Ahn et al., 2010). The conversion of esculin to esculetin could be clearly monitored by the assay developed by Edberg et al. (1977) and Trepeta and Edberg (1987) and for which the results are shown in Figure 45. A dark brown color formation indicating Fe-esculetin complex formation was observed when plant roots were incubated with Fe and esculin, leading to the conclusion that esculin had been de-glycosylated to form the catechol-type Fe(III) chelator esculetin (Figure 45). Such a de-glycosylation could help to explain why esculin was able to alleviate Fe deficiency symptoms in *f6'h1-1* plants even though it was not capable of mobilizing

insoluble Fe (Figure 41A). The conversion of esculin in the root apoplast makes it to those F6'H1-dependent fluorescent coumarins that were effective in Fe(III) mobilization. Such enzymatically accomplished structural modifications of metabolites are also occurring in bacteria. For example, some microorganisms like *Listeria monocytogenes* produce esculetin mainly from the hydrolysis of plant-derived esculin, since these bacteria do not synthesize esculetin by themselves but need it as exogenous siderophore to acquire Fe (Coulanges et al., 1996). Nevertheless, as the assay from Figure 45 is performed in 'semi' sterile conditions, plants from axenic cultures were used, it is unlikely that other processes than enzymatic activities mediated by plants, like microbial actions (Coulanges et al., 1996), were able to catalyze such a reaction in such a short time period. Furthermore, since Fe supply during the pre-culture of either wild-type or mutant plants did not affect the rate of Fe(III)-esculetin complex formation (Figure 45), it can be concluded that the capacity for esculin de-glycosylation in the root apoplast is not regulated by Fe.

In an attempt to investigate whether scopoletin also undergoes structural modifications in the rhizosphere, de-methylation of this metabolite would result in esculetin, roots where incubated in a solution containing Fe and scopoletin. Unfortunately no color formation was detected in the medium (Figure 46A to D). Unexpectedly, roots incubated at pH 7.2 developed a blue coloration (Figure 46A, B and C). In fact, blue color formation may result from Fe bound to several metabolites (Roschzttardtz et al., 2009; Schwyn and Neilands, 1987). However, it remains to be elucidated if the color was indeed caused by the formation of an Fe(III)-complex or if other reactions were involved. In order to investigate more directly if scopoletin can give rise to esculetin in the rhizosphere, extracts from *f6'h1* roots supplied with scopoletin could be analysed by hydrophilic interaction chromatography/Fourier transform ion cyclotron resonance coupled to high-resolution MS (HILIC-FTICR/MS) to detect the presence of Fe(III)-esculetin complexes (Weber et al., 2006; Köster et al., 2011). Alternatively, esculetin concentrations could be measured in these extracts via LC-MS.

The large amount of scopoletin that was found in the root exudates was noteworthy (Figure 20B, F). Therefore it is tempting to speculate that it might play a dual function in the rhizosphere. On the one hand scopoletin likely serves as the

precursor for catechol-type Fe(III) chelators. On the other hand, the coumarin scopoletin has been linked to plant defense due to its antimicrobial and antioxidative activities (Kai et al., 2006; Gachon et al., 2004; Garcia et al., 1995; El Modafar et al., 1993; Goy et al., 1993). Interestingly, the transcriptional regulation of *F6'H1* responds to various biotic stresses (Genevestigator; Zimmermann et al., 2004). In addition, MYB72 responds not only to Fe deficiency (Figure 8) but also to colonization with *Pseudomonas fluorescens* WCS417 bacteria, which activates induced systemic resistance in plants (Van der Ent et al., 2008). Thus the synthesis of scopoletin is not solely a response to Fe deficiency but rather responds to other stresses as well, therefore making a dual function of this metabolite especially in the rhizosphere even more likely.

Furthermore, possible allelopathic activities of the phenolic compound scopoletin (Schumacher et al., 1983) might be crucial in the rhizosphere. It has been described that some phenolics are released in significant amounts in the rhizosphere in order to decrease microbial populations, as they can act as nutrient competitors or to stimulate microbial metabolism in favor of auxin or siderophore production (Jin et al., 2006; Jin et al., 2010). Moreover, it is not yet clear if released coumarins might also be subject to microbial degradation as it is the case for phytosiderophores or citrate (von Wirén et al., 1993; Pinton et al., 2007). Thus, the release of huge amounts of scopoletin could eventually secure a sufficient quantity to serve for Fe nutrition purposes. It would be interesting to assess if *F6'H1* expression is also diurnally regulated, as described for *FRO2* and *IRT1* (Vert et al., 2003) and if the release of F6'H1-dependent fluorescent metabolites occurs in a comparable diurnal rhythm as the release of phytosiderophores by barley. In fact, in this plant species phytosiderophores are released in a concentrated fashion right after sunrise to increase the probability that they successfully deliver Fe before microbial degradation takes place (Marschner, 2012).

In summary, it can be proposed that esculin and most likely also scopoletin undergo modifications in the rhizosphere rendering them effective to become catechol-type Fe(III) chelators. Further investigations will be necessary, especially in the case of scopoletin, to determine the exact nature of the involved enzymatic reactions.

5.6 The synthesis and release of coumarins is part of the Fe acquisition machinery in *Arabidopsis thaliana*

The results presented in this thesis allow an extension of the current model of Strategy I-type Fe acquisition in *Arabidopsis thaliana* (Kobayashi and Nishizawa, 2012). This extension includes a mechanism that involves the F6'H1-dependent synthesis of coumarins that are released in order to mediate mobilization and under particular conditions, reduction of Fe(III) in the rhizosphere (Figure 48).

According to this model, once Fe deficiency is sensed within *Arabidopsis thaliana* plants (1), a signaling cascade is triggered (Giehl et al., 2009) that ultimately leads to the activation of the bHLH transcription factor FIT (Colangelo and Guerinot, 2004) (2). FIT in turn directly regulates the expression of plasma membrane-expressed Fe acquisition genes that are required for proton extrusion by the H^+-ATPase (AHA2, Santi and Schmidt, 2009), the reduction of Fe(III) (FRO2, Robinson et al., 1999; Connolly et al., 2003) and the uptake of Fe(II) (IRT1, Eide et al., 1996; Varotto et al., 2002; Vert et al., 2002). Furthermore, FIT also regulates *F6'H1* (3), a key enzyme of the phenylpropanoid pathway which is required for the biosynthesis of fluorescent coumarins (5). Additionally, the Fe deficiency-induced synthesis of these coumarins is also dependent on the transcription factor MYB72 (4) (Van der Ent et al., 2008; Zamioudis, 2012) which is regulated by FIT as well (Colangelo and Guerinot, 2004; Sivitz et al., 2012). The up-regulation of *F6'H1* and *MYB72* expression in plants experiencing Fe deficiency induces the synthesis of several F6'H1-dependent metabolites within the phenylpropanoid pathway (5). These metabolites include e.g. the coumarins scopolin, scopoletin, esculin and esculetin that accumulate in roots and are secreted into the rhizosphere most likely via the ABC transporter ABCG37/PDR9 (6) (Fourcroy et al., 2014). In order to become effective in Fe(III) mobilization, two adjacent hydroxyl groups must be accessible for Fe(III) chelation. In scopoletin and esculin, for example, these groups are occupied and hence structural modifications like de-glycosylation and de-methylation processes (7) must occur in the rhizosphere. These processes can convert them into catechol-type siderophores that have Fe(III)-chelating properties and are able to mobilize Fe(III) especially at high pH (8). In this way, chelated Fe(III) reaches the proximity of the plasma membrane, where reduction of Fe(III) (9) and subsequent uptake as Fe(II) can occur (11). Additionally, in low pH

conditions, coumarin-chelated Fe(III) can also be reduced within the complex (10) and is therefore prepared for uptake via IRT1 (11) without the requirement of an additional reduction step.

With the results presented in this thesis the components of Strategy I-type Fe acquisition must be expanded by adding a so far uncharacterized mechanisms that involves F6'H1-dependent synthesis and secretion of fluorescent coumarins that have Fe(III) chelating and reducing abilities. This contributes to closing a gap that has long-existed in our understanding of the Strategy I-type Fe acquisition, namely the process of mobilization of Fe(III) from soil particles and its subsequent transfer to the plasma membrane of plant roots.

The outcome of this work is of agronomical significance as it might mark the basis for the design of effective chelators for Fe fertilization of plants growing on calcareous soils. Regarding the field of plant nutrition and plant breeding, the present work might stimulate the development of root fluorescence-based screening procedures and visual or biochemical markers that are useful for the identification of Fe-efficient genotypes. Furthermore, the root specific- and Fe deficiency-induced overexpression of the genes from the phenylpropanoid pathway in transgenic crop plants could eventually contribute to increase Fe efficiency.

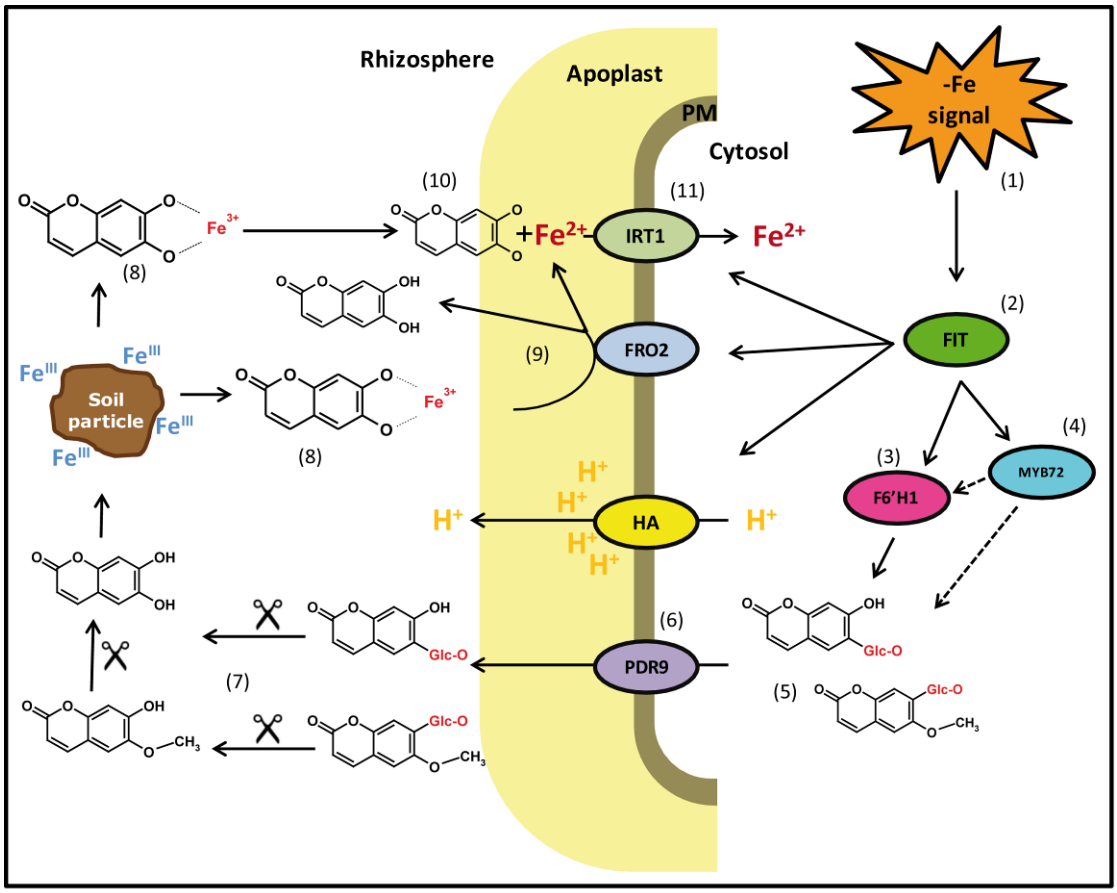

Figure 48. Working model depicting the role of F6'H1 in Fe acquisition in Strategy I plants. An Fe-deficiency signal leads to the activation of FIT, which mediates the up-regulation of the Fe-acquisition apparatus and of *F6'H1*. Furthermore, *MYB72* is also regulated by FIT and might regulate coumarin synthesis, either or not, via F6'H1. The activation of F6'H1 then results in the synthesis of coumarins, that are secreted into the rhizosphere via PDR9 and likely subjected to several structural modification to result in catechol-type Fe-chelators. Their Fe-mobilizing ability then assists Fe uptake via IRT1 especially in conditions of low Fe availability (e.g. high pH). Abbreviations: FRO2, ferric-chelate reductase oxidase; HA, H^+-ATPase; IRT1, Fe-regulated transporter; FIT, FER-like Fe deficiency–induced transcription factor; F6'H1, 2-oxoglutarate-dependent dioxygenase; -Fe, Fe-deficiency signal; PDR9, transporter of phenolic compounds; MYB72, R2R3-MYB-like transcription factor 72; PM, plasma membrane. Dashed lines indicate putative functions. Illustration modified from Kobayashi and Nishizawa (2012).

6 References

Abadía J, Abadía A (1993) Iron and plant pigments. In: Iron Chelation in Plants and Soil Microorganisms, L.L. Barton and B.C. Hemming, eds., Academic Press INC., San Diego, CA, USA

Abadía J, Álvarez-Fernández A, Rombolaà AD, Sanz M, Tagliavini M, Abadía A (2004) Technologies for the diagnosis and remediation of Fe deficiency. Soil Science and Plant Nutrition **50:** 965-971

Ahn YO, Shimizu B, Sakata K, Gantulga D, Zhou C, Bevan DR, Esen A (2010) Scopolin-hydrolyzing beta-glucosidases in roots of Arabidopsis. Plant and Cell Physiology **51:** 132-143

Alcantara E, Romera FJ, Canete M, de la Guardia MD (2000) Effects of bicarbonate and iron supply on Fe(III) reducing capacity of roots and leaf chlorosis of the susceptible peach rootstock "Nemaguard". Journal of Plant Nutrition **23:** 1607-1617

Alexander DB, Zuberer DA (1991) Use of chrome azurol S reagents to evaluate siderophore production by rhizosphere bacteria. Biology and fertility of soils **12:** 39-45

Alfè D, Gillan MJ, Price GD (2002) Composition and temperature of the Earth's core constrained by combining ab initio calculations and seismic data. Earth and Planetary Science Letters **195:** 91-98

Alonso JM, Stepanova AN, Leisse TJ, Kim CJ, Chen H, Shinn P, Stevenson DK, Zimmerman J, Barajas P, Cheuk R, Gadrinab C, Heller C, Jeske A, Koesema E, Meyers CC, Parker H, Prednis L, Ansari Y, Choy N, Deen H, Geralt M, Hazari N, Hom E, Karnes M, Mulholland C, Ndubaku R, Schmidt I, Guzman P, Aguilar-Henonin L, Schmid M, Weigel D, Carter DE, Marchand T, Risseeuw E, Brogden D, Zeko A, Crosby WL, Berry CC, Ecker JR (2003) Genome-wide insertional mutagenesis of *Arabidopsis thaliana*. Science **301:** 653-657

Álvarez-Fernández A, Abadía J, Abadía A (2007) Iron deficiency, fruit yield and fruit quality. In: Iron Nutrition in Plants and Rhizospheric Microorganisms, L.L. Barton and J. Abadia, Springer, Dordrecht, The Netherlands

Andjelkovic M, Van Camp J, De Meulenaer B, Depaemelaere G, Socaciu C, Verloo M, Verhe R (2006) Iron-chelation properties of phenolic acids bearing catechol and galloyl groups. Food Chemistry **98:** 23-31

Barberon M, Zelazny E, Robert S, Conejero G, Curie C, Friml J, Vert G (2011) Monoubiquitin-dependent endocytosis of the iron-regulated transporter 1 (IRT1) transporter controls iron uptake in plants. Proc Natl Acad Sci U S A **108:** E450-458

Bashir K, Inoue H, Nagasaka S, Takahashi M, Nakanishi H, Mori S, Nishizawa NK (2006) Cloning and characterization of deoxymugineic acid synthase genes from graminaceous plants. J Biol Chem **281:** 32395-32402

Beinert H, Holm RH, Munck E (1997) Iron-sulfur clusters: nature's modular, multipurpose structures. Science **277:** 653-659

Bourgaud F, Hehn A, Larbat R, Doerper S, Gontier E, Kellner S, Matern U (2006) Biosynthesis of coumarins in plants: a major pathway still to be unravelled for cytochrome P450 enzymes. Phytochemistry Reviews **5:** 293-308

Boxma R (1972) Bicarbonate as the most important soil factor in lime-induced chlorosis in the Netherlands. Plant and Soil **37:** 233-243

Briat JF, Ravet K, Arnaud N, Duc C, Boucherez J, Touraine B, Cellier F, Gaymard F (2010) New insights into ferritin synthesis and function highlight a link between iron homeostasis and oxidative stress in plants. Ann Bot **105:** 811-822

Buchanan B, Gruissem W, Jones R (2000) Biochemistry and Molecular Biology of Plants. John Wiley & Sons, Ltd., Courier Companies, Inc., USA

Buckhout T, Yang T, Schmidt W (2009) Early iron-deficiency-induced transcriptional changes in Arabidopsis roots as revealed by microarray analyses. BMC Genomics **10:** 147

Cesco S, Neumann G, Tomasi N, Pinton R, Weisskopf L (2010) Release of plant-borne flavonoids into the rhizosphere and their role in plant nutrition. Plant and Soil **329:** 1 - 25

Cesco S, Rombolà A, Tagliavini M, Varanini Z, Pinton R (2006) Phytosiderophores released by graminaceous species promote 59Fe-uptake in citrus. Plant and Soil **287:** 223-233

Chaney RL, Hamze MH, Bell PF (1992) Screening chickpea for iron chlorosis resistance using bicarbonate in nutrient solution to simulate calcareous soils. Journal of Plant Nutrition **15:** 2045-2062

Chen Y, Barak P (1982) Iron Nutrition of Plants in Calcareous Soils. Advances in Agronomy **35:** 217-240

Chomczynski P, Sacchi N (1987) Single-Step Method of Rna Isolation by Acid Guanidinium Thiocyanate Phenol Chloroform Extraction. Analytical Biochemistry **162:** 156-159

Chong J, Baltz R, Fritig B, Saindrenan P (1999) An early salicylic acid-, pathogen- and elicitor-inducible tobacco glucosyltransferase: role in compartmentalization of phenolics and H2O2 metabolism. Febs Letters **458:** 204-208

Chong J, Baltz R, Schmitt C, Beffa R, Fritig B, Saindrenan P (2002) Downregulation of a Pathogen-Responsive Tobacco UDP-Glc:Phenylpropanoid Glucosyltransferase Reduces Scopoletin Glucoside Accumulation, Enhances Oxidative Stress, and Weakens Virus Resistance. The Plant Cell Online **14:** 1093-1107

Clough SJ, Bent AF (1998) Floral dip: a simplified method for Agrobacterium-mediated transformation of *Arabidopsis thaliana*. Plant Journal **16:** 735-743

Cohen CK, Garvin DF, Kochian LV (2004) Kinetic properties of a micronutrient transporter from Pisum sativum indicate a primary function in Fe uptake from the soil. Planta **218:** 784-792

Colangelo EP, Guerinot ML (2004) The essential basic helix-loop-helix protein FIT1 is required for the iron deficiency response. Plant Cell **16:** 3400-3412

Connolly EL, Campbell NH, Grotz N, Prichard CL, Guerinot ML (2003) Overexpression of the FRO2 ferric chelate reductase confers tolerance to growth on low iron and uncovers posttranscriptional control. Plant Physiology **133:** 1102-1110

Coulanges V, André P, Vidon DJM (1996) Esculetin antagonizes iron-chelating agents and increases the virulence of Listeria monocytogenes. Research in Microbiology **147:** 677-685

Curie C, Cassin G, Couch D, Divol F, Higuchi K, Jean M, Misson J, Schikora A, Czernic P, Mari S (2009) Metal movement within the plant: contribution of nicotianamine and yellow stripe 1-like transporters. Annals of Botany **103:** 1-11

Curie C, Panaviene Z, Loulergue C, Dellaporta S, Briat J, Walker E (2001) Maize yellow stripe1 encodes a membrane protein directly involved in Fe(III) uptake. Nature **409:** 346 - 349

Dakora F, Phillips D (2002) Root exudates as mediators of mineral acquisition in low-nutrient environments. Plant and Soil **245:** 35-47

Delhaize E (1996) A metal-accumulator mutant of *Arabidopsis thaliana*. Plant Physiology **111:** 849-855

Dinneny JR, Long TA, Wang JY, Jung JW, Mace D, Pointer S, Barron C, Brady SM, Schiefelbein J, Benfey PN (2008) Cell identity mediates the response of Arabidopsis roots to abiotic stress. Science **320:** 942-945

Döll S (2013) ”Studies on Scopolin and Scopoletin - Stress-Induced Accumulation and Regulatory Elements". Dissertation. Martin-Luther-Universität Halle-Wittenberg, Halle/Saale

Durrett TP, Gassmann W, Rogers EE (2007) The FRD3-Mediated Efflux of Citrate into the Root Vasculature Is Necessary for Efficient Iron Translocation. Plant Physiology **144:** 197-205

Eckhardt U, Mas Marques A, Buckhout T (2001) Two iron-regulated cation transporters from tomato complement metal uptake-deficient yeast mutants. Plant Mol Biol **45:** 437 - 448

Edberg S, Pittman S, Singer J (1977) The use of bile-esculin agar for the taxonomic classification of the family Enterobacteriaceae. Antonie van Leeuwenhoek **43:** 31-35

Eide D, Broderius M, Fett J, Guerinot M (1996) A novel iron-regulated metal transporter from plants identified by functional expression in yeast. Proc Natl Acad Sci USA **93:** 5624 - 5628

El Modafar C, Clerivet A, Fleuriet A, Macheix JJ (1993) Inoculation of Platanus acerifolia with Ceratocystis fimbriata F. Sp. Platani induces scopoletin and umbelliferone accumulation. Phytochemistry **34:** 1271-1276

Fourcroy P, Sisó-Terraza P, Sudre D, Savirón M, Reyt G, Gaymard F, Abadía A, Abadia J, Álvarez-Fernández A, Briat J-F (2014) Involvement of the ABCG37 transporter in secretion of scopoletin and derivatives by Arabidopsis roots in response to iron deficiency. New Phytologist **201:** 155-167

Frossard E, Bucher M, Mächler F, Mozafar A, Hurrell R (2000) Potential for increasing the content and bioavailability of Fe, Zn and Ca in plants for human nutrition. Journal of the Science of Food and Agriculture **80:** 861-879

Fuglsang AT, Guo Y, Cuin TA, Qiu Q, Song C, Kristiansen KA, Bych K, Schulz A, Shabala S, Schumaker KS, Palmgren MG, Zhu J-K (2007) Arabidopsis Protein Kinase PKS5 Inhibits the Plasma Membrane H^+-ATPase by Preventing Interaction with 14-3-3 Protein. The Plant Cell Online **19:** 1617-1634

Gachon C, Baltz R, Saindrenan P (2004) Over-expression of a scopoletin glucosyltransferase in Nicotiana tabacum leads to precocious lesion formation during the hypersensitive response to tobacco mosaic virus but does not affect virus resistance. Plant Molecular Biology **54:** 137-146

Garcia D, Sanier C, Macheix JJ, D'Auzac J (1995) Accumulation of scopoletin in Hevea brasiliensis infected by *Microcyclus ulei* (P. Henn.) V. ARX and evaluation of its fungitoxicity for three leaf pathogens of rubber tree. Physiological and Molecular Plant Pathology **47:** 213-223

García-Marco S, Martínez N, Yunta F, Hernández-Apaolaza L, Lucena J (2006) Effectiveness of Ethylenediamine-N(o-hydroxyphenylacetic)-N′(p-hydroxyphenylacetic) acid (o,p-EDDHA) to Supply Iron to Plants. Plant and Soil **279:** 31-40

García MJ, García-Mateo MJ, Lucena C, Romera FJ, Rojas CL, Alcántara E, Pérez-Vicente R (2014) Hypoxia and bicarbonate could limit the expression of iron acquisition genes in Strategy I plants by affecting ethylene synthesis and signalling in different ways. Physiologia Plantarum **150(1):** 95-106

Giehl RFH, Meda AR, von Wirén N (2009) Moving up, down, and everywhere: signaling of micronutrients in plants. Current Opinion in Plant Biology **12:** 320-327

Giehl RFH (2011) Identification of Regulatory Factors Determining Nutrient Acquisition in Arabidopsis. Dissertation. Universität Hohenheim, Stuttgart

Goy PA, Signer H, Reist R, Aichholz R, Blum W, Schmidt E, Kessmann H (1993) Accumulation of scopoletin is associated with the high disease resistance of the hybrid Nicotiana glutinosa x Nicotiana debneyi. Planta **191:** 200-206

Guerinot M, Yi Y (1994) Iron: nutritious, noxious, and not readily available. Plant Physiology **104:** 815 - 820

Hansch R, Mendel R (2009) Physiological functions of mineral micronutrients (Cu, Zn, Mn, Fe, Ni, Mo, B, Cl). Curr Opin Plant Biol **12:** 259 - 266

Hansen N, Hopkins B, Ellsworth J, Jolley V (2007) Iron nutrition in field crops. pp23 – 59 In: Iron Nutrition in Plants and Rhizospheric Microorganisms, L.L. Barton and J. Abadia, Springer, Dordrecht, The Netherlands

Harborne J, Baxter H (1993) Phytochemical Dictionary A Handbook of Bioactive Compounds from Plants. Taylor & Francis London, Washington DC

Harrington J, Crumbliss A (2009) The redox hypothesis in siderophore-mediated iron uptake. BioMetals **22:** 679-689

Henriques R, Jasik J, Klein M, Martinoia E, Feller U, Schell J, Pais MS, Koncz C (2002) Knock-out of Arabidopsis metal transporter gene IRT1 results in iron deficiency accompanied by cell differentiation defects. Plant Mol Biol **50:** 587-597

Hider RC, Kong X (2010) Chemistry and biology of siderophores. Natural Product Reports **27:** 637-657

Hindt MN, Guerinot ML (2012) Getting a sense for signals: regulation of the plant iron deficiency response. Biochim Biophys Acta **1823:** 1521-1530

Hinsinger P (1998) How Do Plant Roots Acquire Mineral Nutrients? Chemical Processes Involved in the rhizosphere. In: LS Donald, ed, Advances in Agronomy, Vol Volume 64. Academic Press, pp 225-265

Ishimaru Y, Kakei Y, Shimo H, Bashir K, Sato Y, Sato Y, Uozumi N, Nakanishi H, Nishizawa NK (2011a) A Rice Phenolic Efflux Transporter Is Essential for Solubilizing Precipitated Apoplasmic Iron in the Plant Stele. Journal of Biological Chemistry **286:** 24649-24655

Ishimaru Y, Bashir K, Nakanishi H, Nishizawa NK (2011b) The role of rice phenolics efflux transporter in solubilizing apoplasmic iron. Plant Signal Behav **6:** 1624-1626

Ishimaru Y, Suzuki M, Tsukamoto T, Suzuki K, Nakazono M, Kobayashi T, Wada Y, Watanabe S, Matsuhashi S, Takahashi M, Nakanishi H, Mori S, Nishizawa NK (2006) Rice plants take up iron as an Fe3+-phytosiderophore and as Fe^{2+}. The Plant Journal **45:** 335-346

Ivanov R, Brumbarova T, Bauer P (2012) Fitting into the Harsh Reality: Regulation of Iron-deficiency Responses in Dicotyledonous Plants. Molecular Plant **5(1)**: 27-42

Jakoby M, Wang HY, Reidt W, Weisshaar B, Bauer P (2004) FRU (BHLH029) is required for induction of iron mobilization genes in *Arabidopsis thaliana*. Febs Letters **577:** 528-534

Jin CW, He YF, Tang CX, Wu P, Zheng SJ (2006) Mechanisms of microbially enhanced Fe acquisition in red clover (Trifolium pratense L.). Plant Cell Environ **29:** 888-897

Jin CW, Li GX, Yu XH, Zheng SJ (2010) Plant Fe status affects the composition of siderophore-secreting microbes in the rhizosphere. Ann Bot **105:** 835-841

Jin CW, You GY, He YF, Tang C, Wu P, Zheng SJ (2007) Iron deficiency-induced secretion of phenolics facilitates the reutilization of root apoplastic iron in red clover. Plant Physiol **144:** 278-285

Jin CW, You GY, Zheng SJ (2008) The iron deficiency-induced phenolics secretion plays multiple important roles in plant iron acquisition underground. Plant Signal Behav **3:** 60-61

Jones D (1998) Organic acids in the rhizosphere – a critical review. Plant and Soil **205:** 25-44

Kai K, Mizutani M, Kawamura N, Yamamoto R, Tamai M, Yamaguchi H, Sakata K, Shimizu B (2008) Scopoletin is biosynthesized via ortho-hydroxylation of feruloyl CoA by a 2-oxoglutarate-dependent dioxygenase in *Arabidopsis thaliana*. Plant Journal **55:** 989-999

Kai K, Shimizu B, Mizutani M, Watanabe K, Sakata K (2006) Accumulation of coumarins in *Arabidopsis thaliana*. Phytochemistry **67:** 379-386

Kim S, Guerinot M (2007) Mining iron: iron uptake and transport in plants. FEBS letters **581:** 2273 - 2280

Kim SA, Punshon T, Lanzirotti A, Li L, Alonso JM, Ecker JR, Kaplan J, Guerinot ML (2006) Localization of iron in Arabidopsis seed requires the vacuolar membrane transporter VIT1. Science **314:** 1295-1298

Kobayashi T, Nagasaka S, Senoura T, Itai RN, Nakanishi H, Nishizawa NK (2013) Iron-binding Haemerythrin RING ubiquitin ligases regulate plant iron responses and accumulation. Nat Commun **4:** 2792

Kobayashi T, Nakanishi H, Takahashi M, Kawasaki S, Nishizawa NK, Mori S (2001) In vivo evidence that Ids3 from Hordeum vulgare encodes a dioxygenase that converts 2'-deoxymugineic acid to mugineic acid in transgenic rice. Planta **212:** 864-871

Kobayashi T, Nishizawa NK (2012) Iron Uptake, Translocation, and Regulation in Higher Plants. Annual Review of Plant Biology **63:** 131-152

Kobayashi T, Ogo Y, Itai R, Nakanishi H, Takahashi M, Mori S, Nishizawa N (2007) The transcription factor IDEF1 regulates the response to and tolerance of iron deficiency in plants. Proc Natl Acad Sci USA **104:** 19150 - 19155

Korn M, Peterek S, Mock H-P, Heyer AG, Hincha DK (2008) Heterosis in the freezing tolerance, and sugar and flavonoid contents of crosses between *Arabidopsis thaliana* accessions of widely varying freezing tolerance. Plant, Cell & Environment **31:** 813-827

Korshunova Y, Eide D, Gregg Clark W, Lou Guerinot M, Pakrasi H (1999) The IRT1 protein from *Arabidopsis thaliana* is a metal transporter with a broad substrate range. Plant Molecular Biology **40:** 37-44

Köster J, Shi R, von Wirén N, Weber G (2011) Evaluation of different column types for the hydrophilic interaction chromatographic separation of iron-citrate and copper-histidine species from plants. J Chromatogr A **1218:** 4934-4943

Kranz HD, Denekamp M, Greco R, Jin H, Leyva A, Meissner RC, Petroni K, Urzainqui A, Bevan M, Martin C, Smeekens S, Tonelli C, Paz-Ares J, Weisshaar B (1998) Towards functional characterisation of the members of theR2R3-MYBgene family from *Arabidopsis thaliana*. The Plant Journal **16:** 263-276

Krysan PJ, Young JC, Sussman MR (1999) T-DNA as an Insertional Mutagen in Arabidopsis. The Plant Cell Online **11:** 2283-2290

Lan P, Li W, Wen TN, Shiau JY, Wu YC, Lin W, Schmidt W (2011) iTRAQ protein profile analysis of Arabidopsis roots reveals new aspects critical for iron homeostasis. Plant Physiology **155:** 821-834

Lanquar V, Lelievre F, Bolte S, Hames C, Alcon C, Neumann D, Vansuyt G, Curie C, Schroder A, Kramer U, Barbier-Brygoo H, Thomine S (2005) Mobilization of vacuolar iron by AtNRAMP3 and AtNRAMP4 is essential for seed germination on low iron. EMBO J **24:** 4041-4051

Leong J, Neilands JB (1976) Mechanisms of siderophore iron transport in enteric bacteria. Journal of Bacteriology **126:** 823-830

Li L, Cheng X, Ling H (2004) Isolation and characterization of Fe(III)-chelate reductase gene LeFRO1 in tomato. Plant Mol Biol **54:** 125 - 136

Lingam S, Mohrbacher J, Brumbarova T, Potuschak T, Fink-Straube C, Blondet E, Genschik P, Bauer P (2011) Interaction between the bHLH transcription factor FIT and ETHYLENE INSENSITIVE3/ETHYLENE INSENSITIVE3-LIKE1 reveals molecular linkage between the regulation of iron acquisition and ethylene signaling in Arabidopsis. Plant Cell **23:** 1815-1829

Lemanceau P, Bauer P, Kraemer S, Briat J-F (2009) Iron dynamics in the rhizosphere as a case study for analyzing interactions between soils, plants and microbes. Plant and Soil **321:** 513-535

Lucena C, Romera FJ, Rojas CL, Garcia M, Alcantara E, Perez-Vicente R (2007) Bicarbonate blocks the expression of several genes involved in the physiological responses to Fe deficiency of Strategy I plants. Functional Plant Biology **34:** 1002-1009

Lucena J (2007) Synthetic Iron Chelates to Correct Iron Deficiency in Plants, pp 103-129 In Iron Nutrition in Plants and Rhizospheric Microorganisms, L.L. Barton and J. Abadia, Springer, Dordrecht, The Netherlands

Lucena JJ (2000) Effects of bicarbonate, nitrate and other environmental factors on iron deficiency chlorosis. A review. Journal of Plant Nutrition **23:** 1591-1606

Ma JF, Nomoto K (1996) Effective regulation of iron acquisition in graminaceous plants. The role of mugineic acids as phytosiderophores. Physiologia Plantarum **97:** 609-617

Ma JF, Ryan PR, Delhaize E (2001) Aluminium tolerance in plants and the complexing role of organic acids. Trends in Plant Science **6:** 273-278

Ma JF, Shinada T, Matsuda C, Nomoto K (1995) Biosynthesis of Phytosiderophores, Mugineic Acids, Associated with Methionine Cycling. Journal of Biological Chemistry **270:** 16549-16554

Ma JF, Taketa S, Chang Y-C, Iwashita T, Matsumoto H, Takeda K, Nomoto K (1999) Genes controlling hydroxylations of phytosiderophores are located

on different chromosomes in barley (Hordeum vulgare L.). Planta **207:** 590-596

Malamy JE, Benfey PN (1997) Organization and cell differentiation in lateral roots of *Arabidopsis thaliana*. Development **124:** 33-44

Marschner P, ed (2012) Marschner's mineral nutrition of higher plants, Ed 3rd. Academic Press, San Diego, CA, USA

Marschner P, Crowley D, Rengel Z (2011) Rhizosphere interactions between microorganisms and plants govern iron and phosphorus acquisition along the root axis – model and research methods. Soil Biology and Biochemistry **43:** 883-894

Martinoia E, Klein M, Geisler M, Bovet L, Forestier C, Kolukisaoglu U, Muller-Rober B, Schulz B (2002) Multifunctionality of plant ABC transporters--more than just detoxifiers. Planta **214:** 345-355

Maslak A (2002) Einfluss erhöhter atmosphärischer CO_2-Konzentrationen auf den Sekundärstoffwechsel und Pathogenabwehrmechansimen von *Nicotiana tabacum*. Dissertation. Martin-Luther-Universität Halle-Wittenberg, Halle/Saale

Masse E, Arguin M (2005) Ironing out the problem: new mechanisms of iron homeostasis. Trends in Biochemical Sciences **30:** 462-468

Mayer JE, Pfeiffer WH, Beyer P (2008) Biofortified crops to alleviate micronutrient malnutrition. Current Opinion in Plant Biology **11:** 166-170

McBryde WAE (1964) A SPECTROPHOTOMETRIC REEXAMINATION OF THE SPECTRA AND STABILITIES OF THE IRON (III) – TIRON COMPLEXES. Canadian Journal of Chemistry **42:** 1917-1927

Mehrtens F, Kranz H, Bednarek P, Weisshaar B (2005) The Arabidopsis transcription factor MYB12 is a flavonol-specific regulator of phenylpropanoid biosynthesis. Plant Physiology **138:** 1083-1096

Meiser J, Lingam S, Bauer P (2011) Post-translational regulation of the Fe deficiency bHLH transcription factor FIT is affected by iron and nitric oxide. Plant Physiology **157(4)**: 2154-66

Mengel K, Breininger MT, Bübl W (1984) Bicarbonate, the most important factor inducing iron chlorosis in vine grapes on calcareous soil. Plant and Soil **81:** 333-344

Milagres AMF, Machuca A, Napoleão D (1999) Detection of siderophore production from several fungi and bacteria by a modification of chrome azurol S (CAS) agar plate assay. Journal of Microbiological Methods **37:** 1-6

Mladenka P, Macakova K, Zatloukalova L, Rehakova Z, Singh BK, Prasad AK, Parmar VS, Jahodar L, Hrdina R, Saso L (2010) In vitro interactions of coumarins with iron. Biochimie **92:** 1108-1114

Morrissey J, Baxter IR, Lee J, Li L, Lahner B, Grotz N, Kaplan J, Salt DE, Guerinot ML (2009) The Ferroportin Metal Efflux Proteins Function in Iron and Cobalt Homeostasis in Arabidopsis. The Plant Cell Online **21:** 3326-3338

Mukherjee I, Campbell NH, Ash JS, Connolly EL (2006) Expression profiling of the Arabidopsis ferric chelate reductase (FRO) gene family reveals differential regulation by iron and copper. Planta **223:** 1178-1190

Murakami T, Ise K, Hayakawa M, Kamei S, Takagi S-i (1989) Stabilities of Metal Complexes of Mugineic Acids and Their Specific Affinities for Iron(III). Chemistry Letters **18:** 2137-2140

Murashige T, Skoog F (1962) A Revised Medium for Rapid Growth and Bio Assays with Tobacco Tissue Cultures. Physiologia Plantarum **15:** 473-497

Murata Y, Ma J, Yamaji N, Ueno D, Nomoto K, Iwashita T (2006) A specific transporter for iron(III)-phytosiderophore in barley roots. Plant Journal **46:** 563 - 572

Neilands JB (1981) Iron Absorption and Transport in Microorganisms. Annual Review of Nutrition **1:** 27-46

Neumann G, Römheld V (2007) The Release of Root Exudates as Affected by the Plant Physiological Status, pp 23-73. In: The Rhizosphere: Biochemistry and Organic Substances at the Soil-Plant Interface. Second Edition. R. Pinton, Z. Varanini and P.Nannipieri, CRC Press, Taylor & Francis Group Boca Raton, FL

Norvell WA, Adams ML (2006) Screening Soybean Cultivars for Resistance to Iron-Deficiency Chlorosis in Culture Solutions Containing Magnesium or Sodium Bicarbonate. Journal of Plant Nutrition **29:** 1855-1867

Nozoye T, Nagasaka S, Kobayashi T, Takahashi M, Sato Y, Sato Y, Uozumi N, Nakanishi H, Nishizawa NK (2011) Phytosiderophore Efflux Transporters Are Crucial for Iron Acquisition in Graminaceous Plants. Journal of Biological Chemistry **286:** 5446-5454

Ogo Y, Itai R, Nakanishi H, Inoue H, Kobayashi T, Suzuki M, Takahashi M, Mori S, Nishizawa N (2006) Isolation and characterization of IRO2, a novel iron-regulated bHLH transcription factor in graminaceous plants. Journal of Experimental Botany **57:** 2867 - 2878

Ohwaki Y, Sugahara K (1997) Active extrusion of protons and exudation of carboxylic acids in response to iron deficiency by roots of chickpea (Cicer arietinum L). Plant and Soil **189:** 49-55

Ormö M, deMaré F, Regnström K, Aberg A, Sahlin M, Ling J, Loehr TM, Sanders-Loehr J, Sjöberg BM (1992) Engineering of the iron site in ribonucleotide reductase to a self-hydroxylating monooxygenase. Journal of Biological Chemistry **267:** 8711-8714

Palmgren MG (2001) PLANT PLASMA MEMBRANE H+-ATPases: Powerhouses for Nutrient Uptake. Annual Review of Plant Physiology and Plant Molecular Biology **52:** 817-845

Paoli M, Marles-Wright J, Smith A (2002) Structure-function relationships in heme-proteins. DNA Cell Biol **21:** 271-280

Pfaffl MW (2001) A new mathematical model for relative quantification in real-time RT-PCR. Nucleic Acids Research **29:** e45

Pinton R, Varanini Z, Nannipieri P (2007) The Rhizosphere: Biochemistry and Organic Substances at the Soil-Plant Interface. Second Edition. CRC Press, Taylor & Francis Group Boca Raton, FL

Porra RJ, Thompson WA, Kriedemann PE (1989) Determination of Accurate Extinction Coefficients and Simultaneous-Equations for Assaying Chlorophyll-a and Chlorophyll-B Extracted with 4 Different Solvents - Verification of the Concentration of Chlorophyll Standards by Atomic-Absorption Spectroscopy. Biochimica Et Biophysica Acta **975:** 384-394

Powell H, Taylor M (1982) Interactions of iron(II) and iron(III) with gallic acid and its homologues: a potentiometric and spectrophotometric study. Australian Journal of Chemistry **35:** 739-756

Radzki W, Gutierrez Manero FJ, Algar E, Lucas Garcia JA, Garcia-Villaraco A, Ramos Solano B (2013) Bacterial siderophores efficiently provide iron to

iron-starved tomato plants in hydroponics culture. Antonie van Leeuwenhoek **104:** 321-330

Ravet K, Touraine B, Boucherez J, Briat J-F, Gaymard F, Cellier F (2009) Ferritins control interaction between iron homeostasis and oxidative stress in Arabidopsis. The Plant Journal **57:** 400-412

Reichard PU, Kretzschmar R, Kraemer SM (2007) Dissolution mechanisms of goethite in the presence of siderophores and organic acids. Geochimica et Cosmochimica Acta **71:** 5635-5650

Robinson N, Procter C, Connolly E, Guerinot M (1999) A ferric-chelate reductase for iron uptake from soils. Nature **397:** 694 - 697

Rodriguez-Celma J, Lin WD, Fu GM, Abadia J, Lopez-Millan AF, Schmidt W (2013) Mutually Exclusive Alterations in Secondary Metabolism Are Critical for the Uptake of Insoluble Iron Compounds by Arabidopsis and Medicago truncatula. Plant Physiol **162:** 1473-1485

Rodriguez-Celma J, Vazquez-Reina S, Orduna J, Abadia A, Abadia J, Alvarez-Fernandez A, Lopez-Millan AF (2011) Characterization of flavins in roots of Fe-deficient strategy I plants, with a focus on Medicago truncatula. Plant and Cell Physiology **52:** 2173-2189

Rogers EE, Eide DJ, Guerinot ML (2000) Altered selectivity in an Arabidopsis metal transporter. Proc Natl Acad Sci U S A **97:** 12356-12360

Rogers EE, Guerinot ML (2002) FRD3, a Member of the Multidrug and Toxin Efflux Family, Controls Iron Deficiency Responses in Arabidopsis. The Plant Cell Online **14:** 1787-1799

Rombola A, Tagliavini M (2007) Iron Nutrition of Fruit Tree Crops, pp61-85. In: Iron Nutrition in Plants and Rhizospheric Microorganisms, L.L. Barton and J. Abadia, Springer, Dordrecht, The Netherlands

Romera FJ, Alcantara E, delaGuardia MD (1997) Influence of bicarbonate and metal ions on the development of root Fe(III) reducing capacity by Fe-deficient cucumber (Cucumis sativus) plants. Physiologia Plantarum **101:** 143-148

Römheld V, Marschner H (1981) Iron deficiency stress induced morphological and physiological changes in root tips of sunflower. Physiol Plant **53:** 354 - 360

Römheld V, Marschner H (1983) Mechanism of iron uptake by peanut plants : I. Fe reduction, chelate splitting, and release of phenolics. Plant Physiol **71:** 949-954

Römheld V, Marschner H (1986) Evidence for a specific uptake system for iron phytosiderophores in roots of grasses. Plant Physiology **80:** 175-180

Roschzttardtz H, Conéjéro G, Curie C, Mari S (2009) Identification of the Endodermal Vacuole as the Iron Storage Compartment in the Arabidopsis Embryo. Plant Physiology **151:** 1329-1338

Roschzttardtz H, Séguéla-Arnaud M, Briat J-F, Vert G, Curie C (2011) The FRD3 Citrate Effluxer Promotes Iron Nutrition between Symplastically Disconnected Tissues throughout Arabidopsis Development. The Plant Cell Online **23:** 2725-2737

Salama S, Stong JD, Neilands JB, Spiro TG (1978) Electronic and resonance Raman spectra of iron(III) complexes of enterobactin, catechol, and N-methyl-2,3-dihydroxybenzamide. Biochemistry **17:** 3781-3785

Santi S, Schmidt W (2009) Dissecting iron deficiency-induced proton extrusion in Arabidopsis roots. New Phytol **183:** 1072-1084

Schaaf G, Erenoglu BE, von Wirén N (2004) Physiological and biochemical characterization of metal-phytosiderophore transport in graminaceous species. Soil Science and Plant Nutrition **50:** 989-995

Scheffer F, Schachtschabel P (2002) Lehrbuch der Bodenkunde. Spektrum Akademischer Verlag GmbH Heidelberg Berlin 15. Auflage

Schippers JHM, Nunes-Nesi A, Apetrei R, Hille J, Fernie AR, Dijkwel PP (2008) The Arabidopsis onset of leaf death5 Mutation of Quinolinate Synthase Affects Nicotinamide Adenine Dinucleotide Biosynthesis and Causes Early Ageing. Plant Cell **20:** 2909-2925

Schmidt W (1999) Mechanisms and regulation of reduction-based iron uptake in plants. New Phytologist **141:** 1-26

Schmidt W (2006) Iron Stress Responses in Roots of Strategy I Plants, pp 229-251. In: Iron Nutrition in Plants and Rhizospheric Microorganisms, L.L. Barton and J. Abadia, Springer, Dordrecht, The Netherlands

Scholz G, Becker R, Pich A, Stephan UW (1992) Nicotianamine - a common constituent of strategies I and II of iron acquisition by plants: A review. Journal of Plant Nutrition **15:** 1647-1665

Schumacher W, Thill D, Lee G (1983) Allelopathic potential of wild oat (Avena fatua) on spring wheat (Triticum aestivum) growth. Journal of Chemical Ecology **9:** 1235-1245

Schwertmann U (1991) Solubility and dissolution of iron oxides. Plant and Soil **130:** 1-25

Schwyn B, Neilands JB (1987) Universal chemical assay for the detection and determination of siderophores. Analytical Biochemistry **160:** 47-56

Seguela M, Briat J, Vert G, Curie C (2008) Cytokinins negatively regulate the root iron uptake machinery in Arabidopsis through a growth-dependent pathway. Plant Journal **55:** 289 - 300

Shenker M, Fan TW-M, Crowley DE (2001) Phytosiderophores Influence on Cadmium Mobilization and Uptake by Wheat and Barley Plants. J. Environ. Qual. **30:** 2091-2098

Shin L-J, Lo J-C, Chen G-H, Callis J, Fu H, Yeh K-C (2013) IRT1 DEGRADATION FACTOR1, a RING E3 Ubiquitin Ligase, Regulates the Degradation of IRON-REGULATED TRANSPORTER1 in Arabidopsis. The Plant Cell **25(8):** 3039-51

Shin SH, Lim Y, Lee SE, Yang NW, Rhee JH (2001) CAS agar diffusion assay for the measurement of siderophores in biological fluids. Journal of Microbiological Methods **44:** 89-95

Silva AM, Kong X, Parkin MC, Cammack R, Hider RC (2009) Iron(III) citrate speciation in aqueous solution. Dalton Trans**:** 8616-8625

Sivitz A, Grinvalds C, Barberon M, Curie C, Vert G (2011) Proteasome-mediated turnover of the transcriptional activator FIT is required for plant iron-deficiency responses. Plant Journal **66:** 1044-1052

Sivitz AB, Hermand V, Curie C, Vert G (2012) Arabidopsis bHLH100 and bHLH101 control iron homeostasis via a FIT-independent pathway. PLoS ONE **7:** e44843

Smith RM, Martell AE (1989) Critical Stability Constants. Plenum Press, New York **Vols 1–6**

Stintzi A, Barnes C, Xu J, Raymond KN (2000) Microbial iron transport via a siderophore shuttle: A membrane ion transport paradigm. Proceedings of the National Academy of Sciences **97:** 10691-10696

Stookey LL (1970) Ferrozine - a new spectrophotometric reagent for iron. Analytical Chemistry **42:** 779-781

Sugiura Y, Nomoto K (1984) Phytosiderophores structures and properties of mugineic acids and their metal complexes. In: Siderophores from Microorganisms and Plants, Vol 58. Springer Berlin Heidelberg, pp 107-135

Sugiyama A, Yazaki K (2012) Root Exudates of Legume Plants and Their Involvement in Interactions with Soil Microbes. In: JM Vivanco, F Baluška, eds, Secretions and Exudates in Biological Systems, Vol 12. Springer Berlin Heidelberg, pp 27-48

Susin S, Abadia A, Gonzalez-Reyes JA, Lucena JJ, Abadia J (1996) The pH Requirement for in Vivo Activity of the Iron-Deficiency-Induced "Turbo" Ferric Chelate Reductase (A Comparison of the Iron-Deficiency-Induced Iron Reductase Activities of Intact Plants and Isolated Plasma Membrane Fractions in Sugar Beet). Plant Physiology **110:** 111-123

Susin S, Abian J, Sanchezbaeza F, Peleato ML, Abadia A, Gelpi E, Abadia J (1993) Riboflavin 3'-Sulfate and 5'-Sulfate, 2 Novel Flavins Accumulating in the Roots of Iron-Deficient Sugar-Beet (Beta-Vulgaris). Journal of Biological Chemistry **268:** 20958-20965

Swarbreck D, Wilks C, Lamesch P, Berardini TZ, Garcia-Hernandez M, Foerster H, Li D, Meyer T, Muller R, Ploetz L, Radenbaugh A, Singh S, Swing V, Tissier C, Zhang P, Huala E (2008) The Arabidopsis Information Resource (TAIR): gene structure and function annotation. Nucleic Acids Research **36:** D1009-D1014

Takagi S (1976) Naturally occurring iron-chelating compounds in oat- and rice-root washings. Soil Science and Plant Nutrition **22:** 423-433

Takagi S, Nomoto K, Takemoto T (1984) Physiological Aspect of Mugineic Acid, a Possible Phytosiderophore of Graminaceous Plants. Journal of Plant Nutrition **7:** 469-477

Tato L, De Nisi P, Donnini S, Zocchi G (2013) Low iron availability and phenolic metabolism in a wild plant species (*Parietaria judaica* L.). Plant Physiol Biochem **72:** 145-153

Terano H, Nomoto K, Takase S (2002) Siderophore production and induction of iron-regulated proteins by a microorganism from rhizosphere of barley. Biosci Biotechnol Biochem **66:** 2471-2473

Treeby M, Marschner H, Römheld V (1989) Mobilization of iron and other micronutrient cations from a calcareous soil by plant-borne, microbial, and synthetic metal chelators. Plant and Soil **114:** 217-226

Trepeta RW, Edberg SC (1987) Esculinase (β-glucosidase) for the rapid estimation of activity in bacteria utilizing a hydrolyzable substrate, p-nitrophenyl-β-D-glucopyranoside. Antonie Van Leeuwenhoek Journal of Microbiology **53:** 273-277

Uren NC (2007) Types, Amounts, and Possible Functions of Compounds Released into the Rhizosphere by Soil-Grown Plants, pp 1-23. In: The Rhizosphere: Biochemistry and Organic Substances at the Soil-Plant Interface. Second Edition. R. Pinton, Z. Varanini and P.Nannipieri, CRC Press, Taylor & Francis Group Boca Raton, FL

Van De Mortel JE, Schat H, Moerland PD, Van Themaat EVL, Van Der Ent S, Blankestijn H, Ghandilyan A, Tsiatsiani S, Aarts MGM (2008) Expression differences for genes involved in lignin, glutathione and sulphate metabolism in response to cadmium in *Arabidopsis thaliana* and

the related Zn/Cd-hyperaccumulator Thlaspi caerulescens. Plant, Cell & Environment **31:** 301-324

Van der Ent S, Verhagen BWM, Van Doorn R, Bakker D, Verlaan MG, Pel MJC, Joosten RG, Proveniers MCG, Van Loon LC, Ton J, Pieterse CMJ (2008) MYB72 Is Required in Early Signaling Steps of Rhizobacteria-Induced Systemic Resistance in Arabidopsis. Plant Physiology **146:** 1293-1304

Varanini Z, Pinton R (2007) Plant-Soil Relationship: Role of Humic Substances in Iron Nutrition, pp 153-169. In: Iron Nutrition in Plants and Rhizospheric Microorganisms, L.L. Barton and J. Abadia, Springer, Dordrecht, The Netherlands

Varotto C, Maiwald D, Pesaresi P, Jahns P, Salamini F, Leister D (2002) The metal ion transporter IRT1 is necessary for iron homeostasis and efficient photosynthesis in *Arabidopsis thaliana*. Plant Journal **31:** 589-599

Vert G, Grotz N, Dedaldechamp F, Gaymard F, Guerinot ML, Briat JF, Curie C (2002) IRT1, an Arabidopsis transporter essential for iron uptake from the soil and for plant growth. Plant Cell **14:** 1223-1233

Vert GA, Briat JF, Curie C (2003) Dual regulation of the Arabidopsis high-affinity root iron uptake system by local and long-distance signals. Plant Physiology **132:** 796-804

von Wirén N (1994) Iron efficiency in graminaceous plant species and the role of the microbial degradation of phytosiderophores in iron acquisition. Dissertation. Verlag Ulrich E. Grauer, Stuttgart

von Wirén N, Khodr H, Hider RC (2000) Hydroxylated phytosiderophore species possess an enhanced chelate stability and affinity for iron(III). Plant Physiology **124:** 1149-1158

von Wirén N, Klair S, Bansal S, Briat JF, Khodr H, Shioiri T, Leigh RA, Hider RC (1999) Nicotianamine chelates both Fe-III and Fe-II. Implications for metal transport in plants. Plant Physiology **119:** 1107-1114

von Wirén N, Römheld V, Morel JL, Guckert A, Marschner H (1993) Influence of microorganisms on iron acquisition in maize. Soil Biology and Biochemistry **25:** 371-376

Walker TS, Bais HP, Grotewold E, Vivanco JM (2003) Root Exudation and Rhizosphere Biology. Plant Physiology **132:** 44-51

Wang N, Cui Y, Liu Y, Fan H, Du J, Huang Z, Yuan Y, Wu H, Ling HQ (2013) Requirement and functional redundancy of Ib subgroup bHLH proteins for iron deficiency responses and uptake in *Arabidopsis thaliana*. Mol Plant **6:** 503-513

Waters BM, Chu HH, Didonato RJ, Roberts LA, Eisley RB, Lahner B, Salt DE, Walker EL (2006) Mutations in Arabidopsis yellow stripe-like1 and yellow stripe-like3 reveal their roles in metal ion homeostasis and loading of metal ions in seeds. Plant Physiology **141:** 1446-1458

Weber G, von Wirén N, Hayen H (2006) Analysis of iron(II)/iron(III) phytosiderophore complexes by nano-electrospray ionization Fourier transform ion cyclotron resonance mass spectrometry. Rapid Communications in Mass Spectrometry **20:** 973-980

Welch RM (2002) Breeding Strategies for Biofortified Staple Plant Foods to Reduce Micronutrient Malnutrition Globally. The Journal of Nutrition **132:** 495S-499S

Welkie GW (2000) Taxonomic distribution of dicotyledonous species capable of root excretion of riboflavin under iron deficiency. Journal of Plant Nutrition **23:** 1819-1831

Wendenbaum S, Demange P, Dell A, Meyer JM, Abdallah MA (1983) The structure of pyoverdine Pa, the siderophore of Pseudomonas aeruginosa. Tetrahedron Letters **24:** 4877-4880

White PJ, Broadley MR (2005) Biofortifying crops with essential mineral elements. Trends in Plant Science **10:** 586-593

Yang T, Lin W, Schmidt W (2010) Transcriptional profiling of the Arabidopsis iron deficiency response reveals conserved transition metal homeostasis networks. Plant Physiology **152:** 2130 - 2141

Yi Y, Guerinot ML (1996) Genetic evidence that induction of root Fe(III) chelate reductase activity is necessary for iron uptake under iron deficiency. Plant Journal **10:** 835-844

Yonekura-Sakakibara K, Tohge T, Matsuda F, Nakabayashi R, Takayama H, Niida R, Watanabe-Takahashi A, Inoue E, Saito K (2008) Comprehensive Flavonol Profiling and Transcriptome Coexpression Analysis Leading to Decoding Gene–Metabolite Correlations in Arabidopsis. The Plant Cell Online **20:** 2160-2176

Yuan Y, Wu H, Wang N, Li J, Zhao W, Du J, Wang D, Ling HQ (2008) FIT interacts with AtbHLH38 and AtbHLH39 in regulating iron uptake gene expression for iron homeostasis in Arabidopsis. Cell Res **18:** 385-397

Zamioudis C (2012) Signaling in Arabidopsis roots in response to beneficial rhizobacteria. Dissertation. ISBN 978-90-8891-467-6; Uitgeverij BOXPress, Proefschriftmaken.nl

Zhang FS, Ma J, Cao YP (1997) Phosphorus deficiency enhances root exudation of low-molecular weight organic acids and utilization of sparingly soluble inorganic phosphates by radish (Raghanus sativus L.) and rape (Brassica napus L.) plants. Plant and Soil **196:** 261-264

Zimmermann P, Hirsch-Hoffmann M, Hennig L, Gruissem W (2004) GENEVESTIGATOR. Arabidopsis Microarray Database and Analysis Toolbox. Plant Physiology **136:** 2621-2632

Zuo Y, Ren L, Zhang F, Jiang RF (2007) Bicarbonate concentration as affected by soil water content controls iron nutrition of peanut plants in a calcareous soil. Plant Physiol Biochem **45:** 357-364

7 Abbreviations

°C	degree Celsius
%	percent
µ	micro
µg	microgram
µl	microlitre
µM	micromolar
35S	CaMV 35S promoter
bp	base pair
CaMV	Cauliflower Mosaic Virus
cDNA	complementary DNA
CLSM	confocal laser scanning microscope
CoA	coenzyme A
Col-0	Columbia-0, ecotype of *Arabidopsis thaliana*
DNA	desoxyribonucleic acid
dpi	dots per inch
DW	dry weight
E.coli	*Escherichia coli*
EDDHA	ethylenediamine-N,N'-bis(2-hydroxyphenylacetic acid)
EDTA	ethylenediaminetetraacetic acid
Fe	iron (from Latin: ferrum)
e.g.	for example
FLD	fluorescence detector
FW	fresh weight
g	gram
GFP	green fluorescent protein
h	hour
HPLC	high performance liquid chromatography
HR-ICP-MS	high-resolution-inductively coupled plasma-mass spectrometry
ICP-MS	inductively coupled plasma-mass spectrometry
i.e.	id est (from Latin: that is)
LB	left border
LC-ESI-MS	liquid chromatography-electrospray-ionization-mass spectroscopy
M	molar
m	milli
mm	millimeter
MΩ	megaohm
m/z	mass-to-charge
mg	milligram
min	minute
ml	millilitre
mM	millimolar
MS	mass spectrometry
MYB	myeloblastosis family of transcription factors
n	number of biological replicates
n	nano
n.d.	not detected
n.s.	not significant
nm	nanometer
P	p-value (‘probability’)
p	pico
PCR	polymerase chain reaction
pH	‘power of hydrogen’, measure of the acidity or basicity of an aqueous solution
R2R3-MYB	Repeat2 Repeat3 MYB (myeloblastosis) transcription factor
RB	right border
RNA	ribonucleic acid
ROS	reactive oxygen species
rpm	revolutions per minute
RT	retention time
SAIL	Syngenta *Arabidopsis* Insertion Library
SALK	Salk Institute for biological studies
SE	standard error
sec	second
T-DNA	transfer-DNA
t-test	Student’s *t* distribution test
UPLC	ultra performance liquid chromatography
UPLC-ESI-MS	UPLC-electrospray-ionization-mass spectroscopy
UV	ultra-violet light
V	volt
v/v	volume-to-volume ratio
WHO	world health organization
WT	wild type
x *g*	gravitation force

8 Curriculum Vitae

Name:	Nicole Beate Schmid
Date of birth:	08.04.1983
Place of birth:	Heidenheim a.d. Brenz
Nationality:	German
Address:	Leibniz Institute of Plant Genetics and Crop Plant Research Department of Physiology and Cell Biology Corrensstraße 3, 06466 Gatersleben, Germany
Telephone:	+49 (0)39482 5342
Email:	schmidn@ipk-gatersleben.de

Education

08/2009 – now	PhD on 'Identification and characterization of Arabidopsis genes involved in tolerance to Fe deficiency-mediated chlorosis', Molecular Plant Nutrition Group Department of Physiology and Cell Biology Leibniz Institute of Plant Genetics and Crop Plant Research
10/2003 – 05/2009	Studies in Agricultural Biology at the University of Hohenheim, Stuttgart, Germany (Diploma, Dipl.-Agr.Biol.) Study Abroad at the University of Queensland, Brisbane, Australia (02/2006 - 06/2006) Diploma thesis at Bayer CropScience AG, Department of Biochemistry, Frankfurt am Main, Germany
09/1999 – 07/2002	Secondary school (Wirtschaftsgymnasium Heidenheim, Abitur)

Publication

Schmid NB, Giehl RF, Döll S, Mock HP, Strehmel N, Scheel D, Kong X, Hider RC, von Wirén N, (2014): Feruloyl-CoA 6'-Hydroxylase1-Dependent Coumarins Mediate Iron Acquisition from Alkaline Substrates in Arabidopsis. Plant Physiology **164**: 160-172

Participation in scientific conferences during the PhD study

Oral Presentations

A role of the SNARE protein VTI11 in intracellular iron efficiency in *Arabidopsis thaliana*;
6th Plant Science Student Conference (PSSC), IPK Gatersleben (15. - 18.06.2010)

Identification of a new component in Fe acquisition in *Arabidopsis thaliana*;
26th Symposium "Molecular Plant Biology", Dabringhausen (26.02. - 01.03.2013)

Identification of a new component in Fe acquisition in *Arabidopsis thaliana*;
9th Plant Science Student Conference (PSSC), IPB Halle (28. - 31.05.2013)
Talk Award

Identification of a new component in Fe acquisition in *Arabidopsis thaliana*;
17th International Plant Nutrition Colloquium (IPNC), Istanbul, Turkey
(19. - 22.08.2013)

Poster Presentations

PLANT-KBBE: HOT IRON Approach for the identification of genes improving iron efficiency in Arabidopsis;
Gabi Status Seminar, Potsdam (09. - 11.03.2010)

A role of the SNARE protein VTI11 in intracellular iron efficiency in *Arabidopsis thaliana*;
15th International Symposium on Iron Nutrition and Interactions in Plants, Budapest, Hungary (26. - 30.06.2010)

A role of the SNARE protein VTI11 in intracellular iron efficiency in *Arabidopsis thaliana*;
Symposium of the German Society of Plant Nutrition (Genetics of Plant Mineral Nutrition), Hannover (30.09. - 02.10.2010)

Identification of genes improving or impairing growth of Arabidopsis on calcareous substrates;
7th Plant Science Student Conference (PSSC), IPB Halle (14. - 17.06.2011)

Identification of genes involved in Fe efficiency in Arabidopsis;
Botany Congress, Berlin (19. - 22.09.2011)

Identification of genes involved in Fe efficiency in Arabidopsis;
Plant 2030 Status Seminar, Potsdam (06. - 08.03.2012)

Characterization of an Arabidopsis gene involved in tolerance to iron deficiency-induced chlorosis;
16th International Symposium on Iron Nutrition and Interactions in Plants, Amherst, Massachusetts, USA (17. - 21.06.2012)

Characterization of an Arabidopsis gene involved in tolerance to iron deficiency-induced chlorosis;
8th Plant Science Student Conference (PSSC) at the IPK Gatersleben - *Poster Award* (04. - 07.06.2012)

Supervision activity

Supervision of an undergraduate student for research in molecular plant nutrition on 'the Ferroportin Metal Efflux Proteins IREG 1 and IREG 2 in *Arabidopsis thaliana'* (15.02.2010 - 26.03.2010)

Nicole Schmid

Gatersleben, 11th February, 2014

9 Affirmation

I hereby declare that the submitted work has been completed by me, the undersigned, and that I have not used any other than permitted reference sources or materials or engaged any plagiarism. All the references and the other sources used in the presented work have been appropriately acknowledged in the work. I further declare that the work has not been previously submitted for the purpose of academic examination, either in its original or similar form, anywhere else.

Hiermit erkläre ich, dass ich diese Arbeit selbständig verfasst und keine anderen als die angegebenen Quellen und Hilfsmittel verwendet habe. Die den benutzten Hilfsmitteln wörtlich oder inhaltlich entnommenen Stellen habe ich unter Quellenangaben kenntlich gemacht. Die vorliegende Arbeit wurde in gleicher oder ähnlicher Form noch keiner anderen Institution oder Prüfungsbehörde vorgelegt.

Nicole Schmid

Gatersleben, 11th February, 2014

10 Acknowledgements

I would like to express my deepest thanks to Prof. Dr. Nicolaus von Wirén for accepting me as a PhD candidate. For letting me participate in his enthusiasm and amazing knowledge about science. For representing an example from which I could benefit so much, not only scientifically but also personally. For providing a supportive and trustful environment with opportunities, challenges and also enough freedom to develop as a researcher. I am very grateful that I could be part of your team. Thank you Nico.

I also would like to thank Prof. Dr. Buckhout and Prof. Dr. Humbeck for evaluating my thesis.

For financial support during my PhD I would like to acknowledge the Federal Ministry of Education and Research (BMBF) and the IPK Gatersleben.

My deepest thanks to Dr. Ricardo Giehl. I could not be more grateful for your guidance and support. For always being ready for scientific discussions and offering your best advice at any time. For showing me both, the seriousness and the joy of science and everything that goes with it. I will always cherish and also profit from all that I could learn from you in all these different areas. Thank you Ric.

Thanks so much to Anne. For your scientific and personal support throughout the years. For always offering a capable and helpful hand, no matter which issue. Thank you very much. Also thanks a lot to Albe for his cheerful company and support and for his ability to let time pass without notice.

I would also like to thank all members of the Molecular Plant Nutrition group. It was great to work together with all of you. Thank you Ben, Diana, Susanne, Susanne Schmidt, Bernhard, Anderson, Elis, Lisa, Julia, Heike, Melanie, Andrea, Siva, Syed, Alex, Rongli, Fanghua, Fengying, Polet, Baris, Dima, Sebi, Jule, Uli, Zhaojun, Takao, Markus, Ying, Seckin, Ralf, Alex, Kai, Stefan, Mo, Dagmar, Christine, Barbara, Reeza, Wally, Elmarie and everyone else.

I am also very grateful for the support I received in the greenhouse from Mr. Geyer, Mrs. Braun, Frau Wackermann, Frau Fessel, Frau Jacobs, Anke, Andreas and the whole group. Thank you very much.

I also want to thank Dr. Stefanie Döll, Dr. Hans Peter Mock, Dr. Twan Rutten and several other researchers from all over the IPK as well as Prof. Dr. Hider, Xiaole Kong, Dr. Nadine Strehmel and Prof. Dr. Dierk Scheel for cooperations and support. Thanks also to the members of the administration of the IPK.

Last but not least I want to thank my family and all my friends. I cannot be grateful enough for your continuous love and support in so many ways. For me, you are the greatest gift of all. I could not be happier to have all of you in my life.